Universidade de Lisboa
Faculdade de Ciências
Departamento de Física


# Drug Delivery of Methyl-Carboxilated 5-Fluorouracil by means of Human serum albumin microcarriers

**Ana Rita Estevão Rocha**

Dissertação

Mestrado Integrado em Engenharia Biomédica e Biofísica
Perfil de Engenharia Clínica e Instrumentação Médica

**2014**

Universidade de Lisboa
Faculdade de Ciências
Departamento de Física

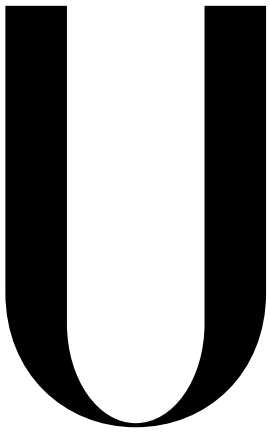

LISBOA

UNIVERSIDADE
DE LISBOA

# Drug Delivery of Methyl-Carboxilated 5-Fluorouracil by means of Human serum albumin microcarriers

**Ana Rita Estevão Rocha**

Dissertação
Mestrado Integrado em Engenharia Biomédica e Biofísica
Perfil de Engenharia Clínica e Instrumentação Médica
Orientador Interno: Dr. Hugo Alexandre Ferreira
Orientador Externo: PD Dr. Hans Bäumler

**2014**

# I. Index

# II. Resumo

De acordo com as estatísticas da Organização Mundial de Saúde, o cancro é a segunda causa de morte em todo o mundo, provocando 7,565 milhões de mortes por ano [1].

As últimas décadas têm sido férteis no aparecimento de novos tratamentos para o cancro, muito devido aos nefastos efeitos secundários que os tratamentos tradicionais infligem aos doentes. Muitos desses avanços têm sido possibilitados pelo crescente conhecimento dos processos fisiopatológicos e bioquímicos característicos do aparecimento e desenvolvimento do cancro. O processo de permeabilidade e retenção aumentadas (PRA) (do inglês "Enhanced Permeability and Retention"- EPR) é um dos poucos processos característico dos tumores sólidos que impulsionou o desenvolvimento de uma nova abordagem no campo da quimioterapia. A teoria do PRA postula que a captação e acumulação de macromoléculas biocompatíveis está aumentada nos tumores, muito devido ao desenvolvimento deficiente da sua vasculatura e sistema linfático e da síntese aumentada de mediadores de permeabilidade [2]. A albumina é uma das referidas macromoléculas que são preferencialmente acumuladas nos interstícios dos tumores e no interior das suas células. Esta proteína encontra-se em maioria na porção proteica do plasma sanguíneo, perfazendo um total de cerca 50-70% das proteínas em suspensão no plasma e apresentando um período semi-vida de cerca de 19 dias. A albumina, que pode ser degradada intracelularmente, torna-se então numa fonte de azoto e energia para as células tumorais, que têm necessidade aumentada de energia e nutrientes devido à sua divisão desregulada. A albumina começa por transpor as paredes dos vasos por transcitose mediada pela proteína gp60 que se encontra à superfície de algumas células epiteliais [3]. Quando se encontra na proximidade de células tumorais há um reconhecimento da albumina por proteínas membranares e a proteína é endocitada e subsequentemente degradada no interior de lisossomas. A albumina liga-se a uma grande variedade de ligandos endógenos tal como ácidos gordos não-esterificados e a bilirrubina em múltiplos locais da sua estrutura. Algumas substâncias activas comuns são também ligadas à albumina em condições fisiológicas, tal como o ibuprofeno, diazepam, varfarina e o 5-fluorouracilo (5-FU) [4][5]. No que diz respeito à ligação do 5-FU à albumina, esta foi descrita como sendo de baixas afinidade e especificidade em comparação com outras substâncias tais como o diazepam.

O 5-FU é uma droga utilizada no tratamento de cancro, nomeadamente da mama e cólon, e está em prescrição clínica há mais de 50 anos [6]. Esta substância análoga das pirimidinas tem-se afirmado como uma droga antineoplásica relativamente bem sucedida. No entanto o rácio entre a dose eficaz e a dose tóxica é pequeno, ou seja, uma resposta terapêutica adequada é pouco provável sem alguma toxicidade. É frequente a ocorrência de episódios mucosite, mielossupressão, diarreia e neurotoxicidade entre os doentes submetidos a regime de

quimioterapia com 5-FU. Sendo uma molécula de pequenas dimensões, é rapidamente distribuída pelos tecidos corporais e catabolizada pelo fígado, que a inactiva através da redução do anel pirimidínico. O 5-FU é assim rapidamente eliminado pelo corpo, apresentado um período de semi-vida em circulação entre 10 e 20 minutos [5]. Devido a esta rápida eliminação, o efeito terapêutico do 5-FU é condicionado pelo que seria desejável conseguir implementar uma estratégia para prolongar o tempo desta substância na circulação sanguínea. Neste sentido há já várias abordagens registadas, nomeadamente através da síntese de partículas onde o 5-FU é incorporado num transportador proteico ou polimérico. Desta forma podem ainda ser exploradas características como a libertação controlada do princípio activo ou até uma conjugação de substâncias ligadas a um veículo [7].

Tada *et al* [8] descreveu a síntese de 5-fluorouracil-ácido-acético (FUAc) numa tentativa de melhorar as capacidade antineoplásicas do 5-FU. No entanto não existem no artigo quaisquer referências a testes de citotoxicidade à referida substância. Mais tarde um grupo coreano utilizou um conjugado de FUAc ligado a albumina humana e testou a suas propriedades farmacocinéticas em soluções fisiológicas, no entanto não há referências quanto ao método de síntese nem ao rácio de moléculas de FUAc por moléculas de albumina [9]. Os resultados descritos por este grupo sugerem que a ligação FUAc-albumina é bastante estável uma vez que a libertação de 5-FU do conjugado se limita a cerca de 1% numa solução fisiológica de pH 9. Do ano seguinte, 1990, data uma outra publicação de um grupo coreano referente ao conjugado FUAc-albumina humana, desta vez por Chung *et al* [10]. Mais uma vez não está descrito o protocolo de síntese, no entanto os resultados obtidos dos testes em coelhos revelaram-se promissores. O conjugado manteve a concentração de 1µg/ml de 5-FU no sangue durante um período de 3 a 24 horas e apenas 5-FU foi libertado das partículas de FUAc-albumina humana, não FUAc. O 5-FU ter-se-á libertado das partículas de FUAc-albumina por um processo ainda desconhecido. Os coelhos receberam uma infusão de suspensão da partícula durante 30 minutos. Foi também descrita a presença de 5-FU no tecido cerebral após a administração de FUAc-albumina humana, ao contrário do que aconteceu com infusões de 5-FU e FUAc.

Tendo por base as publicações acima referidas, Koziol *et al* [11] publicou o protocolo de síntese de um conjugado de FUAc-albumina bovina e ainda a caracterização da mesma partícula e testes de citotoxicidade *in vitro*. A reacção de síntese da partícula de FUAc foi adaptada de Tada et al [8]. De forma a criar uma ligação covalente entre a molécula proteica, neste caso a albumina bovina, e a de FUAc foi utilizado o método EDC/NHS com algumas adaptações [12]. Este método de *cross-linking* cria uma ligação covalente entre o grupo carboxilo da molécula de FUAc e os grupos ε-amina livres nas extremidades das cadeias laterais das lisinas. O sucesso da síntese foi confirmado por ionização-dessorção com laser

assistida por matriz – tempo de voo (MALDI-TOF), havendo uma média de 12 moléculas de FUAc por albumina. De forma a testar a citotoxicidade do conjugado foram selecionadas duas linhas celulares isoladas de carcinoma mamário, MDA-MB-231 e T-47D. Estas duas linhas celulares diferem entre si na expressão de uma proteína de membrana (mABP - *plasma-membrane albumin-binding protei*n) identificada como influente no *uptake* de uma partícula, já em uso clínico, de paclitaxel conjugado com albumina [13], sendo que as células da linhas T-47D expressam esta proteína e as MDA-MB-231 não. Foi encontrada uma relação entre a presença desta proteína e a inibição das células uma vez que o efeito exercido pela partícula de FUAc-BSA e 5-FU mostrou-se similar.

Para o projecto sobre o qual assenta esta tese foram escolhidas três linhas celulares isoladas de carcinoma da mama: MDA-MB-231, T-47D e MCF-7. A terceira linha celular referida expressa a proteína anteriormente referida, mABP, e ainda uma outra também descrita como influente no *uptake* de nab-paclitaxel, a SPARC (de *secreted protein, acidic and rich in cysteine*).

A síntese do da partícula conjugada foi realizada de acordo com o protocolo descrito por Koziol *et al* substituindoa albumina bovina por albumina humana (albumina sérica humana – ASH). O sucesso da síntese foi confirmado por MALDI-TOF e foi obtida uma média de 15 moléculas de FUAc por ASH. A conformação da proteína foi analisada por espectroscopia de dicroísmo circular, o que revelou que a estrutura da proteína sofreu apenas alterações pouco consideráveis quando comparável com a albumina antes da reacção de ligação. De forma a testar a capacidade de inibição que a partícula de FUAc-ASH tem sobre as células, estas foram incubadas durante um período máximo de 96 horas com 6 concentrações diferentes da partícula no meio de cultura celular, assim como das outras substâncias puras (FUAc, ASH e 5-FU), de forma a ser possível estabelecer uma comparação. A avaliação do poder de inibição das substâncias sobre as células foi avaliado através do teste de viabilidade celular MTT e posteriormente confirmado através de contagem celular com azul de tripano. Foram incubadas células nas mesmas condições e período de tempo, sem adição de nenhuma das substâncias a testar como controlo. A inibição registada devido ao FUAc-ASH foi menos pronunciada que a obtida pela administração de 5-FU, no entanto foi clara a inibição exercida tanto pela partícula de FUAc-ASH como pela molécula de FUAc. Tal como seria de esperar, foi o 5-FU o composto que causou uma inibição do metabolismo celular mais acentuada. Pelos resultados obtidos não foi possível destacar a importância das proteínas mABP e SPARC no uptake das partículas de FUAc-ASH. No entanto é de salientar que este efeito é sugerido pelos resultados obtidos após 96 horas de incubação, onde as células da linha MCF-7 apresentam uma maior inibição comparativamente às restantes. Esta linha celular apresenta um período de duplicação mais longo do que as restantes duas linhas celulares, portanto é plausível supor que o

prolongamento do período de incubação com as substâncias a testar produza resultados mais significativos para uma clarificação da importância das referidas proteínas membranares no *uptake* do FUAc-ASH. É também de considerar que existem diferenças estruturais entre as albuminas humana e bovina, sendo que a bovina tem vindo a ser descrita na literatura como mais estável. Este facto pode também influenciar a libertação do 5-FU do conjugado, apresentando assim mais uma razão para a necessidade de uma período de incubação mais prolongado.

Os resultados obtidos sugerem que o conjugado FUAc-ASH possui características passíveis de uma aplicação clínica, no entanto estes devem ser considerados como preliminares e será necessário uma posterior confirmação do potencial da partícula. A confirmar-se que a partícula de FUAc-ASH actua por meios semelhantes a outros conjugados de albumina já no mercado (Abraxane, por exemplo), esta abordagem poderá representar um avanço significativo no tratamento de cancros susceptíveis à acção do 5-FU.

**Palavras-chave:** Cancro, micro-transportador, *drug targeting*, albumina, 5-Fluorouracilo, 5-Fluorouracilo-ácido acético, 5-Fluorouracilo-ácido acético – Albumina sérica humana

# III. Abstract

Nowadays, cancer is one of the major death causes worldwide (7.565 million deaths per year according to WHO statistics). Besides the registered developments in cancer treatments, what leads to improved clinical results; the side effects suffered by the patients are still very hard to bear with mainly referring to chemotherapy. In order to reduce these side effects, one of the explored approaches was to link the chemotherapy drug to a carrier suitable to keep the cytotoxic agent in the circulating blood for a longer period and to minify the drug toxicity for the healthy cells.

Within this drug carrier approach, human serum albumin was chosen as a suitable carrier and for the active substance the choice fell on one adduct of 5-fluorouracil. 5-Fluorouracil is in clinical usage for many years, mainly for treatment of solid cancers (breast and colon cancer) and, as most of the chemotherapy drugs, its toxicity limits the tolerable administered dosage for treatment. In previous works results showed that the coupling of cytostatic drugs to blood proteins could represent an advantage because it reduces the toxicity and is able to keep the cytostatic action.

To synthesize this adduct, named 5-fluorouracil acetic acid (FUAc), an acetic acid side chain was introduce at one of the nitrogen atoms in the » ring. With the attachment of this side chain, 5-FU acquired the ability to bind to the free amine groups of HSA.

An average of 15 FUAc molecules were bound to one HSA. The particle conformation was assessed by Circular dichroism (CD) spectroscopy and minimal differences were registered between the spectra of pure HSA and FUAc-HSA, suggesting that the coupling procedure had not induced major structure alterations.

Three breast cancer cell lines (MDA-MB-231, T-47D and MCF-7) were chosen for the evaluation of the active agents cytotoxicity. These cell lines were chosen mainly due to their difference in mABP and SPARC proteins expression, reported to have a central role in albumin uptake by the cells. MDA-MB-231 cells do not express these proteins, T-47D is positive for mABP and MCF-7 express both the proteins.

Cells were incubated with the four compounds – HSA, FUAc-HSA, FUAc and 5-FU- for periods of 24, 48, 72 and 96 hours. For each compound six different concentrations were taken, from 1 to 500μM. At every 24 hours a MTT assay was performed to assess the inhibition of cell metabolism.

The three cell lines tested were inhibited by 5-FU, FUAc and FUAc-HSA but none of them registered inhibition related to HSA. MCF-7 cell line was the one registering a highest

metabolism inhibition at 96 hours when incubated with FUAc-HSA. In the previous time points, T-47D cell line registered a higher inhibition when compared with the other cell lines. 5-FU was the substance causing the highest in all cell lines. Regarding to FUAc, MDA-MB-231 cell line was the one showing the highest inhibition.

FUAc-HSA might have advantages upon 5-FU for treating solid cancers although further tests should be performed. The dependence on SPARC for FUAc-HSA uptake by the cells was not clear however metabolism inhibition of MCF-7 cells at 96 hours suggested the relation between this protein and enhanced uptake to be valid.

**Keywords:** Cancer, microcarrier, drug targeting, Albumin, 5-Fluorouracil, 5-Fluorouracil-acetic acid, FUAc-HSA

# IV. Acknowledgements / Agradecimentos

First of all I would like to thank to Dr. Bäumler for giving me the opportunity of working with him and his team and for being always helpful and supportive. I am really grateful for this year; it was a great time for me, personally and academically. I learned a lot and I own that to you all! Vielen dank!

I also want to give a special acknowledgement to Dr. Radostina Georgieva for all the support, help and for being always so warm and friendly!

To Michael Koziol (MD candidate), for being such a good teacher, always with so much patience to explain me everything and for making it much funnier during the short periods we worked together! Thank you!

To Kathrin Smuda for being so helpful and nice every single time I needed her. You were a great support for me during this year in Berlin.

Thank you to Dr. Yu Xiong and Axel Stefen for being so helpful and friendly everyday.

It was great to work with you all during this year, thank you again!

Thank you to AG Dorner for all the help provided and for sharing the clean bench.

Also want to thank to Felix Wojcik, Dr. Katharina Janek and Mrs. Agathe Niewienda for MALDI-TOF measurements, to Dr. Margitta Dathe and Mrs. Heike Nikolenko for the help with CD-Spectroscopy.

Thank you to Dr. Hugo Ferreira for supporting and helping me from Portugal.

Agora em português, agradeço a todos aqueles que sempre estiveram comigo e sempre hão-de estar: a minha família e os meus amigos. Aos meus pais, agradeço a paciência e todo o apoio, dado a todos os níveis. Cliché, mas tem de ser dito, sem vocês nada do que tenho feito seria possível. Obrigada!

Aos meus amigos, aqueles que me acompanham desde que me lembro de existir e também aos outros mais recentes mas que vieram para ficar: Ana Patrícia, Sara, Cristina, Ana Margarida, Ricardo, Laura, Lúcia, Zé Manel, João Duarte… e a todos os que me apoiaram à distância mas sempre tão presentes!

Aos meus companheiros de aventuras em Berlim, a Inês e o João, obrigada pela amizade, por serem lindos e pelos bons momentos. Tornaram estes meses muito melhores!

# V. Index of abbreviations

## *

$^{13}C$ ..... Carbon isotope 13
$^{19}F$ ..... Fluor isotope 19
$^{1}H$ ..... Hydrogen isotope 1
µg/mL ..... microgram per mililiter
$^{31}P$ ..... Phosphorus isotope 31
5-FdUMP ..... 5-Fluorodeoxyuridine monophosphate
5-FU ..... 5-Fluorouracil
θ ..... Degree of ellipcity

## A

A ..... Adenine
Acetyl-coA ..... Acetyl-coenzyme A
ALCP ..... Left-handed circularly polarised light
ARCP ..... Right-handed circularly polarised light
ATCC ..... American Type Culture Collection
AUC ..... Area under the curve

## B

$\mathbf{B_0}$ ..... External magnetic field
BSA ..... Bovine Serum Albumin

## C

$C^1$ ..... Carbon in the position 1 of the Uracil ring
$C^2$ ..... Carbon in the position 2 of the Uracil ring
$C^{2'}$ ..... Carbon in the position 2 of the side chain
$C^4$ ..... Carbon in the position 4 of the Uracil ring
$C^5$ ..... Carbon in the position 5 of the Uracil ring
$C^6$ ..... Carbon in the position 6 of the Uracil ring
CD ..... Circular dichroism
CLSM ..... Confocal laser scanning microscope
Cys ..... Cysteine

## D

Da ..... Dalton
DHAP ..... 2,5-Dihydroxyacetophenone

DHR-123 ..... Dihydrorhodamine 123
DMSO ..... Dimethyl sulfoxide
DMSO-$d_6$ ..... Hexadeuterodimethyl sulfoxide
DNA ..... Deoxyribonucleic acid
DNase I ..... Deoxyribonuclease I
DPD ..... Dihydropyrimidine dehydrogenase
dTMP ..... Deoxythymidine Monophospate
dTTP ..... Deoxythymidine triphosphate
dUMP ..... Deoxyuridine monophosphate

## E

EDC ..... 1-Ethyl-3-(3-dimethylaminopropyl)carbodiimide
EDC/NHS ..... 1-Ethyl-3-(3-dimethylaminopropyl)carbodiimide / N-hydroxysulfosuccinimide
EDTA ..... Ethylenediamine tetraacetic acid
EMEM ..... Eagle's minimal essential medium
EPR ..... Enhanced permeability and retention

## F

FBS ..... Fetal bovine serum
FDA ..... Food and Drug Administration
FDHU ..... 5-fluoro-5,6-dihydrouracil
FdUTP ..... Fluorodeoxyuridine triphosphate
FITC-BSA ..... Fluorescein isothiocyanate-bovine serum albumin
FUAc ..... 5-Fluorouracil acetic acid
FUAc-BSA ..... 5-Fluorouracil acetic acid- Bovine serum albumin
FUAc-HSA ..... 5-Fluorouracil acetic acid- Human serum albumin
FUTP ..... fluorouracil triphosphate

## G

G ..... Guanine
g/mol ..... grams per mole
Glu ..... Glutamic acid
Gly ..... Glycine

## H

HER2 ..... Human Epidermal growth factor Receptor 2
HPLC ..... High-performance liquid chromatography
HSA ..... Human serum albumin
Hz ..... Hertz

## I

IC50 ..... Half maximal inhibitory concentration
igG ..... Immunoglobulin G
Ile ..... Isoleucine

## J

*J* ..... Coupling constant
$J_{ij}$ ..... scalar coupling constant

## K

*k* ..... proportionality constant
kDa ..... kilo Dalton

## L

Leu ..... Leucine
Lys ..... Lysine

## M

**M** ..... Net magnetization of a macroscopic piece
mABP ..... membrane albumin binding protein
MALDI-TOF ..... Matrix-assisted laser desorption/ionization - Time of Flight
mbar ..... mili bar
MES ..... 2-(N-morpholino)ethanesulfonic acid
Met ..... Methionine
mg ..... miligram
mg/mL ..... miligram per mililiter
MRE ..... Mean residue ellipcity
MTT ..... 3-(4,5-dimethylthiazol-2-yl)-2,5-diphenyltetrazolium bromide
MTX ..... Methotrexate
MTX-HSA ..... Methotrexate - Human serum albumin

## N

$N^1$ ..... Nitrogen in the position 1 of the uracil ring
$N^3$ ..... Nitrogen in the position 3 of the uracil ring
NADH ..... Reduced Nicotinamide adenine dinucleotide
NCI60 ..... US National Cancer Institute 60 anticancer drug screen
ng ..... nanogram
NHS ..... N-Hydroxysuccinimide
nm ..... nanometer

NMR ..... Nuclear magnetic resonance

## P

PBS ..... Phosphate buffered saline
pH ..... Power of Hydrogen
PLGA ..... Poly(lactic-co-glycolic acid)
pm ..... picometer

## R

RNA ..... Ribonucleic acid
ROS ..... Reactive oxygen species
RPMI ..... Roswell Park Memorial Institute medium

## S

SDS ..... Sodium dodecyl sulfate
SPARC ..... Secreted protein acidic and rich in cysteine

## T

T ..... Temperature in Kelvin
t ½ ..... Half-time period
TMS ..... Tetramethylsilane
Trp ..... Tryptophan
TS ..... Thymidylate synthase

## U

U ..... Uracil

## μ

μ ..... Magnetic momentum
μL ..... microliter
μM ..... micro molar

# VI. Index of Images

# VII. Index of Tables

# 1. Introduction

In the first part of this work a literature review will be presented in order to enframe it theoretically. Through the following chapter the material and methods are listed and explained. On the third chapter the results can be found and, finally, the last chapter regards the discussion of all the procedures and results.

## 1.1 Cancer

Back in the ancient Egypt people already suffered from cancer and physical proofs survived until nowadays, together with fossilized bone tumors in mummies. Written references to cancer, even still not using this word that would appear later, could be found in manuscripts dated from 3000 BC.

From these ancient times to nowadays, numerous improvements in cancer treatment had hopefully been done. Ancient Egyptians classified cancer as having no possible treatment back then, although they described the procedure to remove breast tumors by cauterization with an instrument called fire drill. Scientific evolution made possible to currently have treatments as sophisticated as targeting genetic alterations characteristics of tumors [14].

One of the most remarkable scientific discoveries on the cancer subject was the ability of healthy body cells to go through all the steps from normal dividing and metabolic activity to fast out of control dividing. Several studies have suggested that tumorigenesis is a result of progressive genetic alterations of normal human cells, leading in last instance to highly malignant derivatives. The human is composed of both dividing and no dividing cells. Highly specialized and differentiated cells like neurons, for instance, are able to keep their functions without dividing, however other cells like epithelial and bone marrow need to replicate to maintain their function. The balance is naturally maintained in the whole body by controlling the dividing process and death of cells, but when this balance process fails this can happen to be the starting point of a tumor. Every cell has an intern clock governing its division activity and oncogenes modify it by exerting pressure for the cell to go further on the dividing process. This pressure works at one of the gap phases

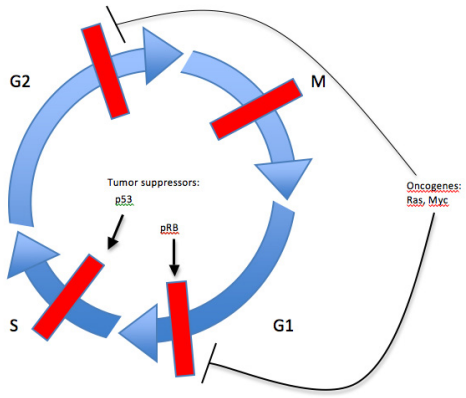


Figure 1: Cell cycle control by tumour suppressor and oncogenes[15]. The red bars represent checking points that the tumours suppressors are to maintain and oncogenes try to overcome.

(either G1 or G2), at S phase or mitosis. Oncogenes are believed to be capable of rescuing cells from programed cell death as well [15]. Even considering that most types of cancers experience different processes to achieve their capabilities, ultimately they all acquire the following characteristics:

- Low sensitivity to anti-growth signals
- Sustained angiogenesis
- Unlimited replicative potential
- Tissue invasion
- Autonomy in growth signals
- Apoptosis avoidance
- Changes in cell metabolism

The invasion of other tissues by cancer cells, the so called metastasis, were described as responsible for 90% of the deaths in oncologic patients [16]. According to the World Health Organization, cancer was responsible for close to 7,6 million deaths in 2008 and predictions for future are far from encouraging: 13,1 million for 2030. Statistically, only heart diseases are more mortal than cancer [17].

Great advances on cancer treatment had been possible due to growing knowledge accessible nowadays related to tumor pathophysiology. One process considered almost like the 'holy grail' for cancer drug delivery research is the Enhanced Permeability and Retention, commonly known as EPR. The referred designation is due to abnormal characteristics of mostly solid tumors, like extensive angiogenesis, what generates hypervasculature, defective vascular architecture, impaired lymphatic drainage and an accentuated increased production of some permeability mediators, as well as an augmented retention of lipid and macromolecular agents (for instance, plasma proteins [18]). The referred overdevelopments occur as a way of providing enough oxygen and nutrients to suppress the tumor demanding needs [2]. There is a large body of evidence demonstrating that tumors in animals and humans have a great need of transferrin and albumin to cover their high demand for iron (III) and amino acids due to their fast grew rate [19]. This high demanding need of nutrients and protein entrapment is suggested to lead to cachexia, a common condition in tumor patients [18].

As the normal cells, tumor cells also need oxygen to survive and proliferate, however, due to the inefficient vasculature; solid tumors frequently experience a lack of oxygen in some locations not close enough to the blood vessels. Oxygenated zones in tumors are that within a distance of about 80pm from a blood vessel and the average tumor cell to capillary distance was reported as being from 33 to 63pm. Plasma proteins, like albumin, reach and accumulate in these tumor regions. After the albumin uptake by cells, the first step for its degradation takes

place in the lysosomes by proteases. The product of this degradation is a stock of free amino acids in the cytosol, which will be used by the cell for further synthesis of proteins necessary for the fast division of cancer cells and also as extra fuel for the Krebs cycle [18], [20].

Cancer cells in hypoxic areas survive mainly by getting energy from anaerobic glycolysis. As protein nutrients are not able to reach these cells as well, only low molecular weight substrates like glucose and free amino acids are the only energy sources available for theses cells [18].

The EPR effect can be observed in almost all tumor types, excepting hypovascular tumors like prostate and pancreatic [21]. The EPR effect with macromolecular drugs or particles like plasma proteins (for example HSA) is a different process from the passive targeting of drugs to tumors. Drug retention in tumors with a registered EPR effect is more than days to weeks contrasting with retention associated with passive targeting reported as being no more than ten minutes [22]. EPR effect can be considered as an advantageous process for cancer drug targeting, however some considerations have to be done since every tumor is different and even in the same tumor huge differences can be registered. Lammers *et al* [23] reported differences with regard to vascular permeability inside the same tumor, where at a certain part particles with 200nm were able to extravasate and in other parts particles with about the size of albumin (3-4nm) were not able to enter the interstitium.

Dreher *et al* [24] investigated the vascular permeability by dextran molecules varying the particles molecular weight and consequently its size. Tumor accumulation was maximal for particles between 40 and 70 kDa however particles of 3,3 and 10kDa penetrated deeply and homogeneously in the tumor. Therefore, it can be assumed that the size of the particle influences the accumulated quantity and how deep it penetrates in the tumor.

Stehle et al [18] reported that macromolecules reach the tumor vasculature by blood convection and after the extravasation to the interstitium of the tumor, by diffusion. The movement by diffusion depends on the molecular weight and by comparing igG (150000 Da) and albumin (66438 Da) diffusion, albumin diffuses around 10 times faster.

## 1.2 Cancer treatments

Cancer is considered one of the biggest health issues, mainly in developed countries as it was already referred in the previous chapter. Many studies had been performed in order to reach significative improvement in treatments, however, besides recent developments in technologies like drug delivery, radiation and chemo therapies, surgery is still pointed as the most effective technique for solid cancers. When used as a single treatment, surgery cures

more patients than any other individual form of cancer therapy since it is assured that 100% of the excised cells are killed, what introduces in most cases a big shrinkage in tumor size [25]. Nevertheless, is not always possible to adopt the surgical intervention due to some cancers location or other restrictions. In those cases, the most widespread approach chemotherapy. Therefore a focus on this technique and the available drugs will be done in the following paragraphs.

Chemotherapy is defined as the use of drugs (usually cytotoxic agents) to treat cancer [26]. It is has been used since 1500s, initially administering heavy metals to the patients and causing severe toxicity and low efficacy. Since then, more effective chemotherapy drugs were studied and commercially available for use as cure, prevention and palliation of a wide range of cancers. Most chemotherapy drugs interfere either with the synthesis of DNA, RNA or proteins.

Antineoplastic agents are classified according to their way of action and the phase of the cell cycle on which they act. If they are specific to a certain cell cycle phase their denomination is cell-cycle specific agents [27][15][28].

### 1.2.1 Cell cycle-specific agents

#### *1.2.1.1 Antimetabolites*

These agents are synthesized to mimic natural metabolites, purines, pyrimidines or folates involved on the DNA synthesis. Their action occurs on the S-phase of the cell cycle and is more effective on high rate growing tumors. Some drugs categorized as antimetabolites are capecitabine, gemcitabine, methotrexate and 5-fluorouracil (5-FU).

#### *1.2.1.2 Mitotic Inhibitors*

They act by causing metaphase arrest. Mitotic inhibitors have activity in G2 and S phase, but are most known as M-phase active. Amongst these drugs are vinca alkaloids and taxanes.

### 1.2.2 Cell cycle-nonspecific agents

This is the denomination for antineoplastic drugs that are active through all the cell cycle process. These drugs affect the DNA and do not have specificity to cells in the dividing process.

#### *1.2.2.1 Alkylating agents*

These agents alter DNA structure by a process known as alkylation. The alkylation process leads to the destruction of DNA template, causing cell lysis in last instance. Cisplatin, carboplatin and Thiotepa are some of the drugs with these properties.

#### *1.2.2.2 Nitrosoureas*

These are lipid-soluble drugs that cross blood-brain barrier and destroy DNA by alkylation process. Some of the drugs being part of this group are lomustine, carmustine and streptozocin.

### 1.2.3 Antitumor antibiotics

Most of antitumor antibiotics were isolated from *Streptomyces* bacteria. These drugs act on DNA-directed RNA synthesis and create toxic oxygen-free radicals what will cause DNA strand breaks. Doxorubicin, daunorubicin and mitomycin-C are part of this group of antineoplastic drugs.

### 1.2.4 Hormones and hormone antagonists

These drugs act by changing the cellular environment and the membrane permeability in a way that affects tumor growth. These drugs antagonize and block natural substances that stimulate tumor growth. Drugs that fit into this group are, for instance, the artificial synthesized sexual hormones.

## 1.3 5-Fluorouracil and 5-fluorouracil-acetic acid

5-fluorouracil is well-established chemotherapy drug in clinical use for around 50 years now [6], mainly prescripted for the treatment of colorectal, breast and aero digestive track cancers [29].

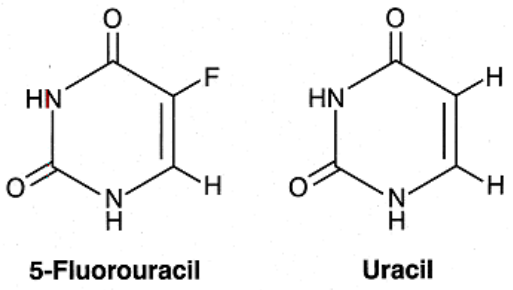


Figure 2: 5-FU and Uracil molecules. These two molecules differ only on the atom linked to $C_5$, where 5-FU has the F and Uracil an H atom. [146]

This drug is a fluoropyrimidine, with a cytotoxicity mechanism attributed to the misincorporation of fluoronocleotides into RNA and DNA and to the inhibition of the nucleotide synthetic enzyme thymidylate synthase [1] (TS). TS is responsible for the conversion of deoxyuridine monophosphate (dUMP) to deoxythymidine monophosphate (dTMP). The TS inhibition results in a decreased concentration of dTMP and subsequently leads to a lack of deoxythymidine triphosphate (dTTP) since dTTP is synthesized from dTMP [29].

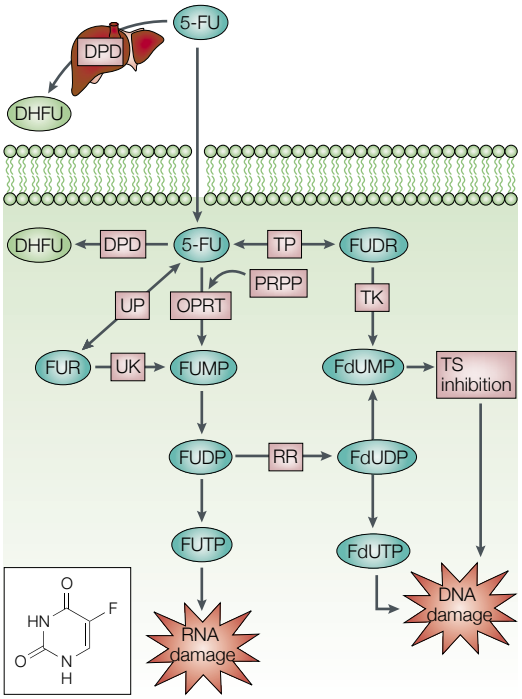


Figure 3: 5-Fluorouracil metabolism. [29]

5-FU is itself a prodrug that has to be converted to fluorodeoxyuridine monophosphate (5-FdUMP), fluorodeoxyuridine triphosphate (FdUTP) and fluorouridine triphosphate (FUTP) – the complete metabolic chain of 5-FU inside the body can be seen in Figure 3.

One mechanism for 5-FU action involves DNA polymerase mediated incorporation of dUTP and 5-F-dUTP into genomic DNA leading to U/A, 5-FU/A, or 5-FU/G base pairs [30].

RNA function is affected through the metabolic conversion of 5-FU in fluorou-uridine (FUTP), which is incorporated into RNA [29].

Only 1 to 3% of the administered doses of 5-FU were found as part of cytotoxic metabolites and more than 80% is fastly degraded. The remaining 19 to 17% 5-FU is excreted in the urine, what will decrease 5-FU antineoplastic activity [31]. Its plasma half-life (t ½) has been reported as being 10 to 20 minutes. DPD is an enzyme essential for the control of 5-FU toxicity since it converts 5-FU to 5-fluorodihydrouracil (FDHU). FDHU is then metabolized to 5-fluoro-b-alanine, which is later excreted in the urine. Patients with deficit in DPD were reported to suffer an increased risk of toxicity [31].

5-FU is one of the phase-specific cytotoxic agents which is more effective in the S phase of the cell cycle, therefore, the longer its plasma half-life, the highest its cytotoxicity.

[1] Thymidylate synthase is an essential enzyme in regulation of DNA replication. Impairments in this enzyme can cause abnormalities like chromosome breakage and exchange, genetic recombination, etc. It has a much higher activity in rapidly proliferating cells than in noncycling cells. [145]

Due to the small size of 5-FU molecule, which makes it capable of penetrating into almost all tissues leading to accumulation through the whole body. This non-selective accumulation contributes the worsen the side effects since healthy cells have contact to 5-FU as well [11].

Considering 5-FU severe side effects, namely myelosuppression and gastrointestinal toxicity [6], many efforts have been done to reduce its toxicity and also to improve its shortcoming pharmacokinetics. Fast body clearance is an issue associated not only to 5-Fluorouracil but also with other widespread drugs, some used in cancer therapy as well. This leads to higher doses treatments applied to patients, which in its turn leads to more severe side effects.

As an attempt to improve 5-FU antitumor activity and reduce side effects, Tada [8] added an acetic acid group to 5-FU having by result a 5-fluorouracil acetate . This molecule modification creates a free group that can be accessed to bind FUAc to proteins. Pure 5-FU has no functional group compatible with protein high affinity binding [10]. Bertucci et al found that 5-FU binds to native human serum albumin with low affinity and low specificity [5].

Based on previous works of Baker and Cheda (1965) and Tada (1975), where an acetic acid group was introduced into the $N^1$ position of 5-FU in order to try an improvement of its antitumor activity, Chung et al. [10] synthesized fluorouracil acetic acid-human serum albumin conjugates and investigated the pharmacokinetics of 5-FU after intravenous infusion of the conjugates. FUAc was chosen due to its carboxylic group, what makes a conjugation with HSA possible. Their results demonstrated that FU rather than FUAC was released from the conjugates in vivo, which indicated that FUAc and polymer conjugates could release pure 5-FU [10].

### 1.3.1 Targeted drug delivery

Conventional chemotherapy drugs are distributed in a non-specific way through the whole body, though its cytotoxicity will be exerted both on healthy and tumor cells. This lack of specificity is a limiting factor since the drug dose achieved in the tumor cannot be as high as desirable in order to protect healthy cells and tissues.

A new approach to chemotherapy started in the last decades, as a try to overcome or at least minimize this drawback of chemotherapy [32]. Based on the research done in the last decades on tumor molecular and cellular environment scientists started to develop targeted delivery of drugs, which, at the same time aim to prolong plasma t ½ of the native drug [33]. Drugs are to be released inside or in the vicinity of the tumor, therefore reducing systemic toxicity and

increasing the drug concentration in the tumor [34]. An ideal molecule for drug delivery should have some characteristics like a relatively high loading capacity for the active substance, to be kept in the proximity of the tumor by some process, not trigger an immunologic response by the body, do not cause adverse effects by itself and have a good biodegradability [33].

Several biological and synthetic substances had been use for targeted drug delivery, most of them filling the requirements referred in the last paragraph. Substances like PLGA, interferin, carbon nanotubes, viruses, liposomes, dendrimers and albumin are in the group of the substances already reported as being suitable as a drug carrier [32][35].

## 1.4 Human Serum Albumin (HSA)

Albumin, a protein of 66478 Da and 585 amino acids, is the most abundant of the blood proteins, with a concentration of around 35-50 mg/mL [19]. It is estimated that a human has about 350g of this protein in total, divided by the blood (150g) and the extravascular space (200g) and having an average half-life of 19 days. HSA contains a single Trp residue at position 214; Met, Gly, and Ile residues are low however Cys, Leu, Glu, and Lys are abundant. The large number of ionized residues gives to HSA a high total charge what enhance its solubility [36]. Around 14g of this protein are catabolized every day by a healthy person and replaced by new albumin, which is synthesized by hepatocytes and about 15mg are lost by the kidneys.

This serum protein can also leave the capillary system (by transcytosis) and previous works showed that during the HSA half-life it runs through 15 000 whole circulation circuits plus about 15 trips to extracellular space, returning back to systemic circulation by lymphatic system [18]. Among several proteins to which drugs can bind once in the circulating blood, albumin is predominantly involved due to its small size and abundance [19]. Albumin is also described as a facilitator for endothelial transcytosis of plasma constituents linked to it to the extravascular space. That starts by the binding of albumin to a cell surface receptor, which leads to formation of transcytotic vesicles by cell membrane invagination [37]. Upon entering the tumor interstitium, the accumulation of albumin is possibly facilitated by SPARC (Secreted Protein, Acidic and Rich in Cysteine), which has binding affinity to albumin and significant homology to gp60, also known as albondin. Gp-60 binds to caveolin-1 (intracellular protein) and transcytotic vesicles are formed (caveolae) [38]. The over-expression of SPARC (or osteonectin) as a key modulator is associated with increased tumor invasion, metastasis and poor prognosis in multiple tumor types [39]. Maeda et al studied the intratumor accumulation of different proteins in solid rat tumors, showing that serum albumin is one of the proteins which the accumulation is more accentuated [2]. Powell et al [40] studied the influence of

estrogen and serum albumin on the proliferation of MDA-MB-231, MCF-7 and T-47D cells. Their work suggests that both a membrane estrogen receptor and a membrane albumin-binding protein (mABP) are involved on this process. The N-terminal part of HSA was associated with the protein inhibitory activity on MCF-7 and T-47D cell lines. MDA-MB-231 suffered no inhibitory effect and it was associated with the lack of mABP expression.

Furthermore, it is a natural carrier of hydrophobic molecules (such as vitamins, hormones and other plasma constituents) and has favorable noncovalent binding characteristics [37]. Lysine residues represent one of the most reactive groups in albumin. HSA has 59 lysine residues [41][42][43].

## 1.5 Albumin and therapeutics

Human serum albumin is a widely used treatment nowadays for several diseases, for instance, shock, burns, trauma, acute respiratory distress syndrome, chronic liver disease, etc. Other applications have been developed in the last years, like implantable biomaterials, surgical adhesives and sealants, biochromotography, ligand traping and fusion proteins [36]. Activated cells such as tumor or inflammatory cells were reported to metabolize albumin in order to cover their increased need for amino acids and energy. HSA can also help to adjust blood pH since it contains a high percentage of acidic (16,8%) and basic (16,9%) amino acids [44].

Recently FDA approved a particle of albumin-binded Paclitaxel under the commercial designation of Abraxane® (Celgene Corporation), which is currently being administered as a first-line treatment to metastic adenocarcinoma of pancreas in combination with gemcitabine [45]. Abraxane particles have an average diameter of 130nm and after intravenous injection, the albumin-paclitaxel particles quickly dissolve into smaller native albumin-sized (approximately 10nm) complexes, which allow intravenous infusion without the risk of capillary blockage [46]. This formulation made possible the delivery of paclitaxel to tumors with a 4.5-fold increase in its transport across endothelial cells, creating an enhanced intracellular paclitaxel delivery and, consequently, increased activity [47].

The nab-paclitaxel reaches the tumor interstitium through the EPR effect. It is believed that the particles' uptake process is the same described for albumin in section 1.4 and illustrated in Figure 4. The expression of SPARC in vivo experiments led to an improved therapeutic response with nab-paclitaxel when compared to pure paclitaxel. Thus, SPARC could serve as a biomarker for the response to therapy with nab- paclitaxel [47].

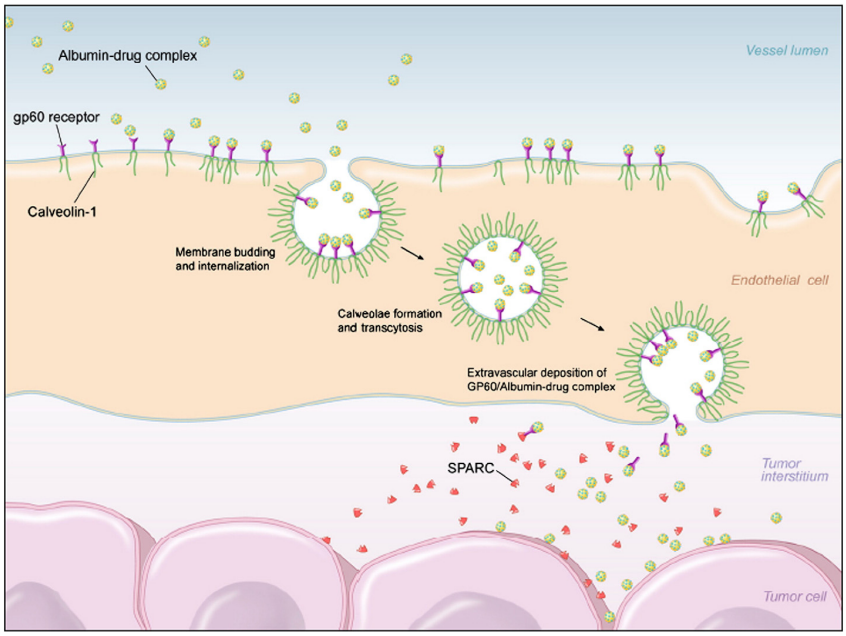


Figure 4 Presumable uptake of albumin-paclitaxel nanoparticles. Possibly, FUAc-HSA walkthrough the same process. Gp60 is a mediator of albumin drug complexes to transcytosis. After the releasing of the complexes in the tumor insterstitium, they bind to SPARC (Secreted Protein, Acid and Riche Cysteine) in the tumor extracellular matrix. [39]

Another conjugate particle with albumin and methotrexate (MTX) was described in several publications and subjected to clinical studies [48][49][50]. They found that MTX-HSA had a delayed effect on the cell cycle compared with MTX and that free MTX was more cytotoxic than MTX-HSA conjugates on a tumor cell line. An interesting fact reported was the plasma half-life of MTX-HSA, estimated to be up to 3 weeks, contrasting with pure MTX plasma half-life of up to 24 hours. The distribution pattern of these conjugates (1M MTX per HSA) in healthy rats and rats with tumor was indistinguishable from the distribution of native HSA. High tumor accumulation rates for both HSA and the MTX-HSA conjugate were observed (more than 15%) after 72 h in rats with Walker-256 carcinoma.

Chung *et al* [10] tested a FUAc-HSA conjugate in rabbits, however the procedure followed for synthesize the particles was not described. An infusion of FUAc-HSA for 30 minutes was reported to maintain a plasma concentration of 5-FU of 1μg/mL from 3 to 24

hours. Pure 5-FU plasma half-life was of approximately 8 minutes. It was suggested that the releasing of pure 5-FU from the compound was triggered by the breaking of the side chain occurring in the slightly acidic environment in tumors. No 5-FU was detected after the infusion of FUAc. Free FUAc was not detected in rabbits' blood when after infusion of FUAc-HSA.

Koziol *et al* [11] published a work similar to the one described in this thesis, although binding FUAc to Bovine Serum Albumin (BSA) instead of Human Serum Albumin. 12 molecules of FUAc were covalently bound to each BSA molecule and the cytotoxicity of the conjugate was tested with breast carcinoma cell lines (MDA-MB-231 and T-47D). These two cell lines differ in one membrane receptor, the gp60, considered to play a central role in cell uptake of albumin conjugates. The results obtained suggested an influence of this receptor in the conjugate cytotoxicity. For T-47D cell line, the one with gp60 receptor, the reported IC50 value was 88,6μM against 408μM for MDA-MB-231. These two cell lines were also incubated with FITC-BSA for 72 hours and there was an obvious discrepancy in albumin uptake between them when observed under the confocal laser scanning microscope.

## 1.6 Drug discovery procedures

Drugs are, usually, discovered through insights into specific disease processes, unexpected effects of treatments in test and due to new technologies, providing the opportunity of trying a new approach [51].

When a promising compound is identified, researchers should conduct their experiments in order to assess, amongst others variables, to how the drug is absorbed, distributed, metabolized and excreted, its potential benefits and mechanisms of action, side effects, interaction with other drugs and its effectiveness when compared with similar drugs [51]. Once this phase is completed, tests with cells in culture are nowadays quite a wide spread practice. In the case of promising results with the cell culture, animal and clinical trials could be approved in to test further treatment efficiency and side effects.

### 1.6.1 Cell lines

Nowadays, hundreds of cell lines are commercially available. Only The American Type Culture Collection (ATCC) itself, one of the most important cell line suppliers worldwide, currently holds more than 4000 cell lines from 150 species.

When it comes to drug discovery procedures, isolated cell lines play an important role by making possible to evaluate if the tested agent is effective and by enabling access to toxicity

profiles of the drug in a certain tissue. Drug screening in cells represent an important early evaluation insofar as it can stop a drug screening before animal and human tests if *in vitro* results are not enough satisfactory [52].

Cells isolated from a disease site, containing genetic or biochemical abnormalities, alteration in receptors, ion channels and receptor signaling pathways are a particularly useful tool as they provide a preview of particular pathways in a drug action [53].

With anti-cancer drugs being one of the most research-focused areas worldwide, panels of cancer cell lines have been used in order to test the crescent number of novel-developed drugs, namely by The US Cancer Institute (NCI). This American organism, maybe the best known working in this matter, developed in the late 1980s the 60 human tumor cell line anticancer drug screen (NCI60) intended to be a tool to supplant the use of transplantable animal tumors for antitumor drug screenings [54]. MDA-MB-231, MCF-7 and T-47D are included in NCI60 as part of the breast cancer cell lines panel. These are object of numerous published works and therefore very well characterized.

#### 1.6.1.1 Membrane receptors and proteins expressed by the three cell lines

The three breast cancer cell lines (MDA-MB-231, T-47D and MCF-7) were already subject of many publications; therefore it was possible to collect information about the expression of proteins relevant to cells characterization.

It is advocated by several health institutions that breast cancers should be tested for estrogen and progesterone receptors and HER2 as a standard [55][56]. To test cancers for these receptors can make the difference when it comes to choose an adequate treatment. Breast cancers classified as triple negative (negative for estrogen, progesterone and HER2) are often associated with poor prognosis since most drugs are set to target one of those three receptors.

Other receptors have been referred as playing a role in breast cancer characterization and therefore, in a better treatment design. mABP, SPARC and caveolin were reported to be involved on the uptake of albumin and albumin-bound drugs [13]. SPARC and mABP are referred later on this work in a more detailed manner. Calcitonin was referred as involved in cell growth, differentiation and tissue development [57]. The androgen receptor was associated with lower risk of recurrence in patients with all breast cancer types [58]. Breast cancer positive for estrogen receptor was found to be inhibited by glucocorticoids [59]. Referring to prolactin, an excess of this hormone was reported as an indicator of disease progression and poor prognosis [60]. Higher concentrations of the CD133 protein are correlated with increasing in tumor size, metastasis and advanced clinical stage [61].

In Table 1 are listed the receptors and membrane-proteins already referred and the characterization of the three cell lines chosen for this work.

| Cell line | Receptors and membrane-proteins | | | | | | | | | | |
|---|---|---|---|---|---|---|---|---|---|---|---|
| | mABP | SPARC | Calcitonin | Androgen | Estrogen | Progesterone | Glucocorticoid | Prolactin | HER2 | CD133 | Caveolin-1 |
| T-47D | + | - | + | + | + | + | + | + | + | - | reduced |
| MDA-MB-231 | - | - | - | - | - | - | - | + | - | + | low |
| MCF-7 | + | + | + | + | + | + | + | + | - | - | very low |

Table 1: Relevant receptors of T-47D, MDA-MB-231 and MCF-7 cell lines. [62][63][40][64][65]

## 1.7 Motivation – resume of the theoretical background

The antineoplastic drug 5-Fluorouracil is used for treating several types of cancer, namely breast cancer. Its plasma half-life was reported to be approximately 20 minutes, which is a very short period, and its toxicity affects both healthy and tumor cells. HSA is an abundant serum protein with a circulating life of approximately 19 days and benefiting of EPR to achieve tumors interstice. HSA was described to be preferentially accumulated in the tumors vicinity [66][2]. Considering HSA attributes, it appears as a strong candidate for drug targeting vehicle.

However, in order to bind covalently 5-FU to HSA a linker needs to be considered since 5-FU does not have a free reactive group to bind a protein.

Chung *et al* [10] reported the pharmacokinetics of a FUAc-HSA conjugate, however the synthesis process was not clarified. 5-FU was detected in blood for up to 24 hours when rabbits received an infusion with FUAc-HSA conjugates.

Kim et al [9] tested 5-FU release from FUAc-HSA particles in physiological solutions and varying pH and reported a high stability of the conjugate. The percentage of 5-FU released from the particles at a pH of 9 was 1%.

The cytotoxicity power of a FUAc-albumin conjugate in breast cancer cells was published by Koziol et al [11]. The conjugates were synthesized with bovine serum albumin for economical reasons, since it is considerably cheaper and highly similar to the human

protein. FUAc-HSA was reported to cause strong inhibition of cell metabolism mainly in cells with mABP, a membrane protein that is a recognition site for albumin.

Considering these facts, the work reported in this thesis followed the line of the work performed previously by Koziol et al, however substituting BSA for HSA. As the protocol for FUAc-BSA was available and already tested it was decided to follow it for FUAc-HSA synthesis. One more cell line was added to the test panel, another breast cancer cell line positive both for SPARC and mABP (gp60). The concentrations to test in cell culture were also adjusted to lower values to keep concentrations closer to the ones reported for plasma of oncologic patients in clinical treatments.

# 2 Materials and Methods

## 2.1 Materials

In this section will be listed the materials used within this project. Chemical substances and equipment are listed in separate.

### 2.1.1 Equipments and consumables

| Material | Model | Supplier |
|---|---|---|
| Centrifugal filtration tubes | Amicon Ultra-15 Centrifugal Filter Units (30 kDa) | Millipore GmbH |
| Centrifuge | Heraeus Labofuge 400 | Heraeus Instruments GmbH |
| 50 mL centrifugal tube | Red cap, assembled, sterile, non-pyrogenic | Sarstedt AG & Co. |
| Rolling mixer | Assistent RM 5 | Karl Hecht GmbH |
| Laboratory glass material | - | KAVALIERGLASS, a.s. Ltd |
| Magnetic mixer | Hytrel HTR 8068 | Carl Roth GmbH |
| Digital pH meter | Jenco model 60 | Jenco International |
| Cell culture flasks | 75 $cm^2$ Growth surface | TPP Techno Plastic Products |
| Centrifuge | Heraeus Labofuge 400 | Heraeus Instruments GmbH |
| 50 mL centrifugal tube | Red cap, assembled, sterile, non-pyrogenic | Sarstedt AG & Co. |
| Clean bench | Thermo HERAsafe | Heraeus Instruments GmbH |

| | | |
|---|---|---|
| $CO_2$ Incubator | BINDER CB Series | BINDER GmbH |
| Automatic pipette | Automatic-Sarpette | Sarstedt AG & Co. |
| Serological pipettes (5, 10 and 25 mL) | Individual wrapped, sterile | Corning GmbH |
| Counting chamber | Nebauer Improved | LO Laboroptik |
| Scale | Explorer Ohaus | Ohaus Europe GmbH |
| Inverted microscope | Leica Leitz DM IL | Leica Mikrosysteme Vertrieb GmbH |
| 8 channel pipettor | 20-200 µL | VWR GmbH |
| Microplate Spectrophotometer | Power wave 340 | Bio-Tek |
| BD Falconcell strainer | 40 µm Nylon | Corning GmbH |
| Cryopresrvation cell tubes | CryoPure Tube, 1.6 mL white | Sarstedt AG & Co. |
| 96 well plates | Falcon, flat bottom, low evaporation | Corning GmbH |
| 24 well plates | Costar, flat bottom | Corning GmbH |
| Microscopy cell culture plates | Ibidi µ-Slide 8 well | Ibidi GmbH |
| Syringe Sterile Filter 0.24µm | MiniSart | Sartorius AG |
| Vortex | Vortex-Genie 2 | Scientific Industries |
| Water bath | Lauda MS | Lauda Dr. R. Wobser GmbH |
| MALDI-TOF analyzer | Bruker Autoflex Speed | Bruker equipment (Rheinstetten, Germany |
| CD-Spectrometer | JASCO J-720 Japan (Tokyo, Japan) | JASCO Labor-und Datentechnik GmbH |

| | | |
|---|---|---|
| Confocal laser scanning microscope | ZeissLSM 510 meta | Zeiss MicroImaging GmbH, Jena, Germany |
| NanoDrop Spectrophotometer | NanoDrop 1000 | Thermo Scientific |

Table 2: Equipment and consumables used for the work in this project

### 2.1.2 Chemicals and reagents

All the substances used during this work are listed below, together with its molecular weight and the supplier.

| Substance | Molecular Weight (Da) | Supplier |
|---|---|---|
| 5-Fluorouracil >99% (HPLC) powder | 130,08 | Sigma Aldrich GmbH |
| Albumin from Human serum, 96-99%, Lyophilized | 66478 | Sigma Aldrich GmbH |
| Phosphate Buffered Saline (PBS), powder, pH 7.4 | - | Sigma Aldrich GmbH |
| Ampuwa Water, steril and endotoxin free | - | Fresenius Kabi Deutschland GmbH |
| FUAc (previously synthesized) | 188,1 | - |
| Sodium chloride (NaCl) | 58,44 | Merck KgaA |
| Sodium Hidroxide (NaOH) | 39,99 | Merck KgaA |
| 2-(N-Morpholino) ethanesulfonic acid (MES) | 195,2 | Sigma Aldrich GmbH |
| 1-ethyl-3-(3-dimethylaminopropyl)carbodiimide hydrochloride (EDC) | 191,7 | Sigma Aldrich GmbH |

| | | |
|---|---|---|
| *N*-hydroxysuccinimide (NHS) | 115,1 | Sigma Aldrich GmbH |
| GIBCO Fetal Bovine Serum | - | Life Technologies GmbH |
| Penicillin/Streptomycin (PenStrep, 10.000 Units/mL, 10 mg/mL) | 334,39/581,57 | Life Technologies GmbH |
| Roswell Park Memorial Institute Medium (GIBCO RPMI 1640 Medium) GlutaMAX | - | Life Technologies GmbH |
| Trypsin (0,25 % + EDTA (1x) with Phenol red) | - | Life Technologies GmbH |
| Chloroacetic Acid ($C_2H_3ClO_2$) | 94,5 | J.T. Baker |
| Eagle's Minimum Essential Medium (EMEM) | - | American Type Culture Collection (ATCC), LGC Standards GmbH |
| Human recombinant insulin 0.5 mg/mL, 5mL bottle ($C_{254}H_{377}N_{65}O_{75}S_6$) | 5808 | Biochrom AG |
| Dimethylsulfoxid (DMSO, $C_2H_6OS$) 99.5% | 78,13 | Carl Roth GmbH |
| Acetic Acid 99-100% ($C_2H_4O_2$) | 60,05 | J.T. Baker |
| Hydrochloric Acid Fuming 37% (HCl) | 36,46 | Merck |
| Potassium Chloride (KCl) | 74,55 | VEB Jenapharm |
| 3-(4,5-Dimethylthiazol-2-yl)-2,5-Diphenyltetrazoliumbromid (MTT,$C_{18}H_{16}BrN_5S$) | 414,32 | Sigma Aldrich GmbH |
| Sodium Hydrogen carbonate ($NaHCO_3$) | 84,01 | Merck KgaA |
| Hydrochloric Acid 37% (HCl) | 36,46 | J.T. Baker |

| | | |
|---|---|---|
| Sodium dodecyl sulfate (SDS, $C_{12}H_{25}NaO_4S$) | 288,38 | Sigma Aldrich GmbH |
| Dihydrorhodamine 123 | 346,38 | Glycotope Biotechnology |
| Trypan Blue (0,25% [w/v], $C_{34}H_{28}N_6O_{14}S_4$) | 872,88 | BioChrom AG |

Table 3: Chemicals and reagentes used during the work in this project

The formulation of solutions prepared in the laboratory is described in the table below.

| Solution | Formulation |
|---|---|
| Culture media for MDA-MB-231 and T-47D cell lines | RPMI 1640, 10% FBS, 1% PenStrep |
| Culture media for MCF-7 | EMEM, 10% FBS, 1% PenStrep, 0,01 mg/mL human recombinant insulin |
| MTT stock solution | 1 mg/mL MTT powder in RPMI 1640 or EMEM (depending on the cell line being used) |
| Solubilization solution for MTT | 0,1 g/mL SDS, 0,6% Acetic Acid, 99,4% SDS |

Table 4: Solutions prepared in the laboratory and its formulation

For DNA extraction from cultured cells, a commercial kit from Qiagen® was purchased. Its commercial designation is QIAamp® DNA Mini and Blood Mini kit.

### 2.1.3 Cell Lines

From the 3 cell lines kept in culture, T-47D and MDA-MB-231 were obtained from other research groups working at Charité (MDA-MB-231 from PD Dr. Diana Lüftner working at Department of Medicine - Division of Hematology, Oncology and Tumor Immunology; T-47D from Prof. Dr. Kurt Possinger from Medical Clinic of Oncology and Hematology) and MCF-7 was purchased from ATCC.

All of them were isolated breast cancers cells and grow as adherent in culture.

#### 2.1.3.1 T-47D cell line

This cell line was isolated from a 54-year-old female, from the mammary gland with ductal carcinoma. It is an epithelial cell type, hypotriploid, derived from a pleural effusion in a metastic site.[62]

#### 2.1.3.2 MDA-MB-231 cell line

This is an epithelial cell line, isolated from 51-year-old Caucasian female mammary gland with adenocarcinoma. The cells were collected in a pleural effusion derived from metastic site. Cells are aneuploid female. [62]

#### 2.1.3.3 MCF-7 cell line

Epithelial cells isolated from mammary gland with adenocarcinoma of a 69 year old Caucasian woman. Collected from a pleural effusion derived from a metastic site. [62]

## 2.2 Methods

In this section are described the methods and techniques performed within this work. The first FUAc synthesis was performed by Dr. Torsten Sievers and later repeated by me and Michael Koziol according to the protocol developed by Dr. Sievers. The first FUAc-HSA synthesis was performed by Michael Koziol and Dr. Yu Xiong. NMR spectroscopy was performed by Dr. Torsten Sievers and MALDI-TOF by Dr. Felix Wojcik. The CD-Spectroscopy was performed by me and Heike Nikolenko. All the procedures related with cell culture and cytotoxicity assays (MTT and cell counting) and DNA extraction were performed by me, with the help of Kathrin Smuda whenever necessary. Kathrin Smuda and Michael Koziol introduced me o these procedures. Dr. Radostina Georgieva and I performed CLSM procedures. Every step of this work was discussed within the workgroup in order to find the most suitable way to proceed.

### 2.2.1 FUAc synthesis

FUAc reaction was adapted from previous works of Baker and Cheda (1965) and Tada (1975), where an acetic acid group was introduced into the $N^1$ position of 5-FU (see Figure 5).

FUAc firstly used in this work was synthesized by Michael Koziol and Torsten Sievers as described in Koziol et al. [11].

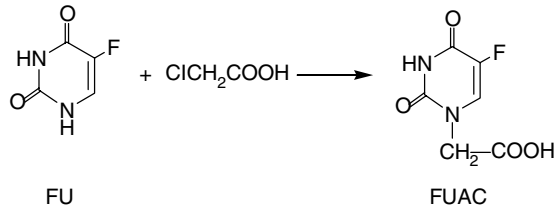


Figure 5 Reaction of 5-FU to FUAc [147]

A new charge of FUAc was synthesized by June at Biotechnology laboratory from the Institute of Transfusion Medicine of Charité, according to the procedure described by Tada [8] and adapted as described at Koziol et al [11]. All procedures were performed at room temperature and most steps took place in the fume hood due to the possible occurrence of harmful fumes. Chemicals were used as provided by suppliers (see at Materials section) with no further purification.

First, 9,76g of 5-Fluorouracil (0,157 g/mL) were dissolved in 62mL of water containing 8,41mg of KOH (0,1356 mg/mL) (solution 1). 7,05mg of chloroacetic acid were dissolved in 28,2mL (0,25 mg/mL) of water and poured into the 5-FU solution (solution 1) and stirred for 15 minutes. A white precipitate was formed and was solved by adding enough potassium hydroxide (KOH) for the precipitate to solve, what happened around pH 10. Mixture was again stirred for 15 minutes, keeping pH at 10. The solution was then heated to 100°C and boiled under reflux for 2 and a half hours. Solution was then cooled down to room temperature and pH adjusted to 2 by the addition of concentrated hydrochloric acid. Then, the solution was kept at 4°C for 1 hour and pH was readjusted to 2. After setting the pH, solution was left at 4°C for 24 hours to allow the crystallization of FUAc.

After the 24 hours, the tube was centrifuged to separate FUAc needles from the supernatant. The FUAc needles were then solved in saturated aqueous $NaHCO_3$, in the necessary volume to obtain a clear solution.

Afterwards, the remaining supernatants were left to crystalize more 2 times, at 4°C and with pH adjusted to 2 with hydrochloric acid, followed by centrifugation to separate needles and supernatant. The last step was to dry FUAc, what was done with the help of a vacuum bomb, at the pressure of approximately 0.1mbar at room temperature. The product obtained from the 3 crystallizations was dried separately in order to confirm their possible different conformation later, by NMR.

### 2.2.2 Nuclear Magnetic Resonance Spectroscopy

Nuclear magnetic resonance is one of the most important tools available to characterize molecules. It gives information about relative positions and numbers of spin active nuclei and makes it possible to identify the structure of a compound.

In dependence on the applied magnetic field and the used resonance frequencies you can measure the spectra of different atoms present in the molecules.

There are several NMR different spectra, namely $^{1}$H-NMR, $^{13}$C-NMR, $^{19}$F-NMR and $^{31}$P-NMR. These referred spectra correspond to the NMR record of different atoms present in the molecules that constitute the material under analysis. These come from different characteristic spin (I) and spin angular momentum that nuclei of some elemental isotope has, and consequently, a magnetic momentum (μ). When applied an external magnetic field (**$B_0$**), nuclei's magnetic moment will be affected by it, resulting in an energy change [67].

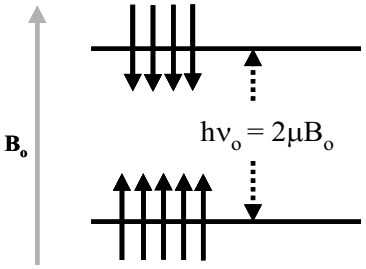


Figure 6: Energy levels for a nucleus with spin ½, in the presence of a magnetic field (**$B_0$**). The top energy level has the nuclear spins aligned in parallel (mI=½) with $B_0$ and the lowest energy level has the spins aligned anti-parallel (mI=-½) with $B_0$. Image adapted from [67]

These so called spin states can have 2I+1 values for a nucleus with spin I, what corresponds to the direction of the angular momentum relative to a z-axis, which is by convention chosen as having the same orientation of the applied magnetic field. When a nuclei has spin of ½ or -½, these corresponds to the magnetic quantum number $m_I$=½ and -½, respectively (Figure 6).

When there is no applied **$B_0$**, the two levels have equal energy, -½γ**$B_0$** for parallel with **$B_0$** and ½γ**$B_0$** for anti-parallel to **$B_0$**, with γ being the gyromagnetic ratio, a property of the nucleus under analysis.

ΔE, the energy separation of 2 levels is described by Bohr's resonance condition: $\Delta E = h\nu_0 = \left(\frac{h}{2\pi}\right)\omega_0$ (Equation 1) and by knowing this and the temperature in Kelvin (T), the Boltzmann relation gives the distribution of

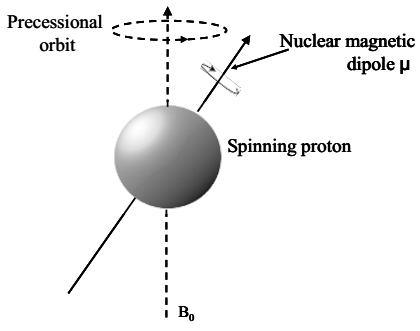


Figure 7: Illustration of the different physical quantities to define the Larmor frequency. [67]

spin population in a sample, with $\kappa$ being the Boltzmann constant, $\upsilon_0$ the Larmor frequency and $h$ the Planck constant:

$$exp\left(-\frac{\Delta E}{\kappa T}\right) = \exp\left(-\frac{h\nu_0}{\kappa T}\right) \approx 1 - \frac{h\nu_0}{\kappa T}$$

Equation 2: Boltzmann relation

Larmor frequency (Figure 7) or the precessional frequency of the nucleus is usually expressed in Hertz and $\omega_0(2\pi\nu_0)$, the angular precessional frequency of the nucleus, is expressed in radians per second. These frequencies depend on both the gyromagnetic ratio ($\gamma$) of the nucleus and $\mathbf{B_0}$.

$\left(\frac{h}{2\pi}\right)\boldsymbol{\omega_0} = \boldsymbol{2\mu B_0}$ Equation 3

so $\boldsymbol{\omega_0} = \boldsymbol{\gamma B_0}$, with $\boldsymbol{\gamma} = \frac{\mu}{I}\left(\frac{h}{2\pi}\right)$ Equation 4

From Equation 3 and Equation 4 it is possible to conclude that the resonance frequency ($\omega_0$) is different for different nuclear spins as the gyromagnetic ratio is different for each spin and it is proportional to the applied magnetic field.

NMR signals are usually detected by means of a receiver coil in the x-y plane, taking the z-axis as defined according to the $\mathbf{B_0}$ orientation. The above theory refers to the quantum mechanical model for nuclei.

In the classical model, the main variable is the net magnetization (**M**) of the macroscopic piece composed by a large number of nuclei. When a magnetic field is applied, the angular momentum of the nucleus will cause a precession around the $B_0$ orientation, with the same nature as described for the nuclei (Figure 7) with angular velocity $\boldsymbol{\omega_0 = -\gamma B_0}$**.**

Nuclear magnetic resonance decoupling is a technique where the analyte is irradiated with a specific frequency to eliminate completely or partially the coupling effect between nuclei. This coupling effect is the effect exerted from one atom to the others in its proximity.

Common NMR spectroscopy spectra are presented as a chemical shift on x-axis vs signal intensity (y-axis). Chemical shift is a measure of how far the registered signal is from a reference signal (usually tetramethylsilane - TMS).

$$\delta(ppm) = \frac{distance\ downfield\ from\ reference\ signal\ (Hz)}{operation\ frequency\ of\ the\ spectrometer\ (MHz)}$$

Equation 5: Chemical shift definition

By distance downfield it means considering signal at higher frequencies [68].

The y-axis, corresponding to signal intensity, is dependent on the number of equivalent nuclei in the analyte at a certain chemical shift. Not all atoms can be detected by NMR-

spectroscopy, only some isotopes generate NMR signals. Among the most common detected isotopes are $^{1}H$, $^{13}C$ and $^{19}F$.

The coupling constant (***J***) is another definition commonly present in NMR-spectroscopy. The J-coupling gives information about the multiplicity (number of peaks), the magnitude and the sign of the coupling. For simple systems like $^{1}H$-$^{1}H$, the multiplicity refers to the number of adjacent and magnetically nonequivalent protons connected to the one that generates the signal. The splitting occurs because each spin interacts with its neighborhood through a mechanism described by the coupling Hamiltonian in Equation 6

$$\mathcal{H}_J = 2\pi J_{ij} \boldsymbol{I}_i . \boldsymbol{I}_j$$

Equation 6: The coupling Hamiltonian

Where i and j are the nuclear spins and $J_{ij}$ is the scalar coupling constant. This is valid only in an isotropic situation. For other situations $J_{ij}$ is not scalar and it is a tensor. A number comes usually associated with J, which gives information about the number of chemical bonds between the two involved spins.

The magnitude of J-coupling provides information about the proximity of the coupling molecule from the other molecule when referring to $^{1}H$-$^{1}H$ coupling. When the interacting nuclei are different, the magnitude of J is related to the nuclear magnetic moment of the coupling isotopes [69][70][68].

Nuclear Magnetic Resonance was performed at Institute for Chemistry of the Humboldt University of Berlin, AG NMR, by Prof. Dr. Clemens Mügge team.

Samples were provided lyophilized in a tube to be dissolved in DMSO-$d_6$ later.

### 2.2.3 FUAc-HSA synthesis

The procedure followed by us to synthesize FUAc-HSA was adapted from the described by Grabarek [12] and was very similar to the recently described process by Koziol *et al* [11], however replacing Bovine Serum Albumin by Human Serum Albumin. The binding procedure of FUAc to HSA was the procedure known as EDC/NHS. It is based on the capacity of EDC to couple carboxyl groups to primary amines. By adding EDC to a carboxyl group the product is an unstable reactive o-acylisourea derivative, which will interact with the amine group of proteins.

NHS works as stabilizing agent for the active ester created by addition of EDC to carboxylic molecule and it will increase the efficiency of EDC-mediated coupling reaction [12][71].

The amount of reagents used was higher than the quantities referred by Koziol *et al* [11] however the molar concentrations were kept the same as described in the same publication.

A buffer solution (6mL PBS and 6mL water) was previously prepared and afterwards 300mg of HSA was dissolved in it (25 mg/mL). This mixture was mixed inside a Falcon tube in the roller mixer for one hour.

300mg of FUAc (25 mg/mL) and 350mg of Sodium Chloride (29,17 mg/mL) were dissolved in 12 mL of water in a glass container. The pH of this solution was then adjusted to 7 using 1M NaOH solution and stirring the mixture in a magnetic mixer. 234mg MES (19,5 mg/mL) were added to the last solution once the pH was adjusted.

600mg EDC (300 mg/mL) and 900mg NHS (450 mg/mL) were dissolved in 2mL of water and immediately poured into the FUAc solution. The ratio between EDC/NHS and FUAc solutions should be close to 1:6 and pH should be then close to 5.2. This solution was stirred for 20 minutes and after this, pH was again adjusted to a value between 7.2 and 7.5 with NaOH 10M solution.

The HSA solution was poured into the FUAc solution (keeping a volume ratio of 7:6) and was stirred for 2 hours.

The following step was the centrifugal filtration, when approximately 10mL were put inside the centrifugal filtering (cut-off 30 kDa) tubes at each time, and the centrifugation was set for 5000x g at 4ºC, for 15 min, with no break. After centrifugation, the supernatant was removed to another tube and 7mL of deionized water were added to the solution left in the filter. This washing step was repeated three times and for each centrifugation the supernatant was saved and frozen for possible posterior analysis.

Once all centrifugation steps were complete, the FUAc-HSA solution was carefully collected from the filtering tube with a micropipette and transferred to a 50mL Falcon tube. FUAc-HSA solution was then frozen at -30°C for 24 hours.

The last step was lyophilisation, what took place for 24 hours. The yielding substance was posteriorly kept at -30°C in a Falcon tube.

### 2.2.4 Matrix-assisted Laser Desorption/ Ionization Time of Flight (MALDI-TOF)

Matrix-assisted Laser Desorption/ Ionization Time of Flight (MALDI-TOF) is a mass spectroscopy technique that uses soft ionization by a short laser pulse, with great utility to analyze biological molecules. The principle of this technique is ionization of compounds without its fragmentation. The substance to be analyzed is, after ionization, mixed and co-crystallised with a photoactive organic acid matrix (like dihydroxyacetonephosphate (DHAP), for instance) that absorbs energy from laser irradiation. Next step is to put the matrix plus analytes in the laser bombardment site and charged analytes will be accelerated into a gas phase subjected to an electric field [72]. A scheme of this procedure is shown in Figure 8.

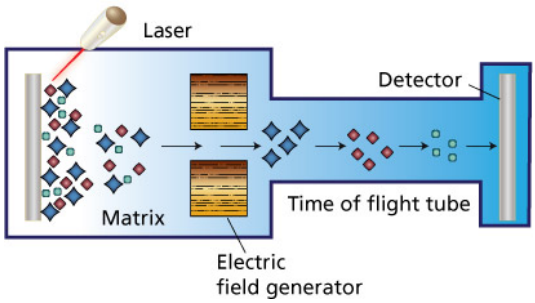


Figure 8 MALDI-TOF principle scheme [148]

Ions travel in a straight and linear direction to detector, on the opposite end of TOF tube. The detector measures particle events as a function of time. Time of flight is proportional to the square root of molecule mass to charge ratio (m/z) and has a mass resolution of 0,03%, approximately.

The time of flight t is given as:

$$t = k\sqrt{\frac{m}{q}}$$

Equation 7: MALDI-TOF unit equation [73]

where $k$ is a proportionality constant representing factors related to the instrument settings and characteristics.

MALDI-TOF spectrum for FUAc-HSA was recorded with an Autoflex Speed, Bruker equipment (Rheinstetten, Germany) in Linear Positive Mode with dihydroxyacetonephosphate (DHAP)-matrix, at Max Planck Institute. We provided samples of HSA and FUAc-HSA (approximately 2mg each) and Felix Wojcik performed the procedure.

### 2.2.5 CD-Spectroscopy

Circular Dichroism-Spectroscopy is a Spectroscopy technique with a great utility in drug discovery [74].

CD-Spectroscopy determines the stereochemistry of chiral drugs and proteins, accessing the absolute configuration of chiral compounds in solution. [74] More specifically, circular dichroism (CD) is the difference in the absorption A of left-handed circularly polarised light (ALCP) and right-handed circularly polarised light (ARCP), so CD can be expressed as ΔA= ALCP – ARCP. It occurs when a molecule contains one or more chiral light-absorbing groups. Ellipcity is another concept connected to CD-spectroscopy. When linearly polarised light pass through a circular dichroic sample it becomes elliptically polarised. This light is not fully circular polarised but has elliptical shape due to the differential absorbance (circular dichroism).

The degree of ellipcity (θ) is defined as the tangent of the ratio of minor to major elliptical axis.

Molar circular dichroism is a common unit used in literature, calculated by the following relation:

$$[\theta] = 100x\theta/(C\times l)$$

Equation 8: molar ellipcity

with C being the analyte in Molar and l the probe cell length in centimetre.

An important use of CD-Spectroscopy is to access the secondary structure of proteins

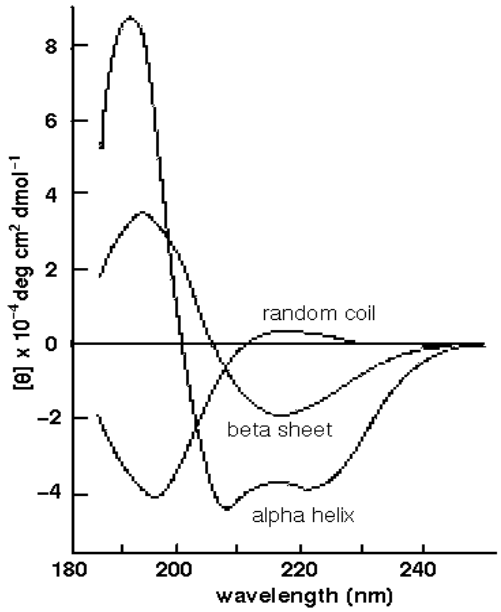


Figure 9: Standard CD-Spectroscopy curves for proteins according to its folding. [149]

and how it can be changed. The signal can be positive or negative depending on whether side-handed is absorbed in a greater extent. This concept is related to the wave nature of light. As above-mentioned, CD-Spectroscopy is widely used to find out secondary structure of proteins, mainly secondary elements of proteins like α-helix and β-sheets. Standard spectra for these cases are seen in Figure 9 [75][76].

The CD-Spectroscopy spectra were recorded with JASKO J-720 Japan (Tokyo, Japan) with the following settings: band width 1.0nm, response 1 sec, measurement range 260–183nm, data pitch 0.1nm, scanning speed 100nm $min^{-1}$, accumulation 10, cell length 0.1 cm, cuvette: quartz). Solutions of 2μM (of HSA and FUAc-HSA) were prepared, with $H_2O$ and 10 x $10^{-3}$ M phosphate/ 154 x $10^{-3}$ NaF buffer as solvents. The choice of Phosphate/ NaF buffer was due to its similarity with physiological solutions.

CD-Spectroscopy acquisition took place at the Leibniz-Institut für Molekulare Pharmakologie im Forschungsverbund Berlin. Dr. Margitta Dathe kindly provided access to equipment and the lab technician, Heike Nikolenko, guided the procedure.

### 2.2.6 Cell culture procedures

Cell culture methods are performed in accordance to the experience of the work group members and following the suppliers' instructions (Life Technologies for reagents and ATCC for cell lines). Cells in culture are maintained in 75 $cm^2$ culture flasks, at 37°C in a controlled atmosphere with 5% $CO_2$, with 10 mL of RPMI 1640 GLUTAMAX medium supplemented with 10% of FBS plus 1% of PenStrep (MDA-MB-231 and T-47D) and 10mL of EMEM supplemented with 0,01mg/ml human recombinant insulin, 10% FBS and 1% PenStrep (for MCF-7). Cells are controlled 3 times per week, usually Monday, Wednesday and Friday. When checked, if the confluence is between 90 to 100%, cells are passaged to a new flask, if not, medium inside the flask is replaced by 10 mL of fresh medium.

Passaging procedure consists on removing cell medium; wash the cells with 1 mL of trypsin to remove remain medium. The following step is to add 2 to 3 mL of trypsin to detach the cells. They are incubated with Trypsin for about 12 minutes. Once detached, fresh medium is put into the flask (the quantity of medium has to be double the previously added quantity of trypsin) and cells are resuspended by repeated pipetting. After the resuspension, cells are strained through a cell strain in order to obtain single cell suspension.

The last step is to seed cells in a new flask, deciding the splitting rate. Usually a rate of 1:15 is enough for the cells to get completely confluent within a convenient time period.

### 2.2.7 Cell counting procedure

The counting procedure starts by collecting 10µL of cell suspension and filling the space between the glass cover and the chamber. As the counting chamber has 2 couting grids that can be used independently, one was chosen and the correspondent space filled. Pipette tip was placed close the glass cover edge and in the centre of Neubauer chamber. Liquid sample should then enter the chamber by capillarity, paying attention to the possible bubble formation, in that case this proccedure should be repeated.

Once the chamber was prepared was placed under the microscope to count the cells. As seen in Figure 10, grids are divided in nine biggest squares, five divided in smaller areas and, the ones located at chamber corners, divided in twelve squares. The cells found on the big four corner squares were then counted, considereing only those toucing upper and left limits, as seen in Figure 10. After counting all cells from the four squares, an average number was calculated and concentration was calculated according to Equation 9.

$$cell\ concentration = \frac{average\ number\ of\ counted\ cells \times 10000}{Number\ of\ squares\ considered}$$

Equation 9: calculation of cell concentration using Neubauer counting chamber

Depending on the following procedure, further dilutions were then calculated [77][78].

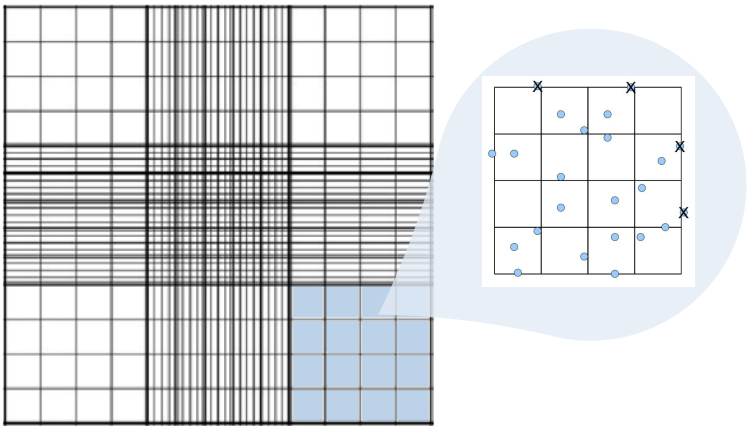

Figure 10: Neubauer counting chamber. The right image shows which cells should be taken into account considering its position in the grid. [150][151]

### 2.2.8 MTT assay

MTT is one of the most widely used cell viability tests due to its reliability and the ease to implementation. The use of a tetrazolium dye was first reported in the early 1980s. It was the first homogeneous cell viability assay developed for a 96-well plate format and suitable for high throughput screening, which strongly contributed for it to be a widely spread assay [79].

MTT substrate should be prepared in a physiological solution and incubated with the cells, such that viable cells convert MTT to formazan. Dead cells have no ability to convert MTT into formazan (Figure 11). Even not being a consensual matter, it is generally accepted that NADH is the responsible for most MTT reduction, transferring electrons to MTT. Is also supported by cellular studies that MTT reduction is not only associated with mitochondria activity but also with cytoplasma and lysosome, endosome and plasma membranes [80].

After MTT reduction, 1-(4,5-dimethylthiazol-2-yl)-3,5-diphenylformazan (insoluble purple-color product) accumulates inside the cells as well as near the cells surface and in culture media. Before reading the absorbance with a spectrophotometer, this insoluble product has to be solubilized in order to have a homogeneous solution. Adding a detergent and an organic solvent can fulfill this requirements [81][82].

The interpretation of results is based on the fact that the more metabolic active cells are in a well, higher is the absorbance value [83].

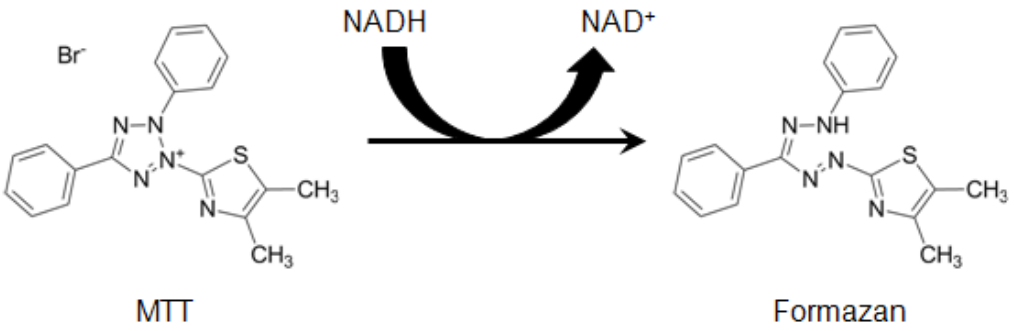


Figure 11: MTT and Formazan molecule [81].

This cell viability assay was performed based on previous team experience and literature descriptions.

First, 5000 cells were seeded in each well of a 96 well plate, except the 6 wells reserved for the blank control. Cell number was calculated by counting cell number in suspension solution with the Neubauer cell counting chamber, as described above.

Cells were left 24 hours to attach to the culture plates in the incubator with 100 µL of media in each well. After the first 24 hours, the media was exchanged for media containing the drugs under study and albumin (5-FU, FUAc, FUAc-HSA and HSA). To each column of the 96 well plates, a solution with different concentration of the tested substances was added; being the concentrations used 1, 5, 10, 50, 100 and 500 µM (each concentration was tested 7 fold and controls 6 fold due to inherent restraints of the culture plate). Concentration of FUAc-

HSA was adjusted to have the same concentration of FUAc as it was in the pure FUAc. FUAc-HSA concentration was calculated according to Equation 10.

$$FUAc - HSA\ concentration = \frac{FUAc\ concentration}{No\ of\ FUAc\ molecules\ per\ HSA\ molecule}$$

Equation 10: FUAc-HSA concentration calculation for experiments

Once the substances were in contact with cells, a MTT test was performed every 24 hours until the 96 hours.

The first step of MTT assay was to remove the 200µL of medium inside each well, wash the well with 100µL of PBS and add the MTT sterile solution to each well (1 mg $mL^{-1}$ in the adequate cell culture media). The plate was then left for 2 hours in the incubator with controlled environment (5% $CO_2$ and 37ºC).

After these 2 hours, MTT solution was removed and 100µL of a solubilization solution was added (99.4% DMSO, 0.6% acetic acid and 0,1 g $mL^{-1}$ SDS). The plate was then agitated in the dark (involved in silver foil) for 15 minutes and, finally read in the plate spectrophotometer at a wavelength of 570 nm [79]. The spectrophotometer (or ELISA reader) software is able to compute the absorbance of each well at 570 nm.

### 2.2.9 Trypan Blue exclusion assay

Trypan Blue is a vital stain used to color dead cells membrane. This can be explained due to membrane selective transport characteristic of healthy cells, therefore when a cell is viable trypan blue cannot pass through its membrane. A characteristic image of trypan blue exclusion in a counting chamber is showed at Figure 12.

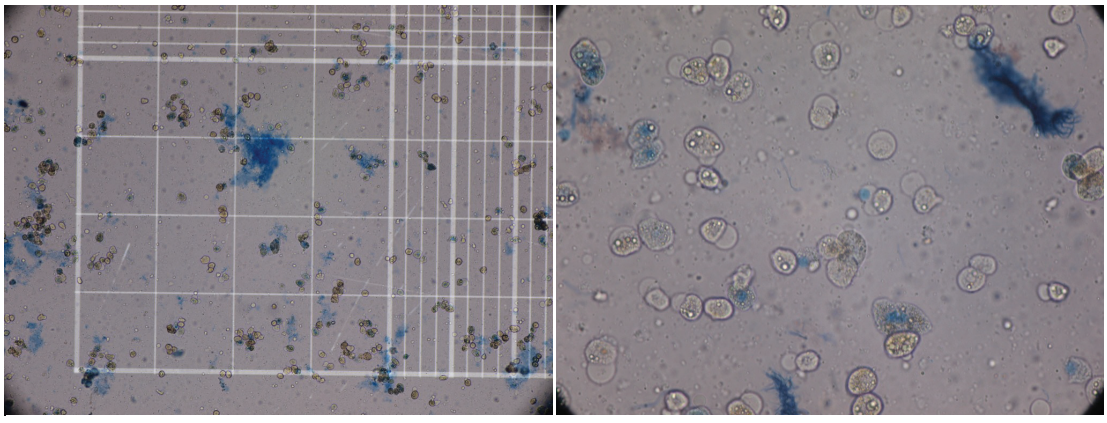

Figure 12: Example of a trypan blue assay, with viable (not stained in blue) and dead cells (stained in blue). Dead cells are permeable to trypan blue. [152]

For Trypan Blue exclusion assay, cells were seeded in 24 well plates with 8 x $10^4$ cells per well (or 1,6 x $10^5$ cells/mL, considering that the seeding volume was 500µL).

24 hours later, media in the wells was replaced by media containing the drugs under test, except for one well were cells were left in normal growing conditions for control (with normal culture media). Cells were then incubated for 72 hours.

After the referred incubation, media in the wells was removed to an eppendorf of 2,5mL, separately, and cells were trypsinized with 0,5mL Trypsin + EDTA for 5 minutes. Once detached, 1mL of culture media was added to inactivate trypsin and the well content was transferred to another eppendorf tube.

From each tube, 50µL were taken and put into another eppendorf tube. 50µL of trypan blue was then added. The mixture was pipetted up and down in order mix it.

Solutions were then checked on a hemocytometer, repeating the counting in 3 grids for every solution [84].

### 2.2.10 Confocal Laser Scanning Microscopy

The confocal laser microscopy technique provides high-resolution optical images with the possibility to depth section select. 3-D images can be obtained by reconstruction made by computer of point-by-point acquisition. CLSM makes possible to image interior of opaque specimens due to lasers usage. A laser beam passes through an aperture and is focused into a

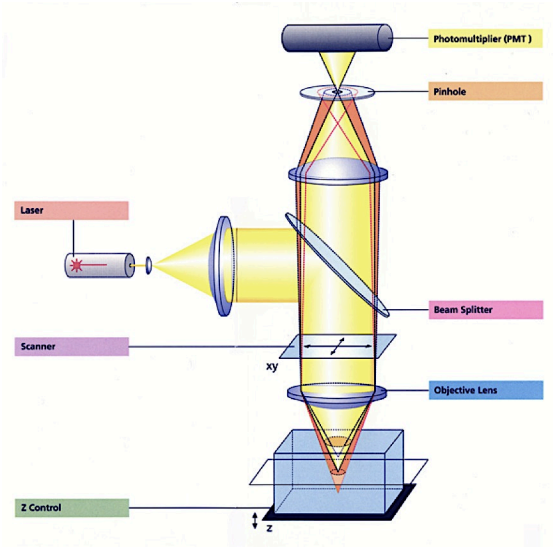


Figure 13: Confocal Laser Scanning Microscopy scheme. [86]

volume of the analyzed probe by an objective lens. Reflected and scattered laser light and possible fluorescence from probe is then collected by the objective lens. The following step is

the separation by the beam splitter of signal corresponding of excitation from emitted light. After crossing the pinhole, light is detected by a photomultiplier, converting light into electric signal in order to be processed by a computer. [85][86]

Cell images from Confocal Laser Scanning Microscopy (CLSM) were obtained to assess cells metabolism, what was achieved by the use of Dihydrorhodamine 123

The fluorogenic probe, DHR-123, is membrane permeable probe, of widely spread usage to detect reactive oxygen species (ROS). The referred ROS are generated inside the cell during proliferation and differentiation processes [87], therefore its existence in the cell is associated with an active cell. DHR-123 has been reported as useful in recognition of active cells by fluorescence-detection methods, such as CLSM [88][89].

For this procedure, five thousand cells were seeded in each well of a 15 µ-Slide 8 well Ibidi plate. Cells were seeded with 200µL of media and incubated for 24 hours. Ended this period, media was changed and media with drugs was added (200µL). Total incubation time with under test drugs was 72 hours. DHR-123 wad added to cells in culture 24 hours before microscopy.

Then, cells were incubated for more 72 hours and, finally, analyzed under the microscope.

The images showed at results chapter were obtained with the confocal laser scanning microscope referred in section 3.3.4, which is equipped with 100x oil immersion objective and numerical aperture 1.3. Images of the samples were prepared applying excitation of DHR-123 at 488nm. The fluorescence was recorded using along-pass filter of 505 nm.

### 2.2.11 4.2.11 DNA extraction and purification

For DNA extraction from cultured cells the first step was to seed cells in 6 well plates, 0.5 x $10^6$ cells per well. Seeding volume was 1mL. 24 hours after, media with 5-FU and FUAc was added, with the concentration of 500µM. 2mL of solution was added to each well, after removing the remaining media inside, and cells were incubated at 37°C for 72 hours.

Ended the incubation period, media was completely removed from wells and cells were detached by trypsinization with 400µL of trypsin+EDTA.

After detaching, cells were resuspended and transferred to 2,5mL eppendorf tubes to be centrifuged (7 minutes, 300x g, no break). Supernatant was removed without disturbing the cell pellet. 1mL sterile PBS was added to each tube and centrifugation step was repeated more 2 times in order to remove any traces of incubation media. After centrifugation cell pellet was

resuspended in PBS (500µL) and cells were counted to assess the concentration (procedure described above). Cell suspensions were then diluted to obtain a concentration of approximately 5 x $10^6$ cells per 200µL (recommended concentration and volume for DNA extraction kit).

DNA extraction and purification was executed as described at the kit protocol [90], without any modifications.

To assess DNA concentration in the final elution the absorbance was checked with NanoDrop spectrophotometer.

Due to technical problems with the DNA isolation kits, what delayed the process, and limited access to NMR spectroscopy, results concerning to 5-FU and FUAc DNA incorporation were not available by the submission date of this work. In the case of positive results, a scientific publication on the matter will be prepared.

### 2.2.12 DNA digestion

In order to measure $^{19}$F-NMR signal of the cells isolated DNA, it had to be degraded in smaller nucleotide sequences. For this purpose the endonuclease Deoxyribonuclease I (commonly known as DNase I) was used. This enzyme is reported to digest DNA into approximately 60% dinucleotides, 25% trinucleotides and oligonucleotides being its smaller substrate a trinucleotide. It is know to cut DNA in an almost randomly way, although it seems to be cleave preferably purine-pyrimidine sequences. [91]

Protocol was established by adapting described procedures in literature [92][68]. Thus, DNaseI quantity was adjusted to DNA concentration having 2 Units of DNase I per 1µg DNA. This mixture was incubated at 37°C for 2 hours. Enzyme was then removed from solution by centrifugal filtration.

### 2.2.13 Software

Through this work different software was used, mainly as interface for laboratory instruments or data processing.

Referring to laboratory instruments handling, KC Junior™ from BIO-TEK® was the operating software for plate spectrophotometer. NMR spectroscopy equipment ran TopSpin™ from Bruker®.

MTT and Trypan Blue data was processed using Microsoft Excel 2011 for Mac and statistical analysis was performed with Prism 6® by GraphPad. NMR spectroscopy images were prepared with iNMR reader, Mestrelab Research. Reference management was done with Mendeley Desktop.

### 2.2.14 Statistical Analysis and IC50

MTT raw data obtained from spectrophotometer results was converted to percentage setting average absorption of control wells to hundred percent. From the seven data points obtained for each concentration, the two extreme values were excluded (the highest and the lowest one). The same procedure was applied to points referring to control. MTT assay was repeated three times with each cell line, for each repetition the above-described procedure was followed.

Once percentages were calculated, the results were transferred to GraphPad PRISM. Results of all the three repetitions for each cell line were considered. From this data group were calculated the mean, standard deviation, IC50 and the chosen non-parametric test to assess significance of the results.

Data was tested for normality with D'Agostino-Pearson omnibus normality test [93] which is an embed function of Prism. As data failed to fit a normal distribution, a non-parametric test was chosen. Assuming to have unpaired data-sets (each data-set refers to different concentration and substance), the Mann-Whitney was chosen [94], with two-tailed P-value and confidence level of 99% (P<0,01).

Calculation of IC50 for each substance with each of the three cell lines was also performed with Prism, choosing an embed model that took logarithm of the concentration and the relative percentage of cell activity into account. Values were calculated according to Equation 11 (Y and X values being the percentage and concentration, respectively) and setting 100% value for the situation where drug had no effect on the cells and 0% as maximum effect (Figure 14).

$$Y = \frac{100}{1 + 10^{X - \log(IC50)}}$$

Equation 11: IC50 calculation [153]

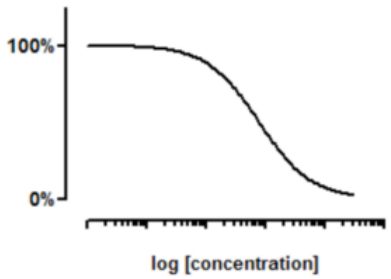


Figure 14: IC50 model description. Y-axi represents relative cell metabolic activity and x-axis logarithm of the respective drug concentration. [153]

Referring to cell counting with trypan blue, data was processed with Microsoft Excel and graphics shown in results section were prepared in Prism. As previously done for MTT data, control was set to 100% and the remaining results compared to control to obtain cell growth in percentage when compared to control. To calculate the standard deviation of each percentage values was used the embed standard deviation function of Microsoft Excel. Further analysis of these data consisted in IC50 calculation with GraphPad.

# 3 Results

In the present chapter will be presented the results obtained through this project.

The NMR-spectroscopy spectra ($^{13}C$, $^{1}H$ and $^{19}F$) are presented in sections 3.1.1.1, 3.1.1.2 and 3.1.1.3. For FUAc-HSA characterization, MALDI-TOF and CD-Spectroscopy results are shown on Sections 3.2.1 and 3.2.2, respectively.

The results obtained from the *in vitro* tests to assess the compounds cytotoxicity are presented in section 3.3.

Confocal Laser Scanning microscopy obtained for the three cell lines can be found in section 3.3.4, the last of this chapter.

## 3.1 FUAc characterization

In order to evaluate the success of FUAc synthesis, NMR spectroscopy was performed. Spectra obtained from $^{13}C$, $^{1}H$ and $^{19}F$-NMR Spectroscopy are shown below.

### 3.1.1 NMR Spectroscopy

For an easier analysis of NMR spectroscopy spectra, the chemical structural of FUAc is shown in Figure 15. The substitutin elements and the chain carbon atoms are highlighted and numl according to its position in the FUAc molecule. For the purpose simplified writing, carbon and the other substituting atoms are re by these notations ($C^2$, $N^1$, etc) within the next subchapters.

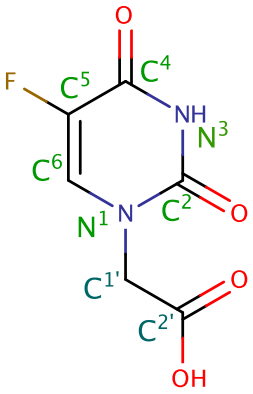


Figure 15: FUAc chemical structure. Scheme created with MarvinSketch software

#### *3.1.1.1 $^{13}C$-NMR Spectroscopy*

Below is shown the $^{13}C$ -NMR spectra. There are six signals; the expected ones for FUAc molecule which has six carbon atoms.

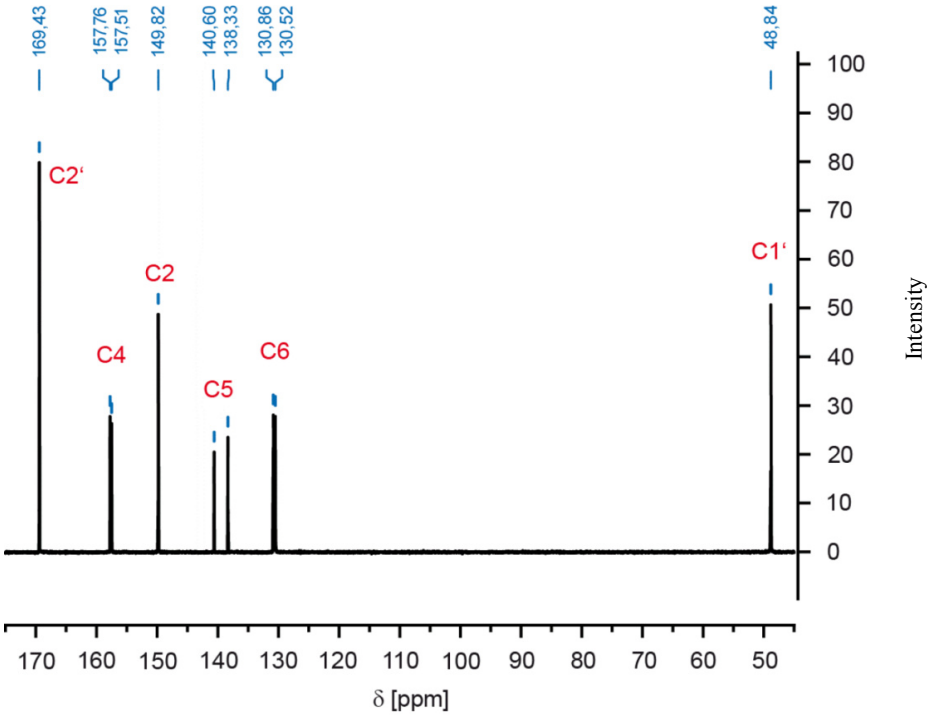


Figure 3.1-b: C-NMR Spectroscopy spectra of FUAc. X-axis represents the chemical shift in ppm and y-axis the signal intensity, which has an arbitrary unit.

$C^1$, $C^2$ and $C^{2'}$ represent singlets and $C^4$, $C^5$ and $C^6$ doublets. The Fluorine atom connected to $C^5$ is strongly electronegative. This electronegativity in the proximity of a carbon atom is in the origin of the double peak at 140,60 and 138,33 ppm. This doublet was assigned to $C^5$ because this is a typical signal for F-C coupling: is a doublet, obeying to N+1 rule (can be applied since $_{19}F$ has a spin of ½) and has a large coupling constant. The other two doublets are a result of the close position to Fluorine atom as well, both corresponding to $J_2$ couplings.

### *3.1.1.2 $^1$H-NMR Spectroscopy of FUAc*

FUAc $^1$H-NMR spectra shows 5 signals, as seen on Figure 17.

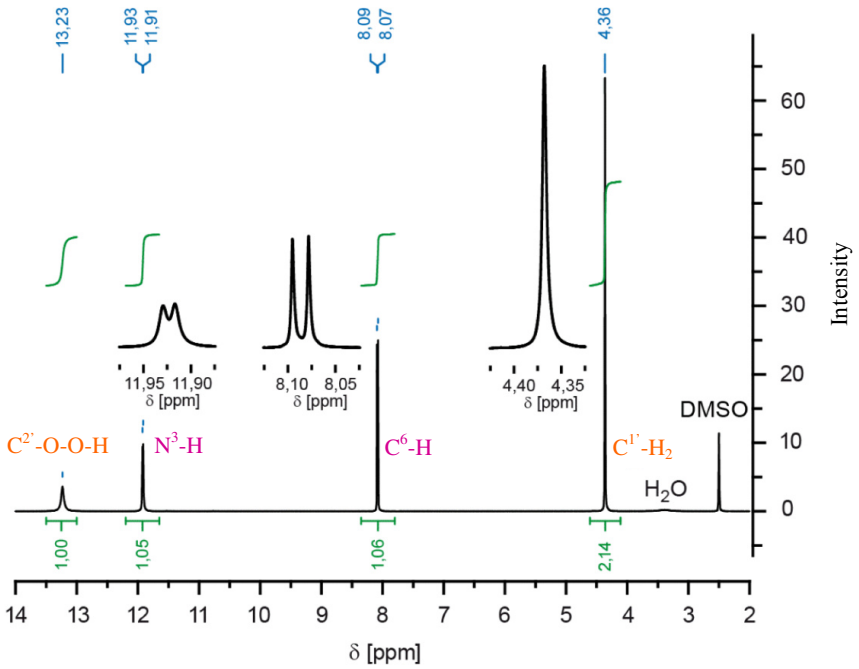


Figure 17: $^{1}$H-NMR spectroscopy of FUAc. X-axis represents the chemical shift in ppm and y-axis the signal intensity, which has an arbitrary unit.

At 13,23 ppm there is a peak corresponding to a carboxylic group in $C^{2'}$. This assignment was due to the presence of two Oxygen atoms, causing deshielding in Hydrogen atom and consequently moving the signal to the downfield. The area under the curve of the peak is 1, so the peak was generated by one Hydrogen atom.

The doublet at 11,93 and 11,91 ppm is likely to correspond to the Hydrogen atom connected to $N^3$ considering that it was created only by one Hydrogen atom (Area Under the Curve (AUC) is one), therefore this atom is under influence of strong electronegative atoms. The proximity of two Oxygen atoms (linked to $C^2$ and $C^4$) is likely to explain this downfield position. Additionally, by the N+1 rule [95], it is known that there is no other Hydrogen atom in the neighborhood of this one.

Another doublet appears with peaks at 8,09 and 8,07 ppm. AUC suggests that it corresponds to one single Hydrogen atom. Chemical shift to downfield suggests the proximity to an electronegative atom. Comparing $J_3$ coupling constant (6,8Hz) with $J_4$ from the previous doublet it is possible to conclude this is larger thus indicating a hydrogen or Fluorine atoms in position $J_3$.

At 4,36 ppm there is a peak with AUC approximate to two, meaning the signal corresponds to two Hydrogen atoms. Considering the chemical shift displacement it is

reasonable to conclude that there is a weak electron withdrawer neighbor or it suffers the influence of both strong electron-withdrawing and strong electron-donating neighbors. This peak was then assigned to Hydrogen atom in $C^{1'}$-$H_2$ since it is influenced by both the electron-donator $N^1$ and $C^{2'}$-OOH.

The DMSO-$\delta_6$ peak was identified according to information in [96].

### *3.1.1.3 F-NMR Spectroscopy of FUAc*

$^{19}$F-NMR spectra shows one signal, a doublet of a doublet.

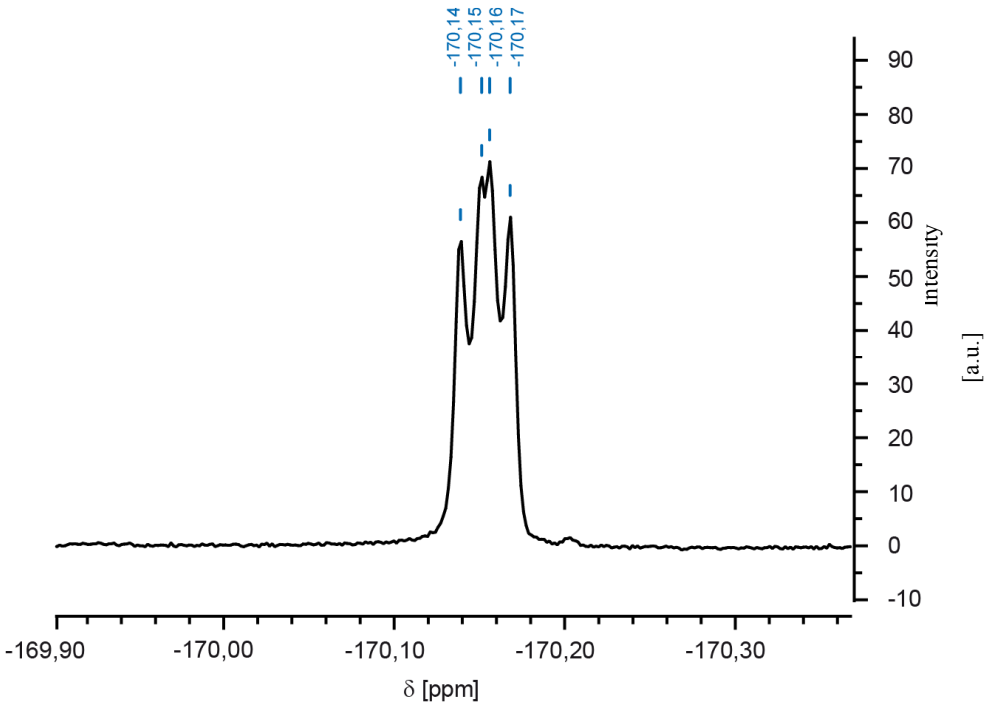


Figure 3.1-d: $^{19}$F-NMR Spectra of FUAc. X-axis represents the chemical shift in ppm and y-axis the signal intensity, which has an arbitrary unit.

The figure above shows a signal with chemical shift of -170.15 ppm split into four peaks. It is a doublet of a doublet that is formed in the following manner. A first doublet occurs by a J3-coupling with 6,4 Hz (corresponds to the J3-coupling from the $^1$H-NMR spectroscopy (6.8 Hz) and is caused by the hydrogen atom coupled C6. A second doublet results from a $J_4$-coupling of 4.7 Hz, the 5.1 Hz corresponds to the $J_4$-coupling from the $^1$H-NMR and is caused by the hydrogen atom coupled $N^3$. The second doublet is a result of subsequent splitting of the first doublet.

## 3.2 FUAc-HSA characterization

### 3.2.1 *MALDI-TOF*

In order to assess the average number of FUAc molecules bound to each albumin particle, a MALDI-TOF analysis was performed.

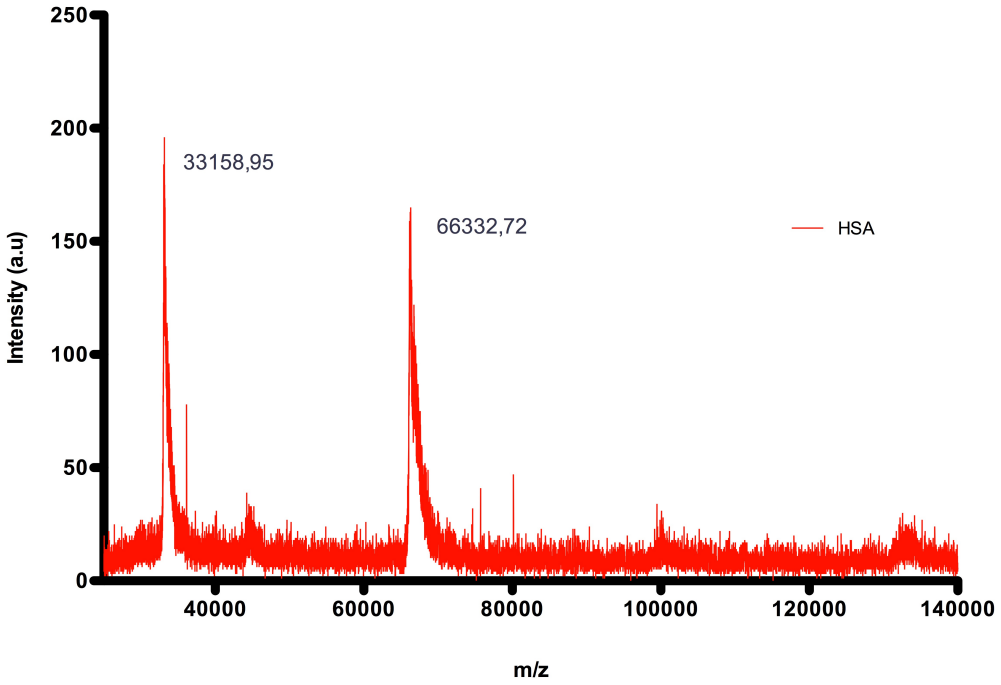


Figure 19: MALDI-TOF spectra of HSA. The two peaks corresponding to monoionised HSA (33158,95 m/z) and to double ionized HSA (66332,72 m/z). X-axys unit, m/z is the mass-to-charge ratio which is the common unit in mass spectroscopy analysis. This unit is defined in chapter 2.2.4. Spectra was acquired in Linear Positive Mode with dihydroxyacetonephosphate (DHAP)-matrix.

First spectrum (Figure 19) refers to HSA, the second (Figure 20) to the superposition of FUAc-HSA and HSA spectra and the third spectrum (Figure 21) shows the peaks corresponding to both molecules monoionised.

Referring to Figure 19, there are two main peaks at 33158,95 and 66332,72 m/z. Considering human serum albumin molecular weight provided by manufacturer as 66437 Da [97], the peak at 66332,72 m/z is assigned to monoionised HSA $[HSA + H]^+$ . Our results indicate thus a molecular weight of 66332,72 Da for the tested HSA.

The origin of the other peak, at 33158,95 m/z, is discussed in Section 4.1.2.1.

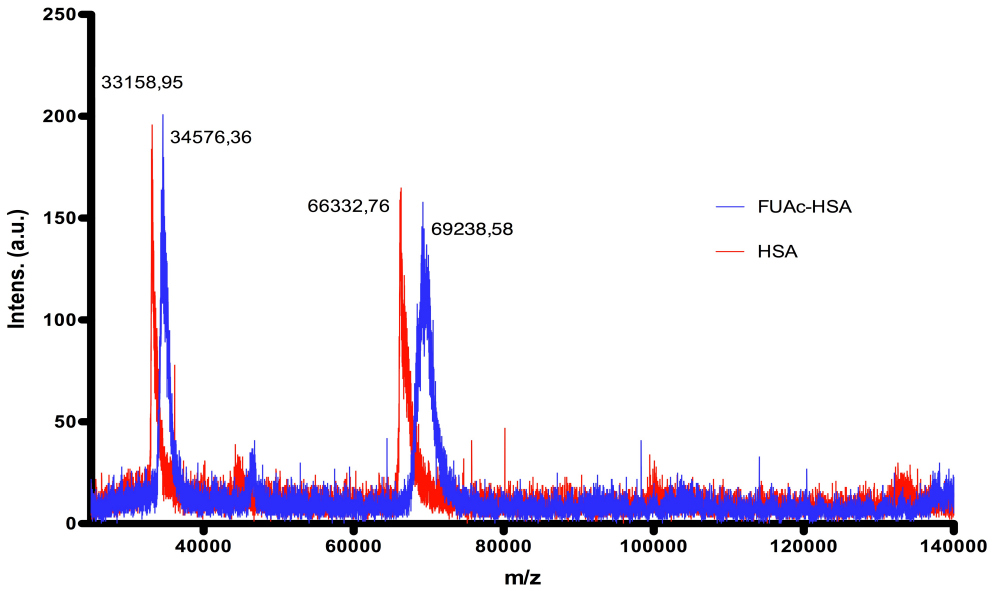


Figure 20: MALDI-TOF spectra of FUAC-HSA (blue) and HSA (red). Measuring conditions and unit definitions as described in Figure 19.

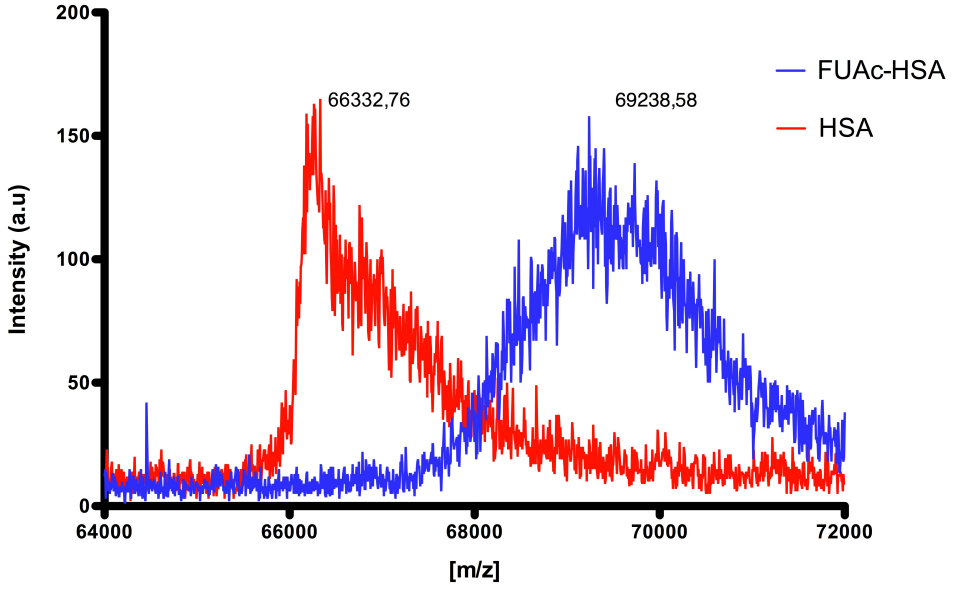


Figure 21: MALDI-TOF spectra of FUAC-HSA (blue) and HSA (red). Measuring conditions and unit definitions as described described in Figure 19.

Both Figure 20 and Figure 21 show the superposition of HSA and FUAc-HSA spectra. In the first figure, all acquired points are visible and the second has a smaller window range, confining only the peaks assigned to monoionised molecules. Resembling to the procedure for HSA spectra, the origin of other visible peaks will be discussed in section 4.1.2.1.

Nevertheless, the obtained spectra support a successful FUAc-HSA synthesis since FUAc-HSA peaks are displaced to the right (higher m/z values) meaning that the analyzed particle has higher molecular mass.

The average number of FUAc molecules bound to each HSA molecule was calculated based on MALDI-TOF results, according to the following procedure:

$$peak\ for\ FUAc-HSA-\ peak\ for\ HSA=\ \text{FUAc weight in FUAc}-\text{HSA}\quad\text{(Equation 12)}$$

so

$$69238{,}58-66332{,}76=2905{,}82\ \text{Da}\quad\text{(Equation 13)}$$

Considering FUAc molecular weight as 188,1 Da [11]

$$\frac{2905{,}82\ \text{Da}}{188{,}1\ \frac{\text{Da}}{\text{FUAc molecule}}}=15{,}4\ \text{FUAc mol. per HSA mol.}\approx 15\quad\text{(Equation 14)}$$

Therefore, for experimental procedures were considered the result of 15 FUAc molecules covalently bound to each HSA molecule.

### *3.2.2 **CD-Spectroscopy***

HSA and FUAc-HSA molecules conformation was investigated by CD-Spectroscopy. Figure 22 shows the spectra for HSA and FUAc-HSA (solved in water and phosphate buffer). The unit in y-axis is mean residue ellipcity (MRE), which reports the molar ellipticity for individual protein residues. MRE values were calculated according to Equation 15.

$$\Theta_{res}=\frac{[\theta]}{585}$$

Equation 15

With [θ] defined in Equation 8 and 585 being the number of amino acids in HSA.

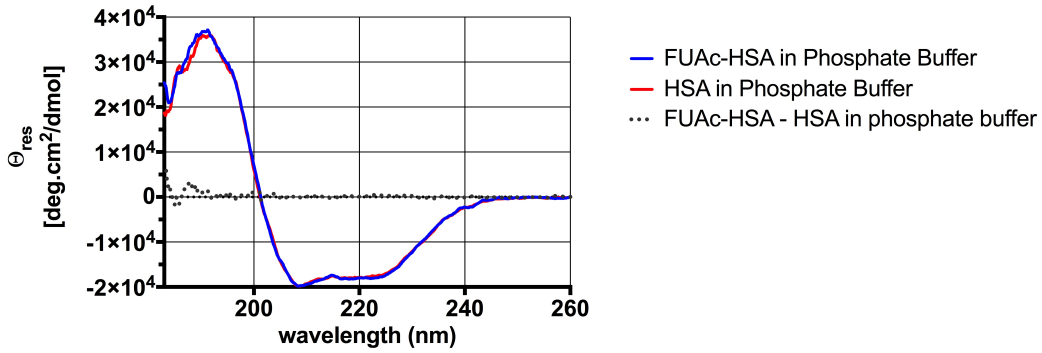


Figure 22 CD-Spectroscopy spectrum in phosphate buffer.

The analysis between HSA and FUAc-HSA CD-spectroscopy spectra can be found in section 4.1.2.2 of discussion. The secondary structure of pure HSA and when bound to FUAc will be compared in order to investigate possible changes in protein conformation due to the coupling process.

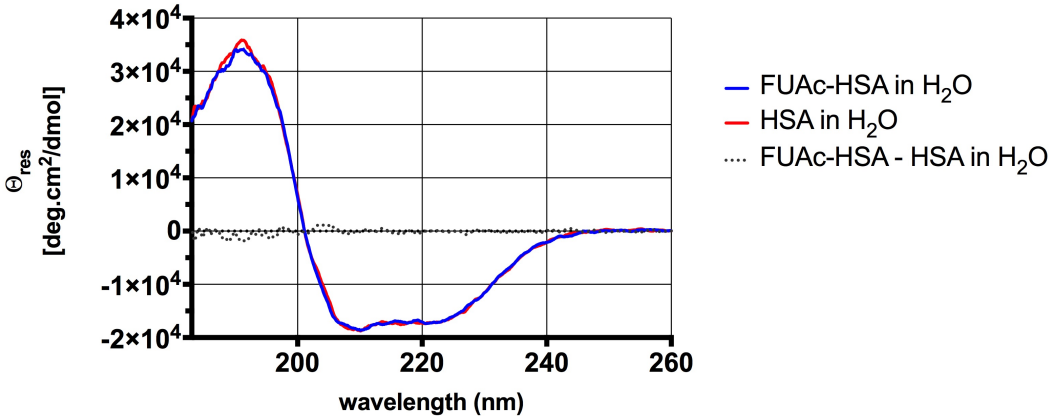


Figure 23: CD-Spectroscopy spectrum in water.

## *3.3* Cytotoxicity studies *in vitro*

Data related to *in vitro* tests is presented in this section. Results are grouped by cell line, 3.3.1, 3.3.2 and 3.3.3 for T-47D, MDA-MB-231 and MCF-7, respectively. In each of the previous cell related subchapters are presented the results of MTT assays and cell counting with trypan blue staining.

### 3.3.1 T-47D cell line

In this subchapter are presented the results obtained for T-47D cell line with MTT assays and cell counting.

#### *3.3.1.1 MTT*

All data in the present subchapter were obtained by processing MTT raw data.

##### 3.3.1.1.1 Relative metabolic cell activity across time

To illustrate compounds influence on T-47D cells its relative metabolic activity is shown on bar charts (Figure 24 to Figure 27) at four time points (24, 48, 72 and 96 hours).

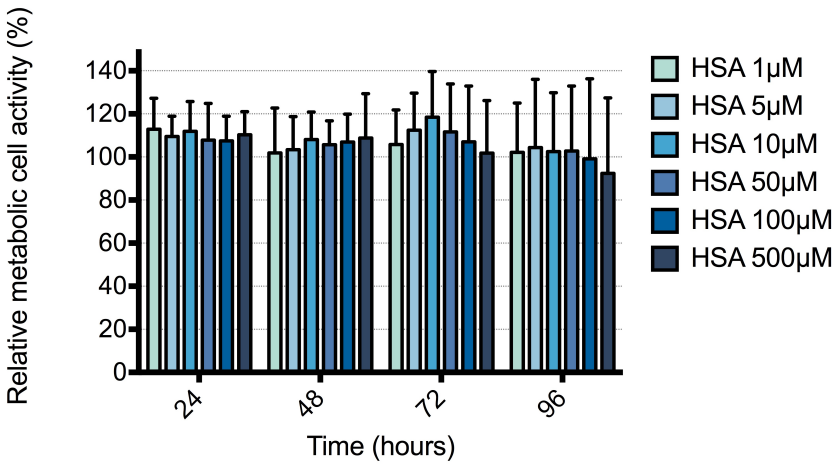


Figure 24: MTT results relative to T-47D for the tested time points and HSA concentrations. Each different coloured column represents a different substance concentration and each group of columns describes results at the x-axis correspondent time point. Y-axis represent the relative metabolic activity of the cell line compared to the control. No significant diferences relative to control were found. Each bar corresponds to the average of 15 data points.

The results referring to cells incubated with HSA (Figure 24) show no significant inhibition at any time point. Tables with all available data points to create these charts are available in Appendix.

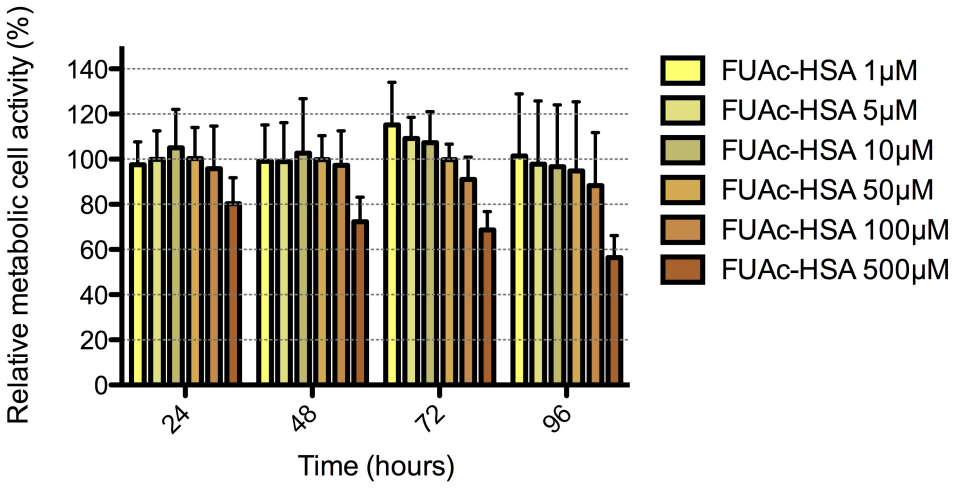


Figure 25: MTT results relative to T-47D for the tested time points and FUAc-HSA concentrations. Each different coloured column represents a different substance concentration and each group of columns describes results at the x-axis correspondent time point. Y-axis represent the relative metabolic activity of the cell line compared to the control. Each bar corresponds to the average of 15 data points.

FUAc-HSA highest concentration (500µM) is associated with a decreasing metabolic activity tendency through the experiment time, with mean value of 80,32% at 24 and 56,42% at 96 hours. Besides the 100µM at 96 hours (88,25%), no other concentration has an associated percentage of less than 90% relative metabolic cell activity. (Figure 25)

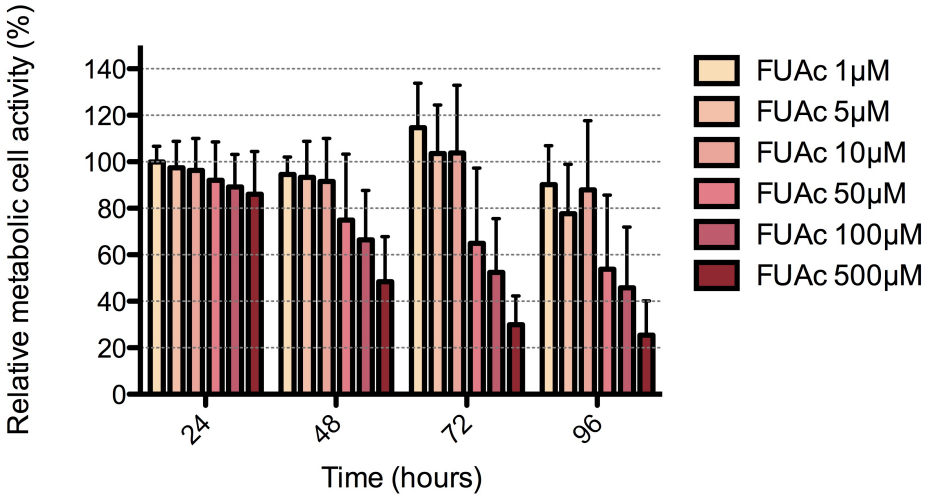


Figure 26: MTT results relative to T-47D for the tested time points and FUAc concentrations. Each different coloured column represents a different substance concentration and each group of columns describes results at the x-axis correspondent time point. Y-axis represent the relative metabolic activity of the cell line compared to the control. Each bar corresponds to the average of 15 data points.

A strong reduction of metabolic activity – less than 50% compared to control- is associated with FUAc highest concentration, from 48 hours time point on, inclusive (Figure 26). At 96 hours time point, 50µM and 100µM concentrations are also associated with relative inhibition of more than 50%. Lower FUAc concentrations (1, 5 and 10 µM) do not exhibit strong inhibition. Inhibition associated with the highest concentrations increases with time.

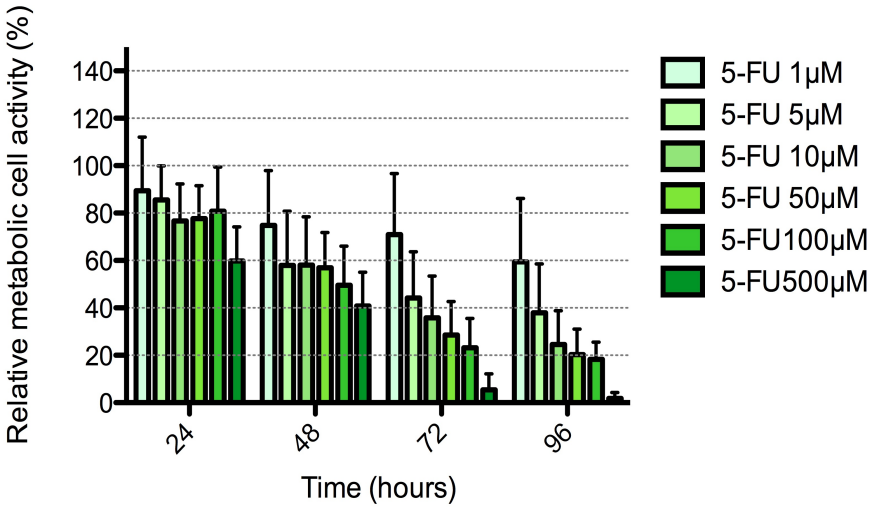


Figure 27: MTT results relative to T-47D for the tested time points and 5-FU concentrations. Each different coloured column represents a different substance concentration and each group of columns describes results at the x-axis correspondent time point. Y-axis represent the relative metabolic activity of the cell line compared to the control. Each bar corresponds to the average of 15 data points.

Metabolic Inhibition associated to 5-FU showed a strong tendency as can be seen in Figure 27. At 96 hours time point, only the lowest concentration is not associated with a cell

metabolic inhibition of more than 50%. Relative Cellular activity decreases with time and reaches a value of 1,83% for 500 µM at 96 hours. Comparing to HSA, FUAc-HSA and FUAc there is a clear stronger reduction on metabolic activity associated with 5-FU.

#### 3.3.1.1.2 Comparative inhibitory activity of substances per time point

Each of the following figures, from Figure 29 to Figure 31, show four box plots corresponding to the tested substances. Each group of box plots is related to one time point (24, 48, 72 and 96 hours). All calculated p-values can be consulted in

Results referring to 24 hours (Figure 29) show significant highest metabolic activity for cells incubated with 1, 5, 10 and 500 µM of HSA (P=0,0006; P=0,0015; P=0,0063 and P= 0,0015). Significant less activity than control is associated with FUAc-HSA highest concentration (P< 0,0001) and all 5-FU concentrations except the lowest (5µM: P=0,0005; 10µM: P<0,0001; 50µM: P<0,0001; 100µM: P<0,0001 and 500µM: P<0,0001).

Only the highest FUAc concentration could be associated with cell metabolism significantly different from control. The Figure 28 refers to 48 hours time point, when HSA had no significant influence on cell metabolism and with FUAc-HSA, only the highest concentration can be associated with activity reduction (P<0,0001). Like in 24 hours time point, 5-FU shows the stronger inhibitory activity with all concentrations being significantly different from control, with P< 0,0001. 500µM FUAc is associated with a strong metabolic activity reduction (P<0,0001) with 50 and 100 µM concentrations showing weaker influence but still statistically different from control (P=0,0017 and P<0,0001, respectively).

At 72 hours time point, as seen in Figure 30, results keep indicating a high inhibitory activity of 5-FU, with all concentrations being significantly different from control (1µM: P=0,0052 and the remaining with P< 0,0001). The three highest concentrations of FUAc exert significant inhibitory activity (P<0,0001) and, concerning to FUAc-HSA, only the highest one shows significant inhibitory effect (P<0,0001). HSA in the concentration of 10µM (P=0,0043) and FUAc-HSA with 1, 5 and 10µM (P=0,0092; P=0,0019 and P=0,0084= are significantly associated with metabolic activity increase compared to control cells.

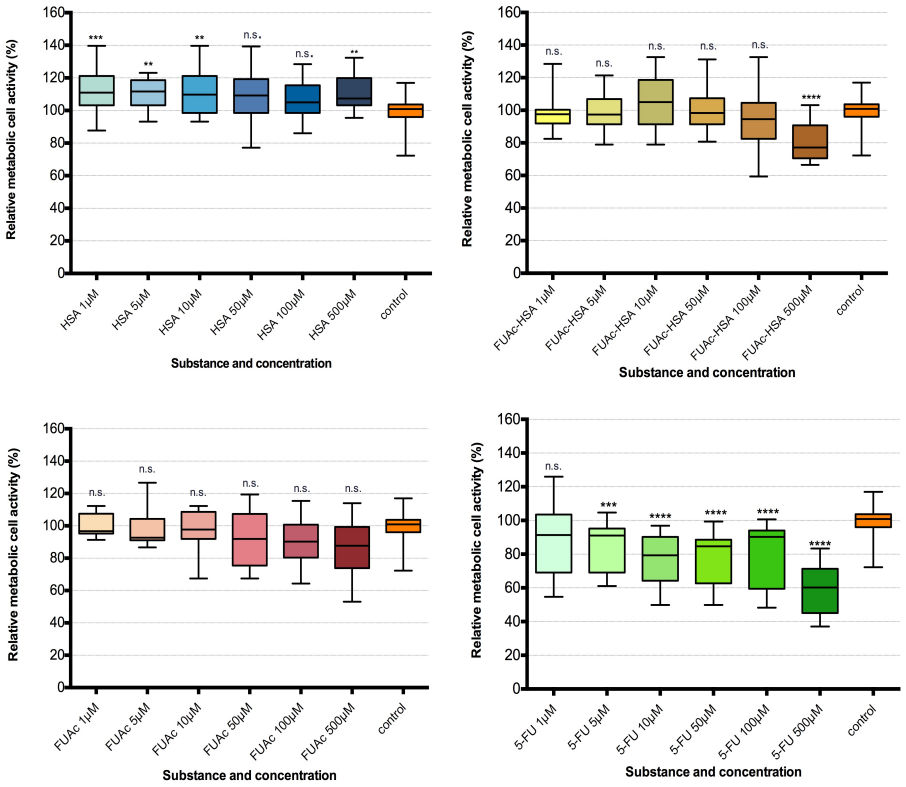


Figure 29: MTT results for T-47D cell line after 24 hours. Control group on orange on the right position in all above-listed plots, the remaining boxes correspond to tested compounds in the concentration referred on x-axis. n.s. states a P-value > 0,05; * a P ≤ 0,05; ** a P ≤ 0,01; *** a P ≤ 0.001; **** a P ≤ 0,0001, when compared to control. Top-left chart shows to HSA results, top-right to FUAc-HSA, bottom-left to FUAc and bottom-right to 5-FU.

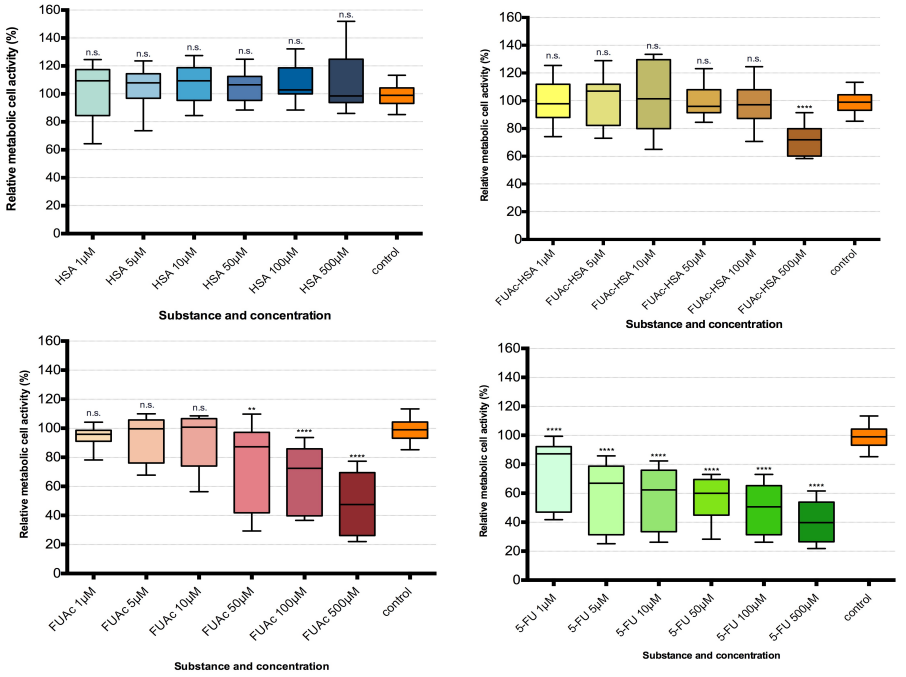


Figure 28: MTT results for T-47D cell line after 48 hours. Control group on orange on the right position in all above-listed plots, the remaining boxes correspond to tested compounds in the concentration referred on x-axis. n.s. states a P-value > 0,05; * a P ≤ 0,05; ** a P ≤ 0,01; *** a P ≤ 0.001; **** a P ≤ 0,0001, when compared to control. Top-left chart shows to HSA results, top-right to FUAc-HSA, bottom-left to FUAc and bottom-right to 5-FU.

Results from 96 hours (Figure 31) lead to similar analysis with the previous time point. Concerning to 5-FU, the statistical analysis is identical with 72 hours. HSA has no significant influence on cell metabolism and only the highest concentration of FUAc-HSA shows significant inhibitory activity (P< 0,0001). Referring to FUAc, the three highest concentrations and 5μM (P=0,0003) have an apparent inhibitory activity on the cells.

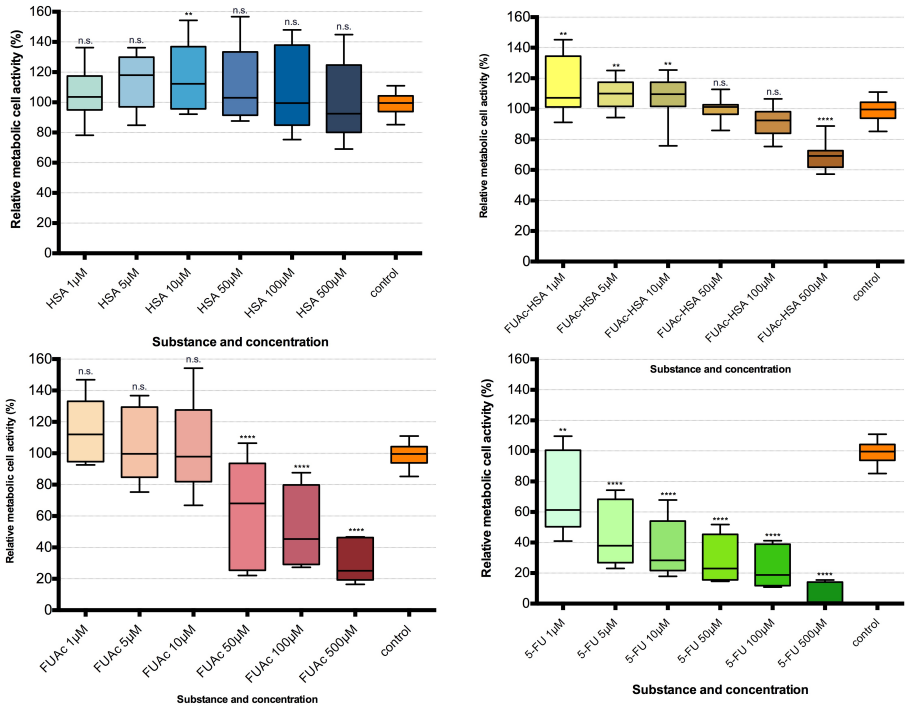


Figure 30: MTT results for T-47D cell line after 72 hours. Control group on orange on the right position in all above-listed plots, the remaining boxes correspond to tested compounds in the concentration referred on x-axis. n.s. states a P-value > 0,05; * a P ≤ 0,05; ** a P ≤ 0,01; *** a P ≤ 0.001; **** a P ≤ 0,0001, when compared to control. Top-left chart shows to HSA results, top-right to FUAc-HSA, bottom-left to FUAc and bottom-right to 5-FU.

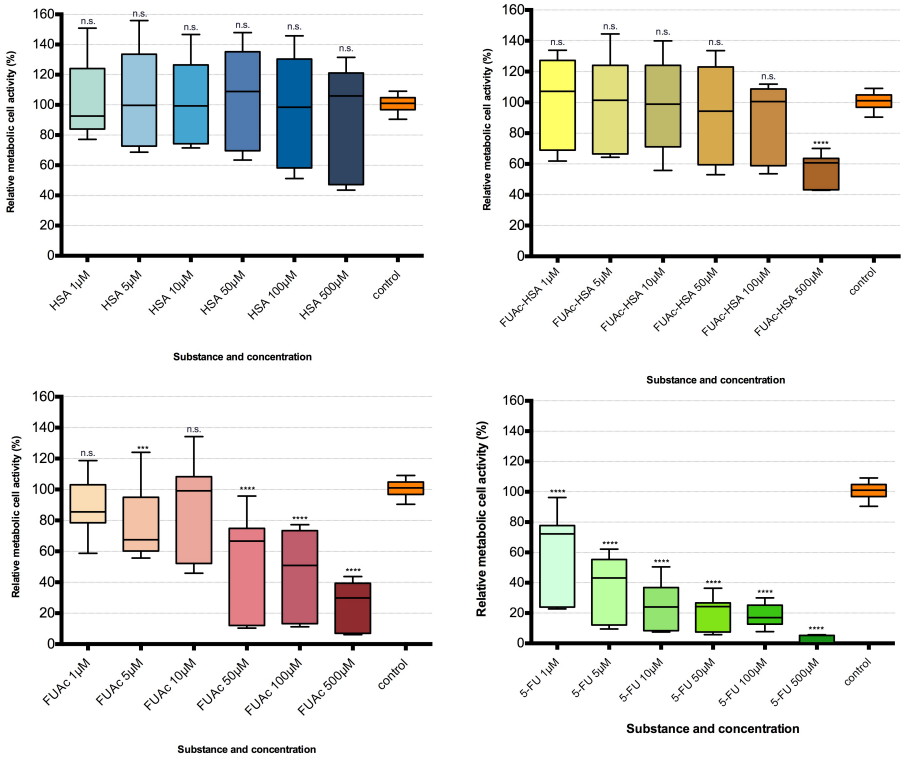


Figure 31: MTT results for T-47D cell line after 96 hours. Control group on orange on the right position in all above-listed plots, the remaining boxes correspond to tested compounds in the concentration referred on x-axis. n.s. states a P-value > 0,05; * a P ≤ 0,05; ** a P ≤ 0,01; *** a P ≤ 0.001; **** a P ≤ 0,0001, when compared to control. Top-left chart shows to HSA results, top-right to FUAc-HSA, bottom-left to FUAc and bottom-right to 5-FU.

### *3.3.1.2 Cell counting*

Cell counting after trypan blue staining was performed to confirm the cytotoxic activity of 5-FU, FUAc and FUAc-HSA suggested by the MTT assay results. As no significant inhibition was registered with lower concentrations with most substances, for this procedure were chosen only the three highest concentrations. Dead cells occurred very rarely.

Comparing results for cells incubated with HSA, cell counting suggests a higher inhibition due to HSA presence in media than MTT did (93,81; 87,79; 68,14 against 111,6; 107;101,8 % for, respectively 50; 100; 500 µM).

For FUAc-HSA, cell counting suggests as strong associated growth inhibition (71,48; 49,20 and 27,27 % of control cell number), contrasting once more with MTT results, reporting a minimum metabolic activity percentage of 68,680% for 500µM.

Related to three FUAc concentrations, the calculated relative cell number percentage suggests very strong growth inhibition (39,75; 25,49 and 11,90 %), values more closely related

to MTT results than the previous. These values were calculated setting control for 100%, following the same procedure adopted for MTT data.

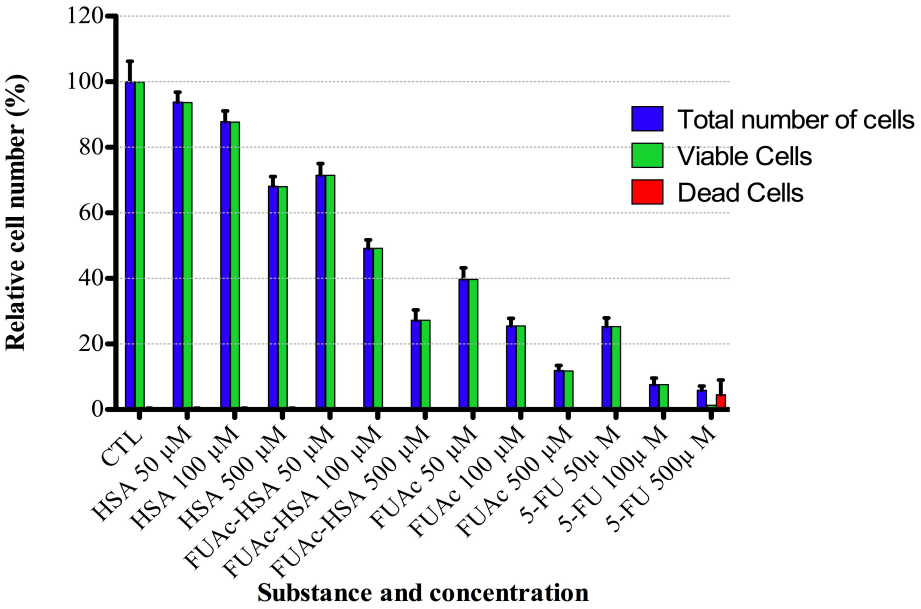


Figure 32: Cell counting results for T-47D cell line. X-axis lists the tested compounds and its concentration and y-axis is relative to cell number percentage compared to control cells. The y-axis represents the relative cell number in percentage compared to the control.

The values calculated for 5-FU were, respectively 25,31, 7,58 and 5,84 %, confirming its stronger inhibitory activity when compared with the other tested substances. As happened for FUAc, 5-FU relative cell number percentage is more similar to MTT values with standard deviation between MTT and cell counting values of 2,333 for 50µM, 11,05 for 100µM and 0,2645 for 500µM.

#### *3.3.1.3 Half maximal inhibitory concentration (IC50)*

The below-shown IC50 values were calculated with MTT and cell counting results in percentage, by means of a non-linear curve fitting.

| Substance / Time (hours) | 5-FU (µM, 95% confidence interval) | FUAc (µM, 95% confidence interval) | FUAc-HSA (µM, 95% confidence interval) | HSA (µM, 95% confidence interval) |
|---|---|---|---|---|
| 48 | 77,77 (29,43 to 205,5) | 407,1 (225,2 to 735,9) | 873,3 (422,3 to 1806) | – |
| 72 | 4,141 (2,696 to 6,361) | 133,7 (91,91 to 194,5) | 911,4 (560,5 to 1482) | – |
| 96 | 1,766 (1,082 to 2,884) | 78,80 (49,34 to 125,9) | 637,6 (365,5 to 1112) | – |

Table 5: Calculated IC50 for T-47D cell line considering the MTT assay results.

| Substance / Time (hours) | 5-FU (μM, 95% confidence interval) | FUAc (μM, 95% confidence interval) | FUAc-HSA (μM, 95% confidence interval) | HSA (μM, 95% confidence interval) |
|---|---|---|---|---|
| 72 | 27,09 (0,09516 to 7711) | 26,24 (1,465 to 469,9) | 125,4 (6,437 to 2444) | – |

Table 6: Calculated IC50 for T-47D cell line considering the cell counting assay results.

It was not possible to calculate IC50 values for HSA with this method. The IC50 values were not calculated for 24 hours data since the data points were disperse and the algorithm could not converge properly.

The lowest IC50 values were assigned to 5-FU, having also an associated narrow confidence interval at 72 and 96 hours time points.

Both FUAc and FUAc-HSA present considerably higher IC50 values and wider confidence intervals.

### 3.3.2 MDA-MB-231 cell line

In this chapter can be found the results corresponding to cytotoxicity in vitro tests with MDA-MB-231 cell line.

#### *3.3.2.1 MTT*

The aim of this MTT subchapter is to present results obtained by processing MTT assay raw data.

##### 3.3.2.1.1 Relative metabolic activity across time

Figures from Figure 33 to Figure 36 show bar charts with relative metabolic cell activity of MDA-MB-231 cells in culture with the substances under test against four time points (24, 48, 72 and 96 hours).

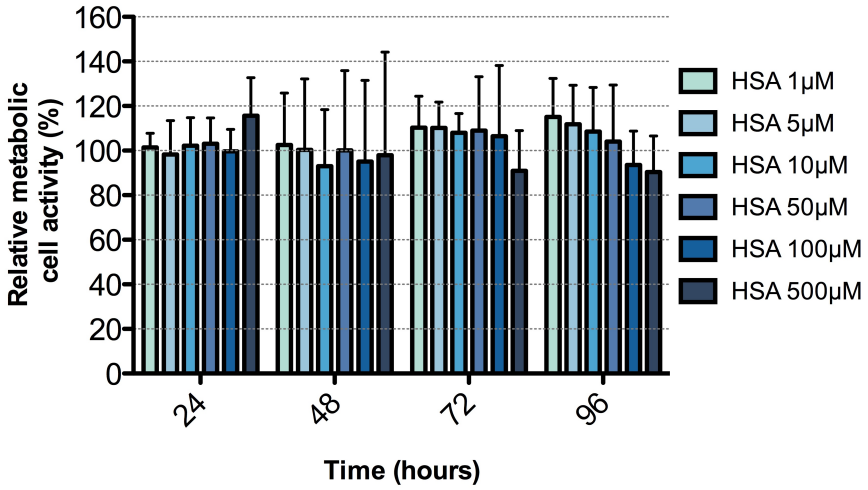


Figure 33: MTT results relative to MDA-MB-231 for the tested time points and HSA concentrations. Each different coloured column represents a different substance concentration and each group of columns describes results at the x-axis correspondent time point. The y-axis represents the relative cell metabolic activity in percentage compared to the control. Each bar corresponds to the average of 15 data points.

By analysis of Figure 33 (referring to HSA), there is no strong percentage increase or decreasing tendency, either associated with time or concentration. Some bars suggest an increasing in metabolic cell activity, mainly the highest concentration at 24 hours (115,70%) and the two lowest concentrations at 96 hours (115,1 and 111,80 %, respectively) nevertheless; the control value (100%) is contained in ±SD interval for these points.

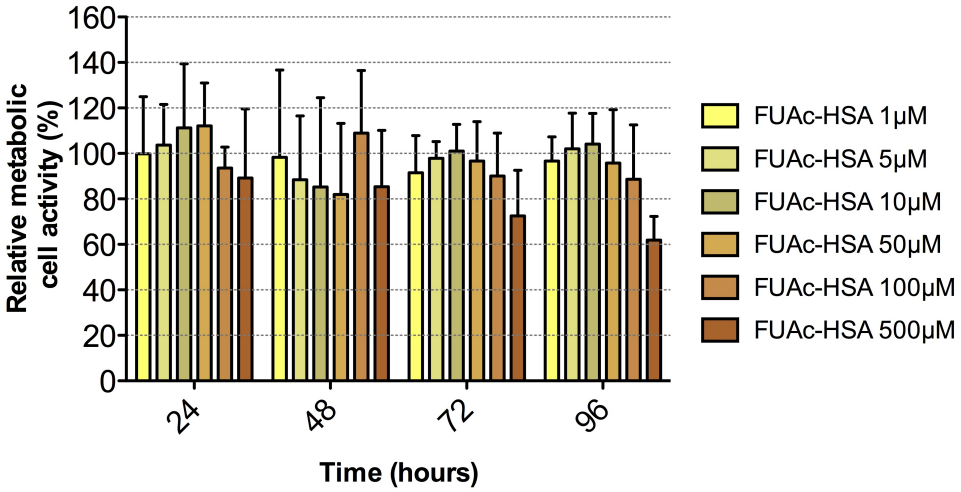


Figure 34: MTT results relative to MDA-MB-231 for the tested time points and FUAc-HSA concentrations. Each different coloured column represents a different substance concentration and each group of columns describes results at the x-axis correspondent time point. The y-axis represents the relative cell metabolic activity in percentage compared to the control. Each bar corresponds to the average of 15 data points.

The chart in Figure 34 refers to FUAc-HSA. There is a decrement in relative metabolic activity associated with the highest FUAc-HSA concentration (500μM) across time, reaching a value of 61,87% (±10,45) at 96 hours. Based on graphic analysis, cannot be reported any other remarkable bias from the control assigned value.

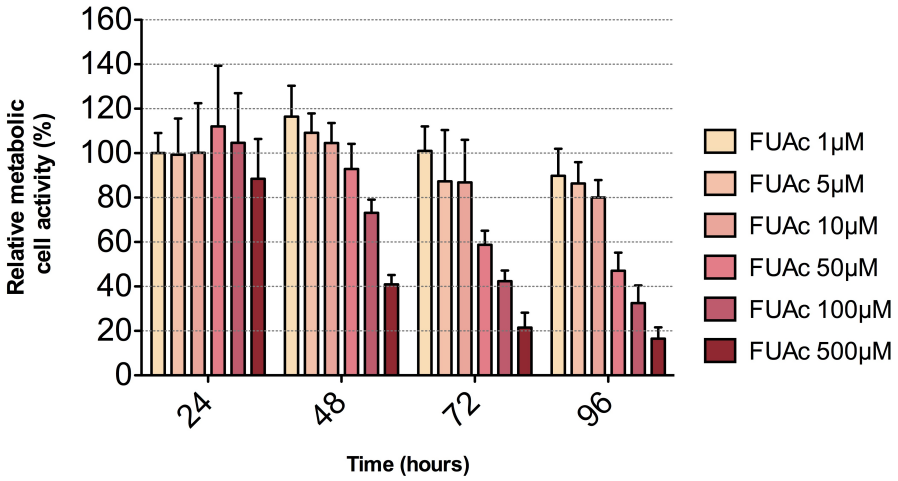


Figure 35: MTT results relative to MDA-MB-231 for the tested time points and FUAc concentrations. Each different coloured column represents a different substance concentration and each group of columns describes results at the x-axis correspondent time point. The y-axis represents the relative cell metabolic activity in percentage compared to the control. Each bar corresponds to the average of 15 data points.

The above placed bar graphic (Figure 35) exhibits results relative to FUAc, which can be associated with a strong reduction of metabolic cell activity. At 24 hours time point, the inhibition was not very pronounced however at 48 hours it is already noticeable a significant decreasing associated with the two highest concentrations, reaching 73,13 ± 5,974 % for

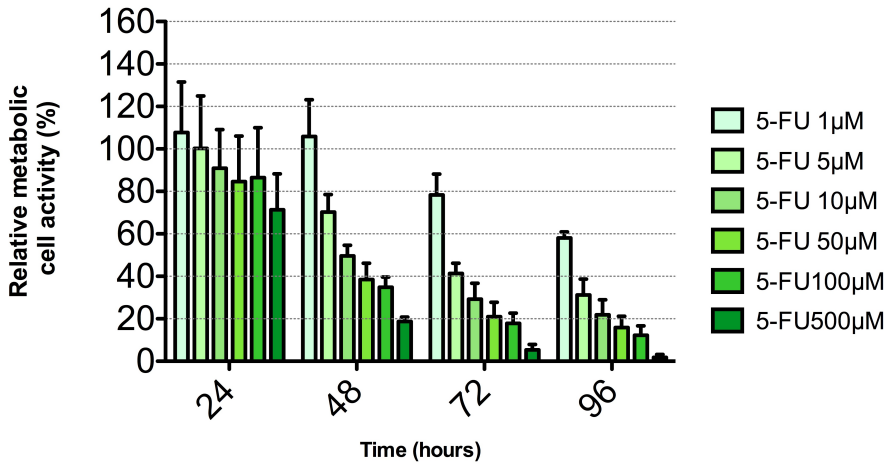


Figure 36: MTT results relative to MDA-MB-231 for the tested time points and 5-FU concentrations. Each different coloured column represents a different substance concentration and each group of columns describes results at the x-axis correspondent time point. The y-axis represents the relative cell metabolic activity in percentage compared to the control. Each bar corresponds to the average of 15 data points.

100µM and 40,98 ± 4,227 % for 500µM. Relative metabolic activity has a minimum value of 16,50 ± 5,144 % for 500µM at 96 hours. The three lowest concentrations do not cause a cell metabolism inhibition of more than 20%.

Making an overall analysis, reduction of metabolic cell activity seems to happen along with time and concentration increasing, excepting however results referring for 24 hours.

The fourth graphic in this section (Figure 36) shows results relative to 5-FU. Based on the above-presented results, 5-FU can be associated with a very strong metabolic activity inhibition, reaching a value of 1,838 ± 1,354% for 500µM at 96 hours. AT 72 and 96 hours, all concentrations are associated with values of less than 80%. Like in previous results, data for 24 hours do not show a clear metabolic activity-decreasing tendency due to concentration. From 48 to 96 hours point there is an obvious concentration and time dependent inhibition.

#### 3.3.2.1.2 Comparative inhibitory activity of substances per time point

The first figure of this section (Figure 37) shows 4 box plots relative to MTT results for the four tested substances at 24 hours time point.

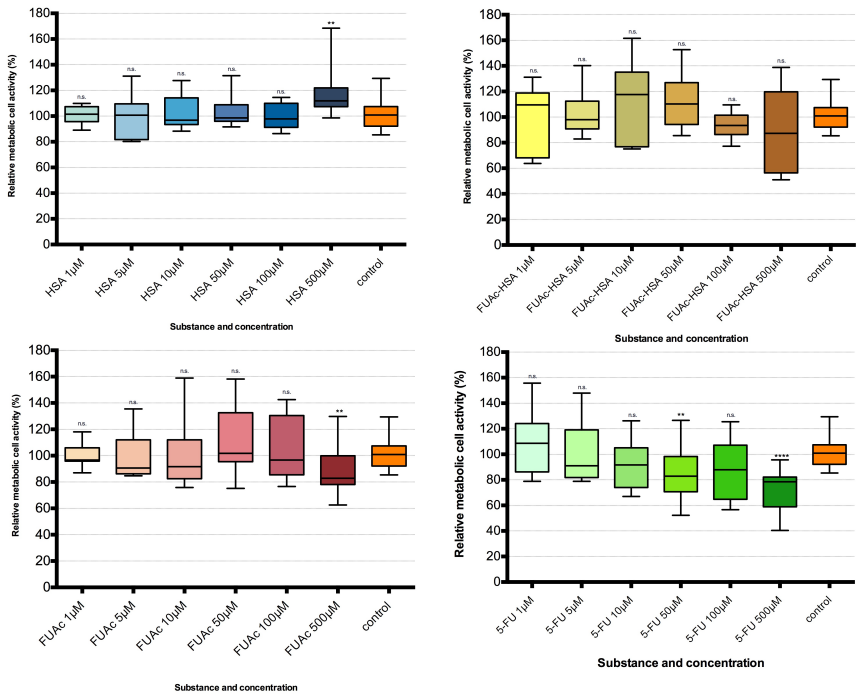


Figure 37: MTT results for MDA-MB-231 cell line after 24 hours. Control group on orange on the right position in all above-listed plots, the remaining boxes correspond to tested compounds in the concentration referred on x-axis. n.s. states a P-value > 0,05; * a P ≤ 0,05; ** a P ≤ 0,01; *** a P ≤ 0.001; **** a P ≤ 0,0001, when compared to control. Top-left chart shows to HSA results, top-right to FUAc-HSA, bottom-left to FUAc and bottom-right to 5-FU.

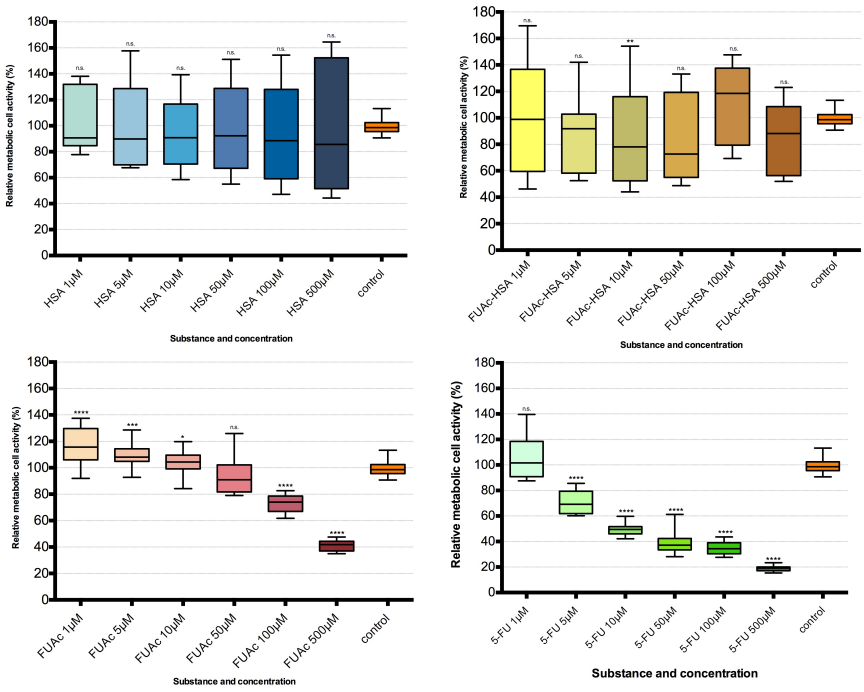


Figure 38: MTT results for MDA-MB-231 cell line after 48 hours. Control group on orange on the right position in all above-listed plots, the remaining boxes correspond to tested compounds in the concentration referred on x-axis. n.s. states a P-value > 0,05; * a P ≤ 0,05; ** a P ≤ 0,01; *** a P ≤ 0.001; **** a P ≤ 0,0001, when compared to control. Top-left chart shows to HSA results, top-right to FUAc-HSA, bottom-left to FUAc and bottom-right to 5-FU.

As referred previously about 24 hours time point data, it usually do not lead to significant conclusions about substances activity on cells. Analyzing the above-presented graphics, there are four data groups differing significantly from control: HSA 500µM, FUAc 500µM and 5-FU 50 and 500µM.

HSA 500µM is associated with an increased metabolic cell activity (P=0,0013). The remaining three referred data groups are associated with a decreasing in metabolic cell activity, however only 5-FU 500µM has a highly significant different value, compared to control (FUAc 500µM: P=0,1443; 5-FU 50µM: P=0,0035; 5-FU 500µM: P<0,0001).

Figure 39 shows the graphics for tested substances at 48 hours time point. Referring to HSA, 5 and 10µM concentrations exert an apparent stimulation on cells metabolism (P=0,0017 and P=0,0009, respectively). For FUAc-HSA, only 500µM concentration shows a notorious associated lower metabolic activity (P<0,0001). Considering 5-FU data, all concentration

resulted in metabolic activity reduction with high statistic significant difference from control (P<0,0001). FUAc is also associated with a sharp cellular metabolism decrease but only for the two highest concentrations (P<0,0001) and moderated inhibition with 10µM (P=0,0017).

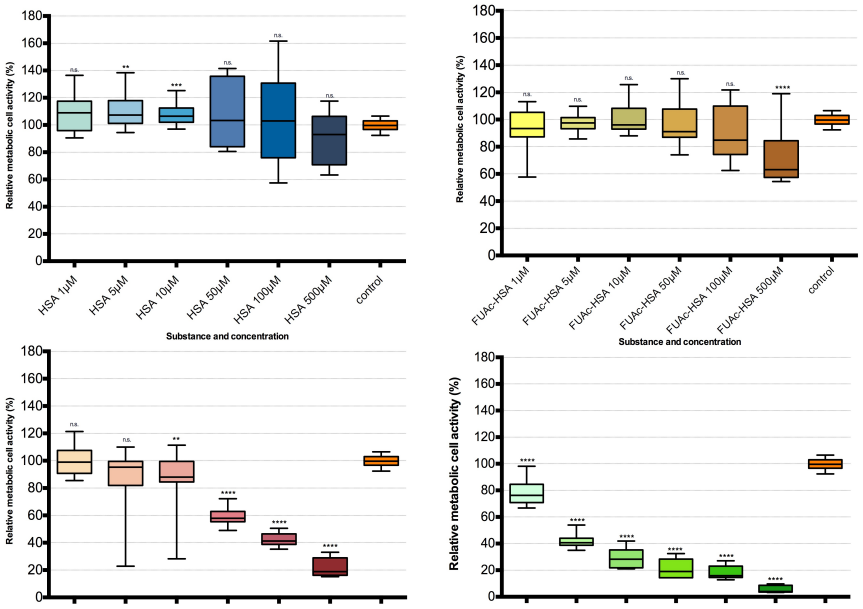


Figure 39: MTT results for MDA-MB-231 cell line after 72 hours. Control group on orange on the right position in all above-listed plots, the remaining boxes correspond to tested compounds in the concentration referred on x-axis. n.s. states a P-value > 0,05; * a P ≤ 0,05; ** a P ≤ 0,01; *** a P ≤ 0.001; **** a P ≤ 0,0001, when compared to control. Top-left chart shows to HSA results, top-right to FUAc-HSA, bottom-left to FUAc and bottom-right to 5-FU.

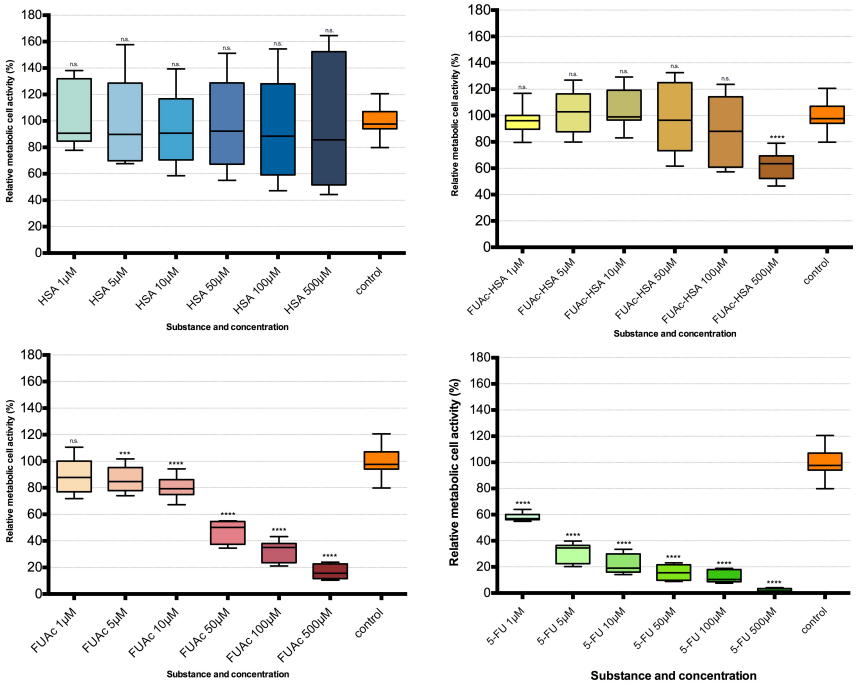


Figure 40: MTT results for MDA-MB-231 cell line after 96 hours. Control group on orange on the right position in all above-listed plots, the remaining boxes correspond to tested compounds in the concentration referred on x-axis. n.s. states a P-value > 0,05; * a P ≤ 0,05; ** a P ≤ 0,01; *** a P ≤ 0.001; **** a P ≤ 0,0001, when compared to control. Top-left chart shows to HSA results, top-right to FUAc-HSA, bottom-left to FUAc and bottom-right to 5-FU.

By the analysis of the 96 hours box plots (Figure 40), can be concluded that none of HSA concentrations leads to significant inhibition or stimulation of cellular metabolic. Concerning to FUAc-HSA, only the highest concentration is related with sharp metabolic activity inhibition (P<0,0001). All 5-FU concentrations led to a strong metabolic activity decrease (P<0,0001).

### *3.3.2.2 Cell counting*

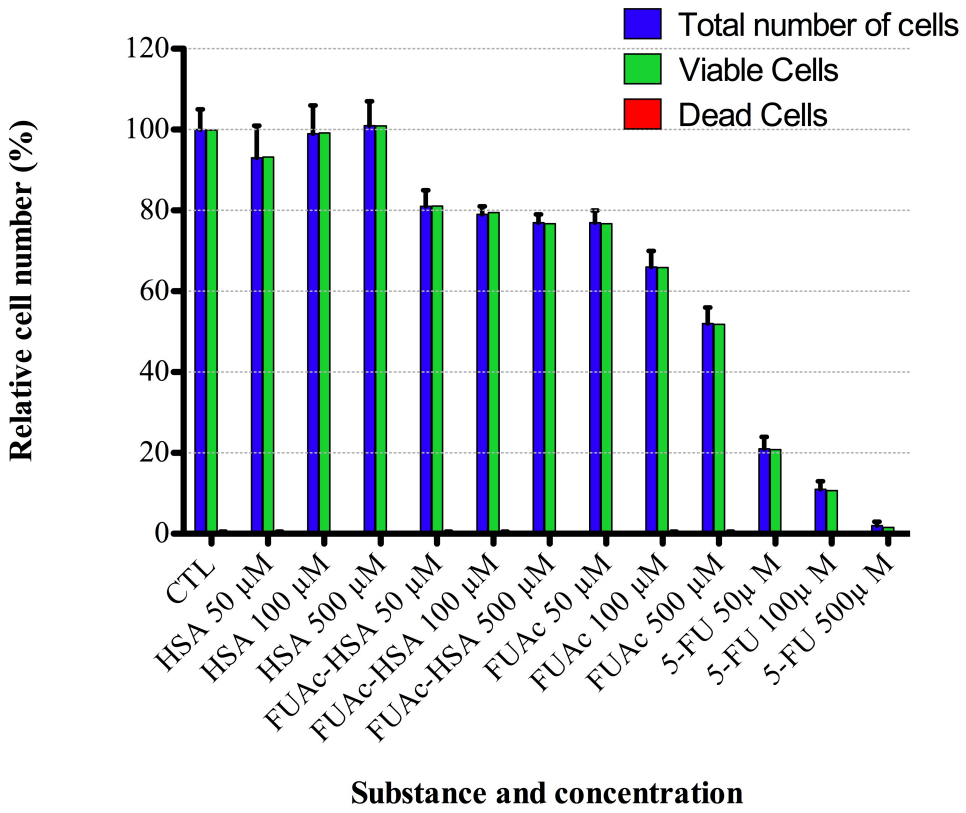


Figure 41: Cell counting results for MDA-MB-231 cell line. X-axis lists the tested compounds and its concentration and y-axis is relative to cell number percentage compared to control cells. The y-axis represents the relative cell number in percentage compared to the control.

The results obtained with cell counting procedure with MDA-MB-231 cell line are shown in Figure 41. As previously noted, negligible number of dead cells were found in the counting procedure.

Analyzing the above bar chart, it is possible to conclude that none of the HSA concentrations is associated with a significantly decreased cell number (50µM: 93% ± 8; 100µM: 99%± 7; 500µM: 101% ± 6). The three chosen FUAc-HSA concentrations show a similar effect on cells if compared to control values, with counted cells being circa 80% of the ones from control (50µM: 81% ± 4; 100µM: 79% ± 2; 500µM: 77% ± 2). FUAc data suggests

that it leads to highest inhibition when compared with the same concentration of HSA and FUAc-HSA and lowest if compared to 5-FU, showing a pronounced concentration-dependent inhibition (50µM: 77% ± 3; 100µM: 66% ± 4; 500µM: 52% ± 4). A very strong growth inhibition associated with 5-FU is suggested by these results, also showing concentration dependence (50µM: 21% ± 3; 100µM: 11% ± 2; 500µM: 2% ± 1).

#### *3.3.2.3 Half maximal inhibitory concentration (IC50)*

The table below (Table 7) list IC50 values in µM calculated from MTT data and Table 8 shows the IC50 for the substances calculated with the cell counting data.

| Substance / Time (hours) | 5-FU (µM, 95% confidence interval) | FUAc (µM, 95% confidence interval) | FUAc-HSA (µM, 95% confidence interval) | HSA (µM, 95% confidence interval) |
|---|---|---|---|---|
| 48 | 24,21 (19,07 to 30,74) | 337,5 (274,4 to 415,2) | – | – |
| 72 | 4,034 (3,416 to 4,765) | 78,61 (63,29 to 97,65) | 1531 (591,9 to 3963) | – |
| 96 | 1,489 (1,257 to 1,764) | 45,74 (39,67 to 52,73) | 766,0 (486,9 to 1205) | – |

Table 7: Calculated IC50 for MDA-MB-231 cell line considering the MTT assay results.

| Substance / Time (hours) | 5-FU (µM, 95% confidence interval) | FUAc (µM, 95% confidence interval) | FUAc-HSA (µM, 95% confidence interval) | HSA (µM, 95% confidence interval) |
|---|---|---|---|---|
| 72 | 15,14 (13,91 to 16,47) | 562,3 (10,71 to 29523) | – | – |

Table 8: Calculated IC50 for MDA-MB-231 cell line considering the cell counting assay results.

5-FU exhibits relatively low IC50 values with a narrow confidence interval. Concerning to FUAc-HSA, the calculated values predict the need of high doses in order to inhibit cell grow by 50%. Associated confidence interval is also relatively wider than for the other compounds. As suggested by previous results, FUAc trigger a weaker response on cells compared to 5-FU, presenting higher IC50 values than 5-FU but lower than FUAc-HSA.

### 3.3.3 MCF-7 cell line

The following sections (from 3.3.3.1 to 3.3.3.3) present results concerning to MCF-7 cell line and in vitro cytotoxicity tests.

### *3.3.3.1 MTT*

Within this section are shown results obtained from MTT assays with MCF-7 cell line.

#### 3.3.3.1.1 Relative metabolic activity across time

The present section comprises four bar charts (from Figure 42 to Figure 45), each corresponding to one of the tested compounds.

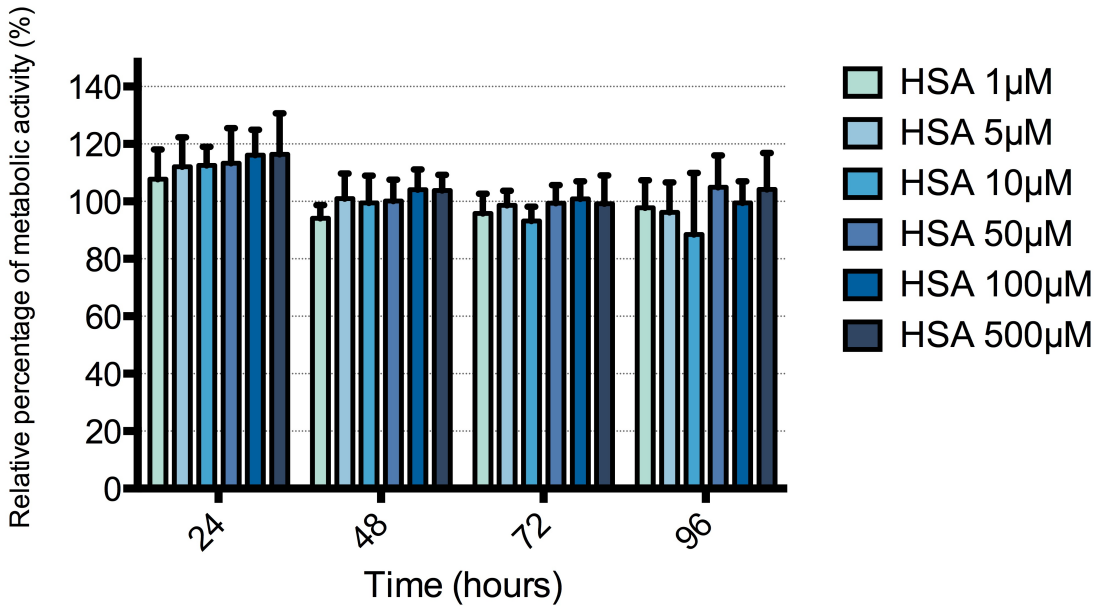


Figure 42: MTT results relative to MCF-7 for the tested time points and HSA concentrations. Each different coloured column represents a different substance concentration and each group of columns describes results at the x-axis correspondent time point. The y-axis represents the relative cell metabolic activity in percentage compared to the control. Each bar corresponds to the average of 15 data points.

Based on the above-shown graphic (Figure 42) can be assumed that HSA exerts no significant inhibition or stimulation on this cell line. Concentration or time dependent metabolic inhibition due to HSA could not be noted.

Referring to the second graphic of this chapter, Figure 43, which illustrates MTT results for cells incubated with FUAc-HSA, there is a consistent tendency of concentration and time-dependent inhibition. Only one data group, FUAc-HSA in the concentration of 500µM at 96 hours time point, appears associated with less than 60% relative metabolic activity, the highest concentration (50,45% ± 4,53).

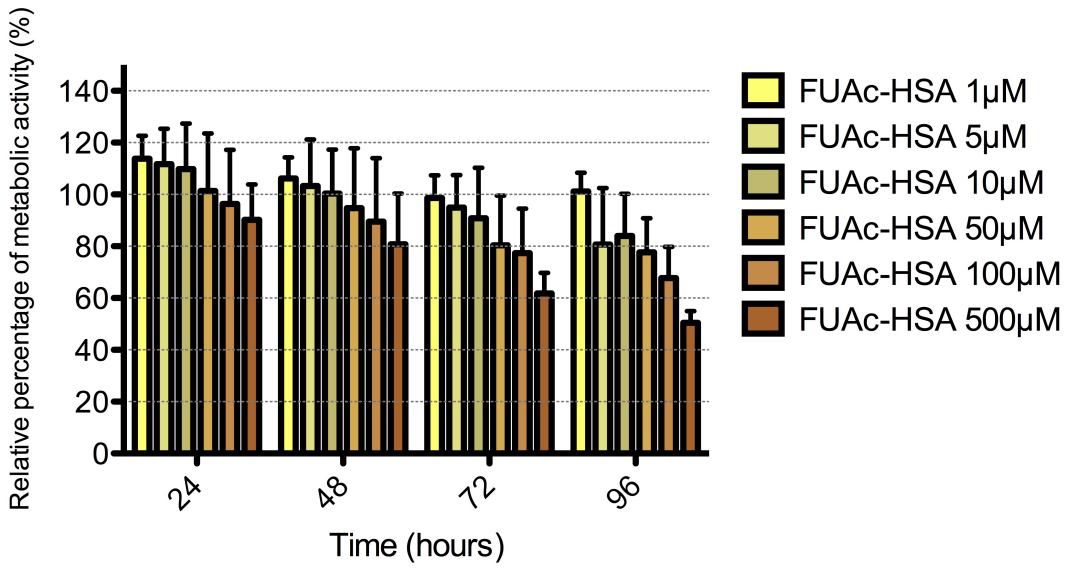


Figure 43: MTT results relative to MCF-7 for the tested time points and FUAc-HSA concentrations. Each different coloured column represents a different substance concentration and each group of columns describes results at the x-axis correspondent time point. The y-axis represents the relative cell metabolic activity in percentage compared to the control. Each bar corresponds to the average of 15 data points.

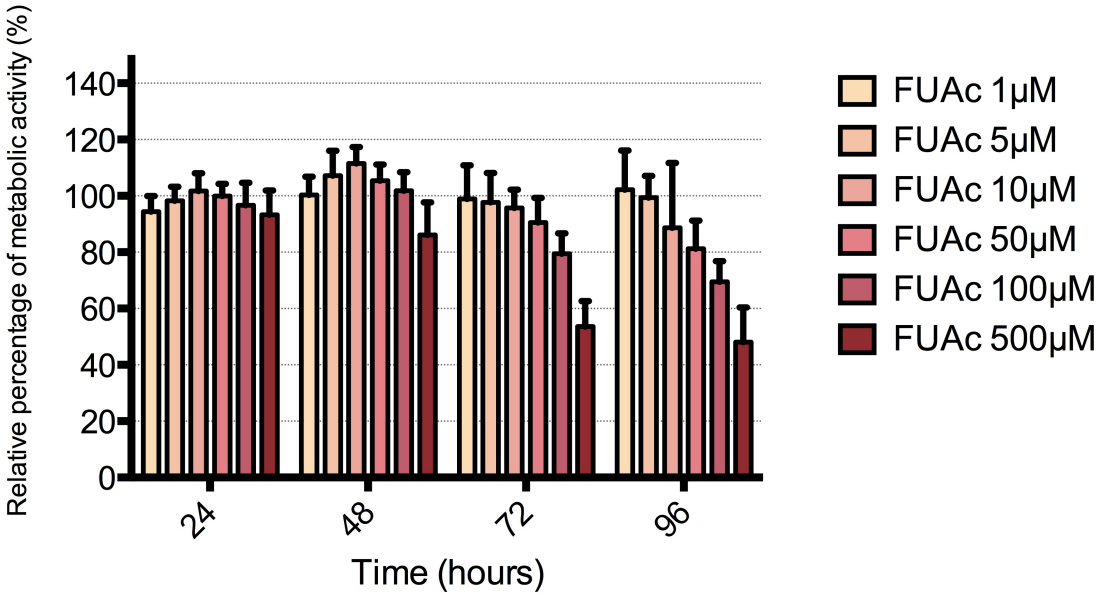


Figure 44: MTT results relative to MCF-7 for the tested time points and FUAc concentrations. Each different coloured column represents a different substance concentration and each group of columns describes results at the x-axis correspondent time point. The y-axis represents the relative cell metabolic activity in percentage compared to the control. Each bar corresponds to the average of 15 data points.

The analysis of FUAc on cell metabolic activity based on the graphic (Figure 44) suggests the existence of direct relation between compound concentration and metabolism inhibition (at 72 and 96 hours time points). The highest the concentration is, the strongest is the associated inhibition. Only at 96 hours time point a relative metabolic activity of less than 60% is achieved corresponding to the two highest concentrations (100µM: 53,63% ± 8,998; 500µM: 48,12% ± 12,24).

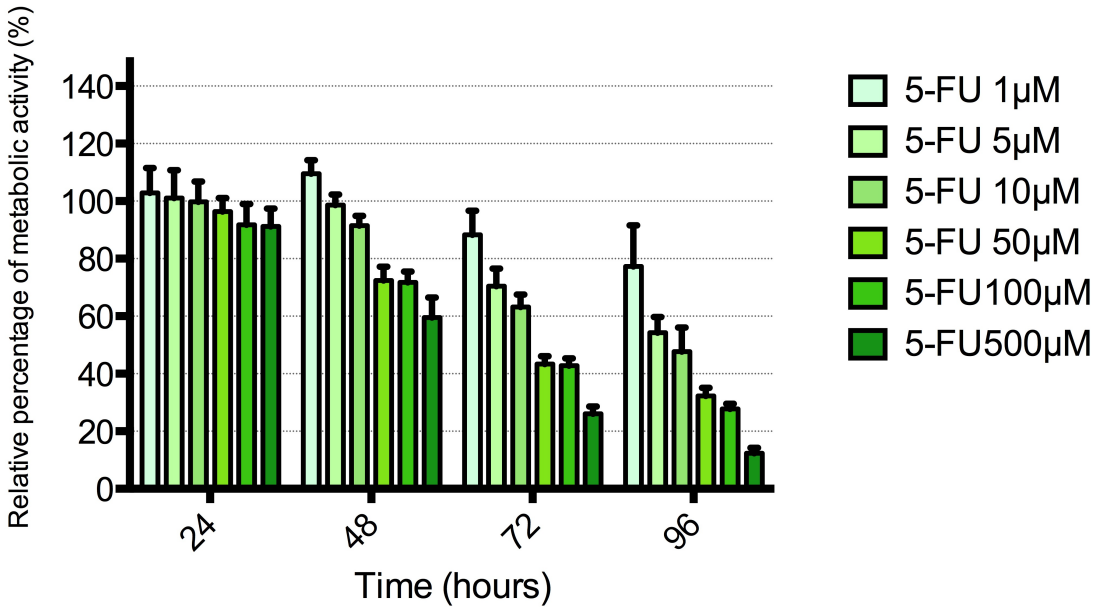


Figure 45: MTT results relative to MCF-7 for the tested time points and 5-FU concentrations. Each different coloured column represents a different substance concentration and each group of columns describes results at the x-axis correspondent time point. The y-axis represents the relative cell metabolic activity in percentage compared to the control. Each bar corresponds to the average of 15 data points.

Concerning to the last graphic in this section, Figure 45 that corresponds to results for 5-FU, there a notorious direct relation between concentration, time and metabolic activity percentage. The higher is the concentration and the longer is the incubation period, stronger is the inhibition. At 96 hours and with 500µM concentration the correspondent relative percentage compared to control of metabolic activity is 12,34% ± 1,898.

#### 1.1.1.1.1 Comparative substances inhibitory activity per time point

The next four chart groups (from Figure 46 to Figure 49) show box plots relative to tested compound at one certain time point.

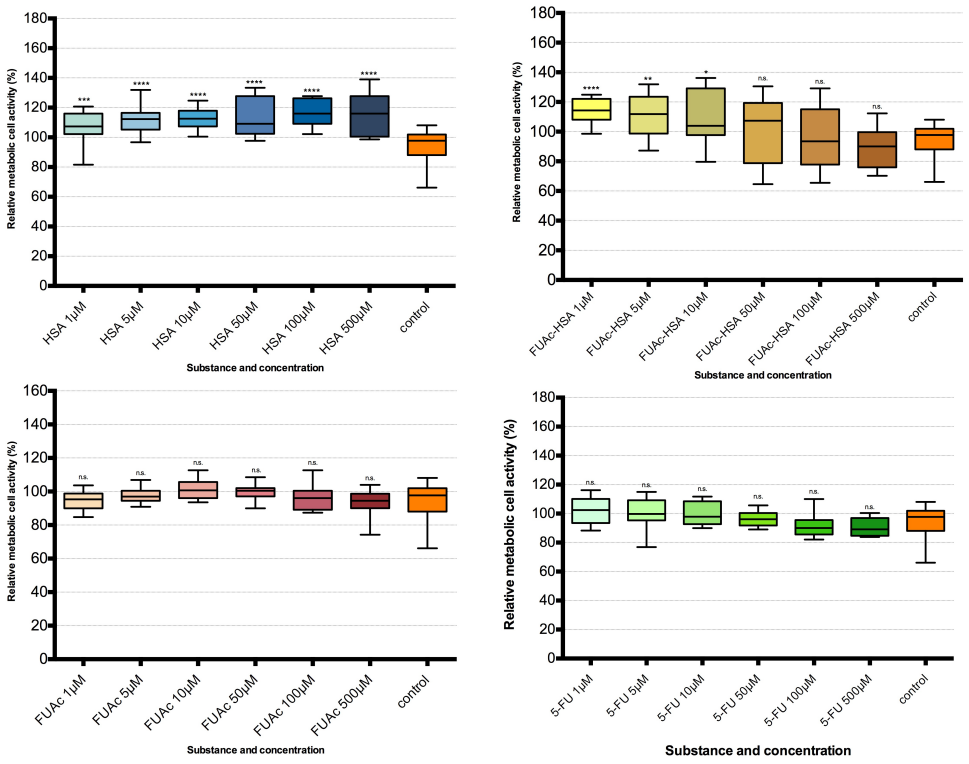


Figure 46: MTT results for MCF-7 cell line after 24 hours. Control group on orange on the right position in all above-listed plots, the remaining boxes correspond to tested compounds in the concentration referred on x-axis. n.s. states a P-value > 0,05; * a P ≤ 0,05; ** a P ≤ 0,01; *** a P ≤ 0.001; **** a P ≤ 0,0001, when compared to control. Top-left chart shows to HSA results, top-right to FUAc-HSA, bottom-left to FUAc and bottom-right to 5-FU.

Above results relative to 24 hours support the fact that 5-FU and FUAc action do not lead to a significant difference in cells relative metabolic activity. On the other hand all HSA concentrations and the three lowest FUAc-HSA concentrations can be associated with metabolic activity stimulation (HSA 1µM: P=0,0008; remaining concentrations: P<0,0001; FUAc-HSA 1µM: P<0,0001; FUAc-HSA 5µM: P=0,0018; FUAc-HSA 10µM: P=0,0159).

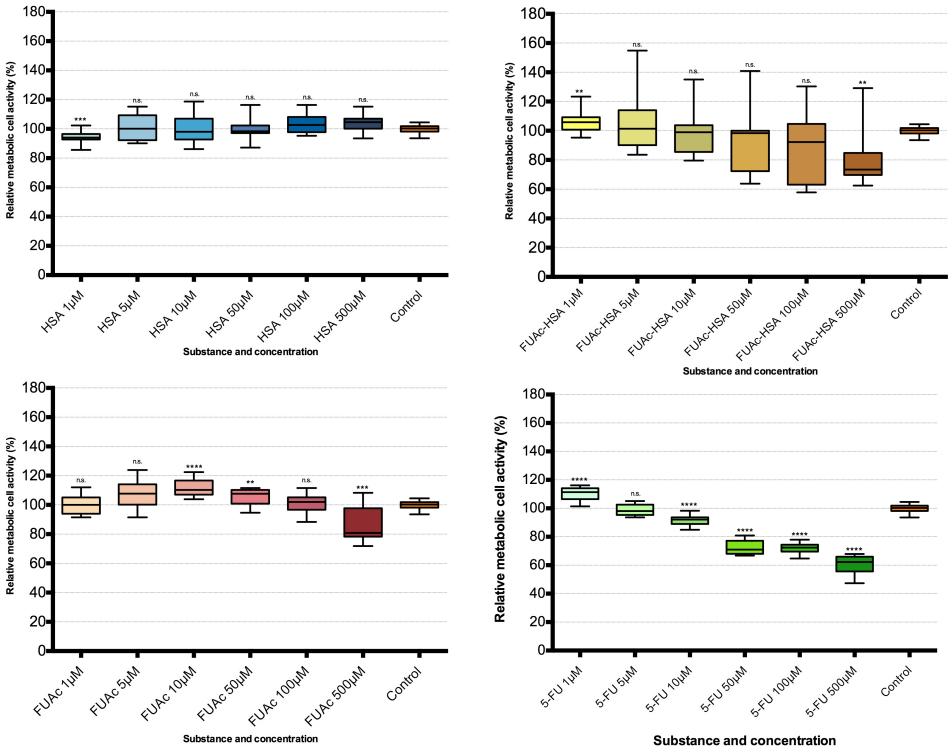


Figure 47: MTT results for MCF-7 cell line after 48 hours. Control group on orange on the right position in all above-listed plots, the remaining boxes correspond to tested compounds in the concentration referred on x-axis. n.s. states a P-value > 0,05; * a P ≤ 0,05; ** a P ≤ 0,01; *** a P ≤ 0.001; **** a P ≤ 0,0001, when compared to control. Top-left chart shows to HSA results, top-right to FUAc-HSA, bottom-left to FUAc and bottom-right to 5-FU.

The Figure 47 refers to results at 48 hours time point, where stimulating effect of HSA and FUAc-HSA is less pronounced, showing both substances statistical significant difference from control only for the lowest concentration (HSA 1µM: P= 0,0001; FUAc-HSA 1µM: P=0,0044). Also at this time point, FUAc-HSA 500µM is associated with cell metabolism inhibition (P=0,0020). Two FUAc concentrations and one from 5-FU are suggested to be associated with metabolism stimulation (FUAc 10µM: P<0,0001; FUAc 50µM: P=0,0034; 5-FU 1µM: P<0,0001). FUAc highest concentration and 5-FU concentrations from 10 to 500µM could be associated with cell metabolism inhibition (FUAc 500µM: P=0,0007; 5-FU 10 to 500µM concentrations: P< 0.0001).

The next chart group, shown at Figure 48, refers to 72 hours time point. HSA 10µM appears as being metabolic stimulating for cells, although with low statistic significance (P=0,0013) and the three highest concentrations of FUAc-HSA exert relative strong metabolic inhibition on cells (FUAc-HSA 50µM to 500µM: P<0,0001). All the considered 5-FU concentrations can be significantly associated with cell metabolic inhibition (5-FU 1µM to 500µM: P<0,0001) and the highest FUAc concentrations can be described as considerably metabolic inhibitory (FUAc 50µM: P=0,0023; FUAc 100µM and FUAc 500µM: P<0,0001).

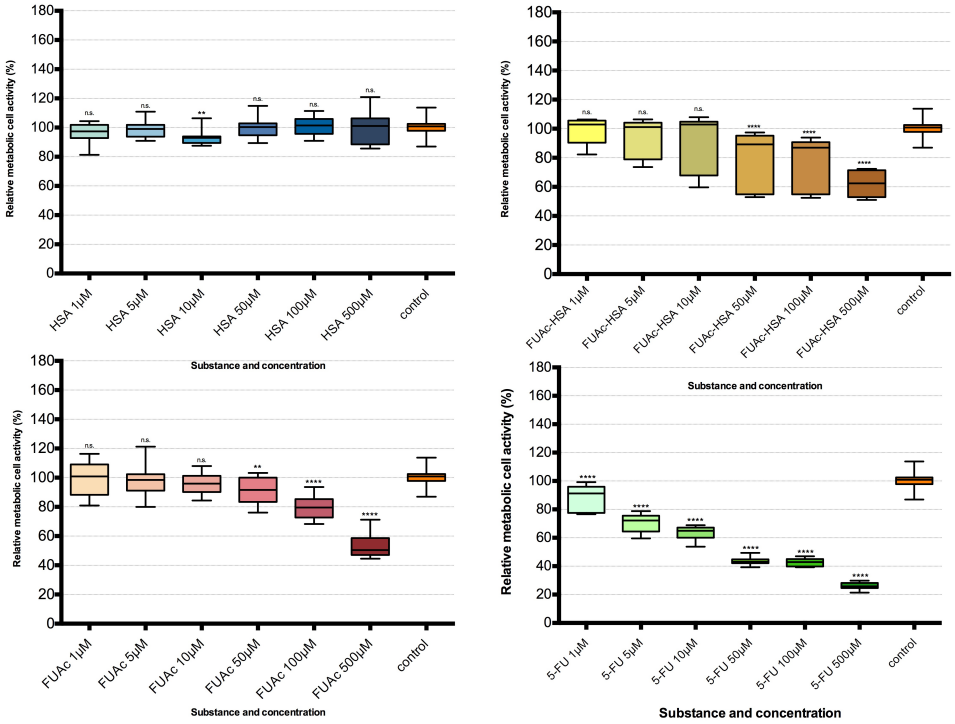


Figure 48: MTT results for MCF-7 cell line after 72 hours. Control group on orange on the right position in all above-listed plots, the remaining boxes correspond to tested compounds in the concentration referred on x-axis. n.s. states a P-value > 0,05; * a P ≤ 0,05; ** a P ≤ 0,01; *** a P ≤ 0.001; **** a P ≤ 0,0001, when compared to control. Top-left chart shows to HSA results, top-right to FUAc-HSA, bottom-left to FUAc and bottom-right to 5-FU.

The last group of charts in this section, Figure 49, suggests that HSA has no significant influence on cell metabolism, considering all the 6 different concentrations. FUAc-HSA is linked to relative strong metabolic inhibition with the highest concentrations (50, 100 and 500 µM) and not so significant with 5µM (FUAc-HSA 5µM: P=0,0044; FUAc-HSA 50 to 500µM: P<0,0001). All 5-FU concentrations and FUAc concentrations from 50 to 500µM show relatively strong association with cell metabolism inhibition (FUAc 50 to 500 µM: P<0,0001; 5-FU all concentrations: P<0,0001).

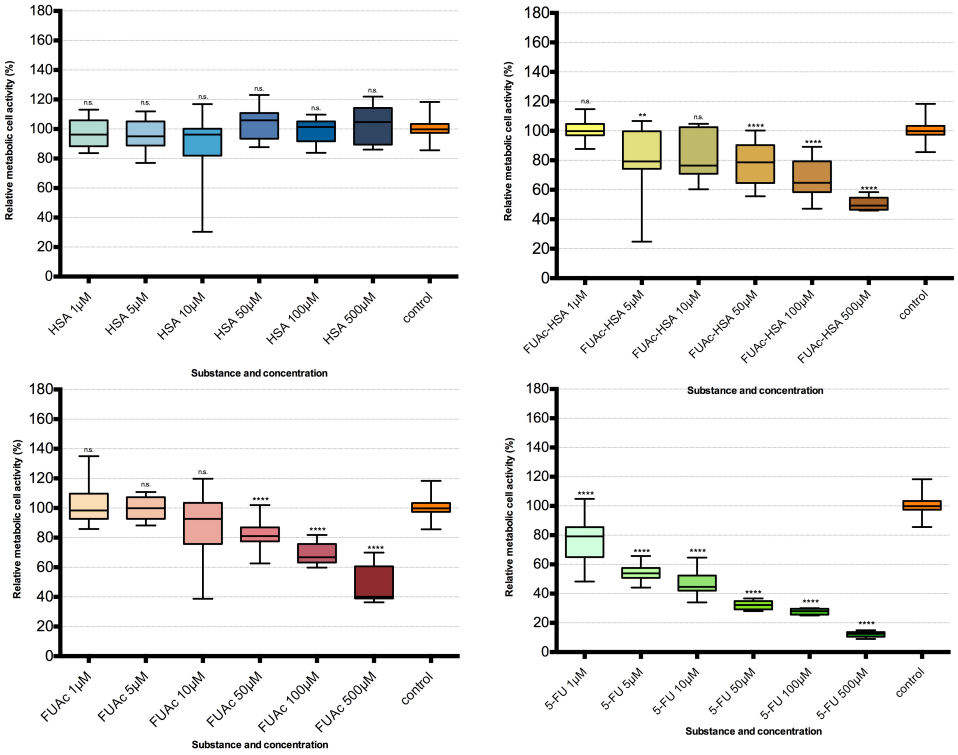


Figure 49: MTT results for MCF-7 cell line after 96 hours. Control group on orange on the right position in all above-listed plots, the remaining boxes correspond to tested compounds in the concentration referred on x-axis. n.s. states a P-value > 0,05; * a P ≤ 0,05; ** a P ≤ 0,01; *** a P ≤ 0.001; **** a P ≤ 0,0001, when compared to control. Top-left chart shows to HSA results, top-right to FUAc-HSA, bottom-left to FUAc and bottom-right to 5-FU.

### *3.3.3.2 Cell counting*

In Figure 50 is shown a bar chart with cell counting results for MCF-7, at 72 hours time point. As reported for the other cell lines, dead cells were inexistent or in a very low number.

Analyzing the present results, the HSA shows to have directly connected to concentration (HSA 50µM: 113% ± 5; HSA 100µM HSA: 98% ± 5; 500µM: 90% ± 3). FUAc-HSA is associated with a maximum cell growth inhibition for 500µM (71% ± 5) and weaker inhibition for lower concentration (FUAc-HSA 50µM: 88% ± 3; FUAc-HSA 100µM: 78% ± 2). Concerning to results for FUAc and 5-FU, relative cell growth associated with FUAc 500µM is similar to the caused by 5-FU 50µM (FUAc 500µM: 48% ± 5; 5-FU 50µM: 45% ± 10), being the lowest relative cell growth registered for 5-FU 500µM (9% ± 4).

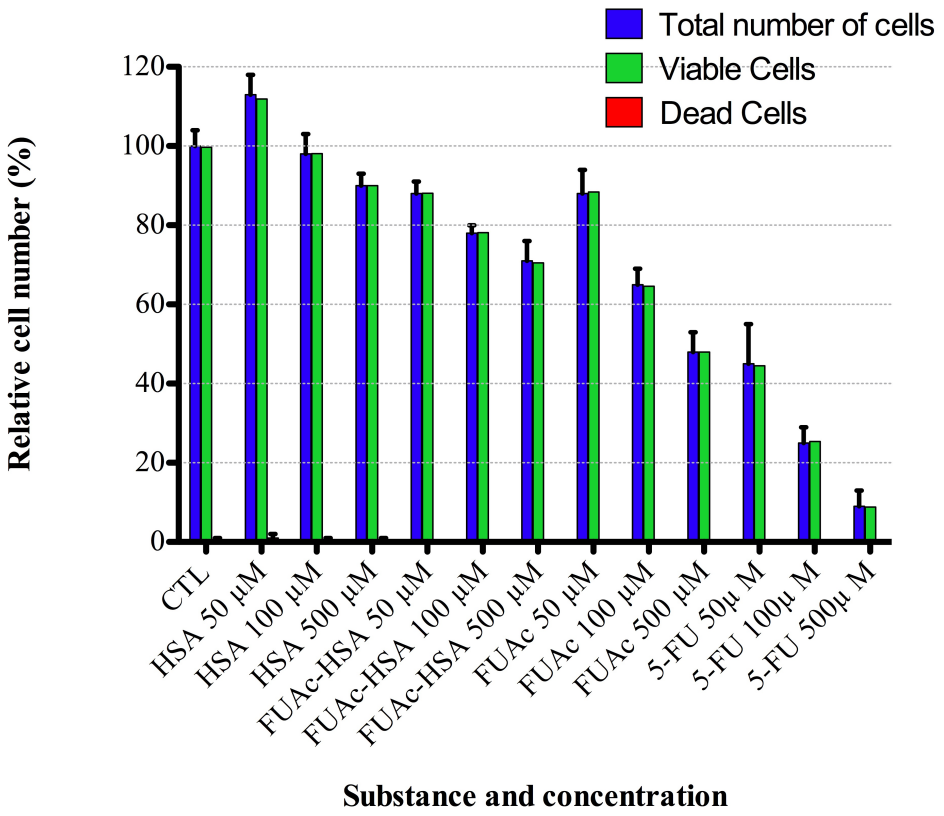


Figure 50: Cell counting results for MCF-7 cell line. X-axis lists the tested compounds and its concentration and y-axis is relative to cell number percentage compared to control cells. The y-axis represents the relative cell number in percentage compared to the control.

### *3.3.3.3 Half maximal inhibitory concentration (IC50)*

In Table 9, above-shown, are lists the IC50 values relative to tested substances with MCF-7 cell line.

.

| Substance / Time (hours) | 5-FU (µM, 95% confidence interval) | FUAc (µM, 95% confidence interval) | FUAc-HSA (µM, 95% confidence interval) | HSA (µM, 95% confidence interval) |
|---|---|---|---|---|
| 48 | 736,6 (523,4 to 1037) | – | 3394 (365 to 31561) | – |
| 72 | 39,66 (34,88 to 45,08) | 592,3 (464,8 to 754,7) | 1276 (548,6 to 2968) | – |
| 96 | 9,456 (7,996 to 11,18) | 413,8 (288,2 to 594,1) | 557,7 (304,3 to 1022) | – |

Table 9: Calculated IC50 for MCF-7 cell line considering the MTT assay results

The algorithm could not converge to a concentration value relative to FUAc at 48 hours neither for HSA relative to the listed three time points. As previously suggested by the other results, 5-FU has the lowest IC50 values and FUAc-HSA the highest.

| Substance / Time (hours) | 5-FU (µM, 95% confidence interval) | FUAc (µM, 95% confidence interval) | FUAc-HSA (µM, 95% confidence interval) | HSA (µM, 95% confidence interval) |
|---|---|---|---|---|
| 72 | 39,03 (4,624 to 329,5) | 401,6 (0,5046 to 319700) | – | – |

Table 10: Calculated IC50 for MCF-7 cell line considering the cell counting assay results.

### 3.3.4 Confocal Laser Scanning Microscopy

In this section are presented confocal laser scanning microscopy images of the three cell lines stained with DHR-123. The referred dye is burst sensitive, being visible as green fluorescence when a cell is active.

#### *3.3.4.1* T-47D cell line

The Effect of 5-FU and FUAc-HSA on T-47D cells activity can be related with the difference in shape and DHR 123 fluorescence seen in Figure 51. A high number of active cells can be seen in control (incubated with cell culture media without tested substances). By comparison with the other two images, there is a notorious difference either referring to the number of cells or the green fluorescence. All visible cells incubated with FUAc-HSA show a decreased fluorescence. In the third image, can be seen a cell with very little fluorescence and one aggregate with unusual shape and strong uniformly distributed fluorescence. This type of fluorescence can be explained by the fact that already dead cells are auto fluorescent.

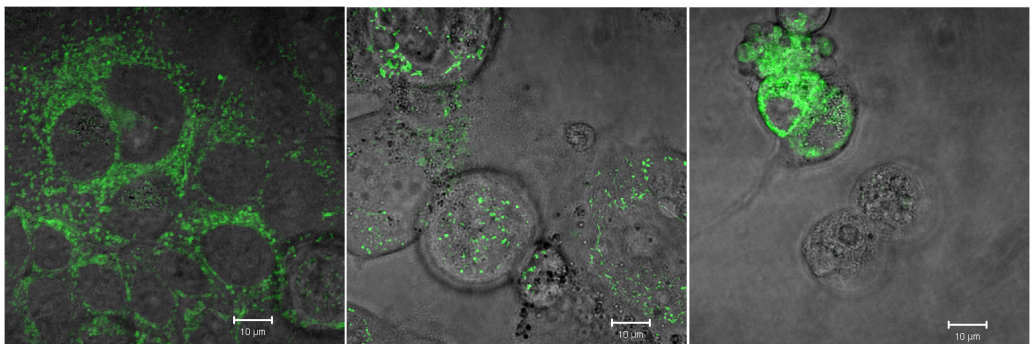

Figure 51: CLSM images of T-47D cells after incubation of 72 hours.

Picture on the left corresponds to control cells incubated with DHR 123; picture in the centre to cells incubated with FUAc-HSA and DHR 123 and picture on the right shows cells incubated with 500µM 5-FU and DHR 123.

### 3.3.4.2 MDA-MB-231 cell line

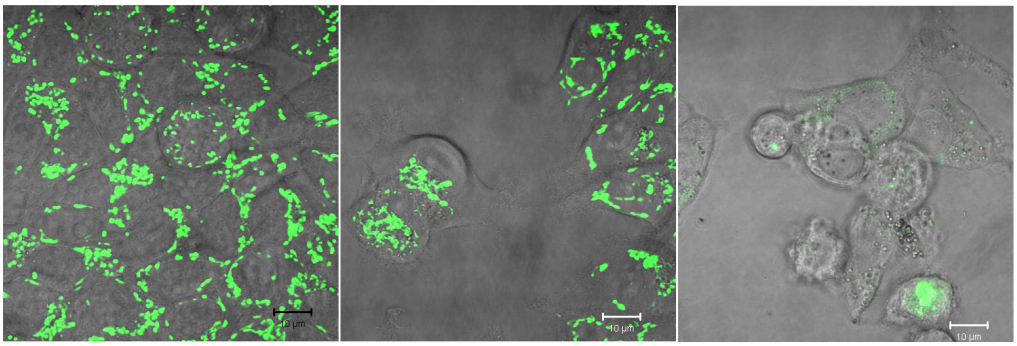

Figure 52 CLSM images of MDA-MB-231 cells after incubation of 72 hours.

Picture on the left corresponds to control cells incubated with DHR 123; picture in the centre to cells incubated with FUAc-HSA and DHR 123 and picture on the right shows cells incubated with 500µM 5-FU and DHR 123.

The inherent conclusions to Figure 52 are similar to the referred ones for Figure 51, a decreasing in fluorescence in cells incubated with FUAc-HSA is however not so evident in this image.

### 3.3.4.3 MCF-7 cell line

Pictures of MCF-7 (Figure 53) can be compared with pictures of the two previously described cell lines. Fluorescence and number of cells decrease is notorious as well as shape modifications on the cells incubated with 5-FU and FUAc-HSA.

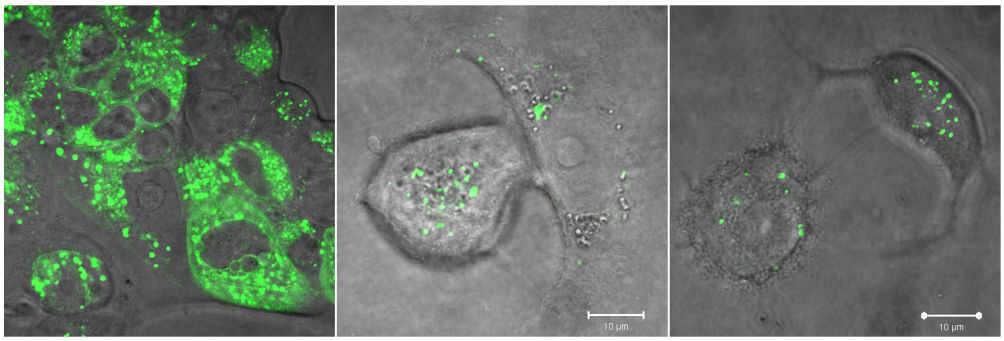

Figure 53: CLSM images of MCF-7 cells after incubation of 72 hours.

Picture on the left corresponds to control cells incubated with DHR 123; picture in the centre to cells incubated with FUAc-HSA and DHR 123 and picture on the right shows cells incubated with 500µM 5-FU and DHR 123.

# 4 Discussion

Cancer is a major health issue worldwide. Treatments for cancer have been contributing to prolong life of oncological patients even without complete remission of the tumor, however the side effects of the available treatments still represent a heavy burden for patients [98]. Within cancer treatments, chemotherapy has played a great highlighted role, being the most widespread approach to treat cancer. Around 1940, the world was experiencing early days of chemotherapy, with the emergence of nitrogen mustard as an effective treatment for lymphoma. From that day on, hundreds of new drugs were developed until the eighties, when the discovery of new drugs slowed down and there was a need of changing strategies namely by using rat models, creating a panel of human cell lines to test drugs and to boost molecular and genetic knowledge of tumors [17]. The last was a starting point for cancer-targeted therapies, what was also the base for this work. There was a previous work with FUAc and albumin at Institute of Transfusion Medicine, however using bovine albumin instead of human. Regarding the achievement of promising results that can be assessed at Koziol et al [11] it was decided to try the synthesis and characterization of similar conjugates with human serum albumin.

The aim of this project was to synthesize, characterize and perform in vitro tests with FUAc-HSA, a particle consisting of 5-FU acetic acid covalently bound to human serum albumin. FUAc-HSA microparticles were expected to overcome 5-FU main drawbacks (fast body clearance, low selectivity and severe side effects [99][29]) and came as the next step to previous work at Institute of Transfusion Medicine, where bovine serum albumin was used instead of the homonymous protein with human origin.

The followed procedures, as well as the obtained results, will be discussed in this chapter. Main technical problems and suggestions for future improvement of this research project will be discussed in the last point of this chapter.

## 4.1 Substances synthesis and characterization

### 4.1.1 FUAc

5-Fluorouracil acetic acid was synthesized according to a procedure adapted from Tada et al [8] that was previously described by Koziol et al [11]. To confirm the successful synthesis, FUAc was analyzed by NMR spectroscopy. There are $^{1}H$ and $^{13}C$-NMR spectroscopy results published however, to the best of our knowledge, there was none $^{19}F$-NMR spectra in published literature. Whenever we registered different results from the ones

reported by Tada et al [8] a suggestion for the reason of this difference is made in the respective subchapter.

#### *4.1.1.1 $^{1}$H-NMR*

As a an adapted version of Tada [8] protocol was followed in this work, a comparison between his $^{1}$H-NMR results and ours seems pertinent. In Tada's paper, reported results concerning to $^{1}$N-NMR were (referring to chemical shift δ): one singlet at 4,40ppm with AUC of two, one doublet at 8,09ppm with AUC of one and broad singlet at 11,18ppm with AUC of one. Reported peaks at 8,09ppm and 4,40ppm by Tada are comparable to the ones we obtained (8,08ppm and 4,36ppm, respectively) but a considerable shift was noted when comparing our peak at 11,9ppm and the one reported by Tada at 11,18ppm. Our results show one peak not reported by Tada, placed at 13,23ppm. According to our knowledge on FUAc molecule, this peak is expected since it corresponds to the carboxyl at $C^{2}$. Peaks reported by Tada are relative to only four hydrogen atoms but FUAc molecule have five.

#### *4.1.1.2 $^{13}$C-NMR*

As reported in the results section, we obtained 6 peaks for $^{13}$C-NMR analysis of FUAc, each peak corresponding to information related to the 6 constituting carbon atoms of the molecule. Tada et al [8] reports no results for $^{13}$C-NMR analysis and Kim et al [100] reports three peaks, with chemical shifts of 49,5ppm, 131ppm and 170ppm and assigned, respectively, to $C^{1'}$, $C^{5}$ and $C^{2'}$. Comparing with the results we obtained, it is noticeable the presence of three peaks with approximate chemical shifts (48,84ppm; 130,86ppm and 130,52ppm; 169,43ppm, respectively). As referred in Results section (3.1.1.1) each of the six carbon atoms should have a correspondent peak in the spectra, so we are lead to think that Kim et al either omitted the remaining peaks or for technical reasons they were not present in spectra. Small differences like the ones registered between our obtained results and the reported results in previous publications can be explained by different experimental conditions or different NMR equipment.

#### *4.1.1.3 $^{19}$F-NMR*

To the best of our knowledge, there is not a published $^{19}$F-NMR spectroscopy spectra of FUAc, therefore a parallel cannot be done. Anyway, based on the analysis presented at section

3.1.1.3, it seemed reasonable for us to conclude that the obtained $^{19}$F-NMR supports the success of FUAc synthesis.

### 4.1.2 FUAc-HSA

As referred in section 2.2.3 which is relative to FUAc-HSA synthesis methods, FUAc was bonded to HSA molecule using the EDC/NHS method [12][101]. There were other options available instead of using water-soluble carbodiimides (EDC) for the coupling of carboxylic group with amine, namely diazomethane, diazoacetyl reagents. Our choice fell on EDC since it was suitable for organic synthesis, versatile and of common use; therefore it was a well-documented substance. NHS played a role in reaction efficiency since it was reported to increase it. The last substance is also a reagent for activating carboxyl groups for conjugation with protein primary amines [102][103].

#### *4.1.2.1 MALDI-TOF*

This particular mass spectroscopy technique is suitable for protein detection and quantification and described as very sensitive, since it allows the detection of sub-femtomole concentrations, it is relatively easy to perform and inexpensive [104] [105].

The molecular weight obtained by MALDI-TOF analysis for human serum albumin is within the accepted range (difference of 200-300 Da), considering the molecular weight value given by the product provider [97][106].

Besides the peak corresponding directly to HSA molecular weight, another peak at 33158,95 m/z (singular ionization) is visible. This value corresponds to approximately double the mass charge of the singular ionization peak. This is a common occurrence in MALDI-TOF spectra as the analyte is ionized by a laser and if it gets double charged ($[HSA + 2H]^{2+}$) its kinetic energy through the time of flight tube will be two-fold the one of the mono-ionized analyte [107].

The amount of FUAc molecules bound to HSA was calculated according to the above-mentioned theory as well. As HSA, FUAc-HSA has two main peaks in spectra, at 34576,36 and 69238,58 m/z, being the last one approximately two-fold the first.

According to the previously referred formula $peak\ for\ FUAc-HSA - peak\ for\ HSA = \text{FUAc weight in FUAc} - \text{HSA}$ (Equation 12) the number of FUAc molecules by HSA molecule was the difference between the peaks corresponding to the two substances. The average number calculated was 15 FUAc per HSA.

Albumin particles prepared with a similar technique and described by Dosio *et al* [108] were reported to achieve a loading of 30 paclitaxel molecules per HSA, so it can be technically possible to load more FUAc into HSA either using a different coupling technique or adjusting the followed coupling procedure. However, it is also described at Dosio *et al* that HSA does not suffer significant change in global charge with up to 10 paclitaxel molecules per HSA so according to this, it is possible that higher HSA loading leads to molecule modifications. Frei and [20], support that albumin maintain its physiological stability and half-life with loading ratio up to 1.4 mole of drug per mole of HSA. Stehle [109] reported that loading ratios close to 1:1 for MTX-HSA achieved optimal conditions for targeting MTX into tumors in rats. Taheri [48] prepared MTX-HSA particles with EDC as crosslinking agent, though this was a process similar to ours. In his work, Taheri compared cytotoxicity of MTX-HSA with loading molar ratios of 12, 8 and 2 MTX per HSA and the best results were achieved with the conjugate of molar ratio 12 (IC50 values, in ng: 14,3; 24,6 and 45,6 corresponding to loading molar ratios of 12, 8 and 2 MTX per HSA, respectively).

Considering the works previously referred and the fact that MTX has a molecular weight (454,44 g/mol) much higher than FUAc (188,1 g/mol), we believed only small changes to occur in HSA structure. In order to evaluate HSA structure before and after the coupling of FUAc we used CD-Spectroscopy. The maintenance of HSA native structure seems to play an important role in its cell uptake.

#### *4.1.2.2 CD-Spectroscopy*

As referred in the previous subchapter, CD-Spectroscopy was performed to assess conformational changes of HSA. This technique was previously chosen for this purpose, namely by Tavirani et al [110], Varlan et al [111] and Zsila et al [112].

The result we obtained was the expected as the probability of FUAc-HSA to behave like pure HSA should be higher without significant protein modification due to FUAc coupling.

Albumin secondary structure was compared with its structure in FUAc-HSA compound. Secondary structure of pure HSA and HSA was calculated according to [113] and the obtained values were 69,99% α-helix and 9,68% of β-strand for pure HSA and 69,45% α-helix and 9,71% for FUAc-HSA. Therefore, no significant change in conformation was observed when comparing HSA to FUAc-HSA. Figure I of Annex III shows the difference between both CD-Spectroscopy spectra, where the little difference between them is also notorious.

## 4.2 *In vitro* tests

In this section will be discussed the obtained results for cytotoxicity tests presented in chapter 3.3.

### 4.2.1 MTT

#### *4.2.1.1 Cell metabolism inhibition due to 5-FU*

This anti-metabolite drug is described as having a strong cell inhibition activity, even with very low doses. It was previously reported [114] that its activity is related with the time of incubation with cells so for incubation of 72 hours with up to 7,7µM an inhibition of 50% of the cells was achieved. IC50 values for 22, 72 and 96 hours with HT-29 cells were, respectively 13,1µM, 8,1µM and 5,8µM. These values are not very different from the values we obtained for MDA-MB-231 and T-47D cell lines.

Concerning to our results, the highest cell metabolism inhibition was caused by 5-FU, as can be confirmed by the results in chapter 3.3. IC50 values obtained from MTT results are very low, mainly for 72 and 96 hours time points. At 48 hours time point, differences on IC50 values referring to the three cell lines were higher, however standard deviation for MTT data is also generally higher.

It is possible that the presence of phenol red in the culture media influences the cell response to 5-FU since T-47D and MCF-7 have estrogen receptors and has been suggested that this compound can promote these cells proliferation acting as a estrogen analog [115]. By this association, MDA-MB-231 is not supposed to be much affected by phenol red because it is a triple negative cell line, so it does not express high levels of estrogen receptors [116]. Results obtained in this work are consistent with the previous stated since MDA-MB-231 cell line is the one with the lowest IC50 values, followed by T-47D and MCf-7, respectively. The last cell line had a slower growing rate when compared to the other two, so a slower response to 5-FU is also explainable in this way because its action mechanism affects preferably dividing cells [117].

#### *4.2.1.2 Cell inhibition due to FUAc*

FUAc exerted a weaker inhibition in all cell lines if compared with 5-FU, with remarkably higher values of IC50 for T-47D and MCF-7 at 48 hours time point. Repeating what occurred with 5-FU, MCF-7 was the cell line less sensitive to FUAc.

Considering FUAc chemical structure, the methyl-carboxyl group at $N_1$ in the uracil group changes the molecule in a way that makes it no longer a direct pyrimidine analog, interrupting the conversion chain from 5-FU to its metabolites. In fact, Luo *et al* and Chung *et al* state that it is not likely to occur a conversion of pure FUAc into 5-FU [118][10].

Terminal carboxyl group present in FUAc is responsible for the molecule charged state at physiological conditions, slightly more hydrophilic and higher polarity than 5-FU [8][119]. Due to these characteristics, FUAc is less likely to penetrate the cell membrane either by the non-privileged interaction with the cell membrane or the lack of resemblance with uracil [120].

#### *4.2.1.3 Cell inhibition due to HSA*

Regarding the three cell lines used through this work, none of them showed considerable reaction to incubation with HSA. At some time points could be considered that it caused a slightly increasing cell activity however it is not significative. Data published on this matter is contradictory. A previous publication reported MCF-7 and T-47D cell growth stimulation due to the presence of HSA in culture media and no influence on MDA-MB-231 [63], however we could not register a strong tendency on this subject. Powell at al [40] reported that serum albumin inhibits the proliferation of T-47D and MCF-7 cell lines, although it showed no effect on MDA-MB-231. Our MTT results had not shown a clear tendency of a cell inhibition caused by HSA either.

An explanation to consider is that HSA concentrations in the performed cell tests were kept under typical physiological concentration, reported as being between 30 and 35 g/L blood (or, less than 526μM) [35], what is perhaps not enough to reach high concentrations for an accentuated response of the cells. Chan et al [121] reported that human serum albumin has its characteristic degradation of N-terminal in temperatures around 30ºC. Serum albumin from other species, namely bovine, chicken and rabbit were also tested and this degradation could not be observed. Since Powell et al described the serum albumin N-terminal as responsible for cell growth inhibition and this undergoes a degradation process at temperatures reached during our experiments, HSA might had lost its inhibitory activity on the cells with mABP receptor.

#### *4.2.1.4 Cell inhibition due to FUAc-HSA*

The synthesized FUAc-HSA particle did not show a strong inhibitory effect in neither of the tested cell lines, not achieving an associated inhibition of more than 50% cell metabolism. By comparing the results obtained for FUAc-BSA by Koziol *et al* [11] and the ones presented in this work it is possible to conclude that FUAc-HSA shows a weaker inhibition on T-47D and MDA-MB-231 cells. An explanation to consider can be the higher loading ratio achieved at FUAc-HSA of 15 FUAc molecules per HSA molecule against twelve FUAc molecules per BSA at FUAc-BSA. This higher loading ratio can modify HSA structure and slow the uptake of the particle by the cell. In previous publication [122] it is referred that BSA has a higher binding constant for Uracil than HSA, in a molecular scale, this can lead to an advantageous particle conformation for FUAc-BSA when compared to FUAc-HSA when considering the cell uptake of the particle. It was already referred in this work that HSA suffer degradation in its N-terminal at 30ºC or higher temperatures. This domain plays a role in MCF-7 and T-47D cell inhibition by HSA. It has also a possible role in the binding reaction of HSA to FUAc [11]. Therefore, this specific degradation of HSA, which does not occur on BSA, can explain the difference between the results obtained for the two particles. These differences in the protein conformation can influence both in the particle synthesis and in cell uptake.

To the best of our knowledge, there are no previously published results related to in vitro cytotoxicity tests with FUAc-HSA. Chung *et al* [10] reported release of 5-FU from FUAc-HSA after administration in rabbits and in PBS with degrading enzymes, however there is no information about HSA loading ratio. FUAc-HSA was reported to be present in rabbit plasma much longer than pure 5-FU (1μg/mL up to 36 hours versus terminal half-life of 8 minutes). This prolonged presence in rabbits blood is related to slow release of 5-FU from FUAc-HSA particles, since the cleavage might happens either due to enzyme activity or zero-order kinetics.

The inhibition of cells should be discussed based on the known process for albumin cell uptake, described previously in this work. The cellular uptake process of albumin runs mainly by endocytosis [39][20] and albumin is subsequently degraded at the endosomes.

Albumin showed affinity with membrane proteins, namely the gp60 that is reported to be present in endothelial cells. This glycoprotein binds to albumin and the endocytic process is triggered, leading the formed endosome through the cell to the extravascular space [19][13]. SPARC is another protein reported to be secreted by some cancer cells to extracellular matrix, to which albumin binds to [39][46]. In fact, this was one of the associated facilitators reported by Desai *et al* [13] for inhibitory effect of nab-paclitaxel. The other protein reported to have an influence on albumin effect on the cells was mABP [40].

The choice of the three cell lines for our in vitro tests was made mainly based on the presence of the last two referred proteins, mABP and SPARC. As so, MCF-7 were described as expressing both, T-47D only one (mABP) and MDA-MB-231 none of them [13][40][123]. Regarding the previously described hypothesis for uptake of HSA particles, MCF-7 should be the most inhibited cells by FUAc-HSA, followed by T-47D and MDA-MB-231 being the less affected. In fact, IC50 value for FUAc-HSA on MCF-7 is the lowest when compared to the other cell lines but only at 96 hours time point. This result can be in fact supportive of the described hypothesis due to this cell line slow growing rate. It was previously referred that FUAc and 5-FU took longer to show strong inhibition on MCF-7 than with the other cell lines. It should also be noted that IC50 relative to FUAc and FUAc-HSA at 96 hours with MCF-7 are more similar between them than in the other cell lines (IC50 FUAc is 413μM and for FUAc-HSA 557,7 μM). MCF-7 is the cell line exhibiting highest inhibition after incubation with the 500 μM of FUAc-HSA for 72 and 96 hours, however not registering a wide difference from the results obtained for the remaining cell lines this difference is statistically significant at 96 hours (MDA-MB-231 vs MCF-7: p-value 0,0019; MDA-MB-231 vs T-47D: p-value= 0,0083; T-47D vs MCF-7: p-value < 0,0001).

Based on this evidence, it should be interesting to either add another time point at 120 hours of incubation or seed more MCF-7 cells when starting the assay because they grow faster when get more confluent, in order to better understand the connection of FUAc-HSA action and SPARC/mABP. Comparing the other two cell lines, the IC50 values are in accordance with the expected and described by Koziol *et al* since T-47D cell were more inhibited by FUAc-HSA at all considered time points.

Evidences of pure 5-FU release from FUAc-HSA particles were published by Wang et al and Chung *et al* [10][118]. The exact process in how the cleavage occurs is however not clear.

### 4.2.2 Comparison between trypan blue cell counting and MTT results

Cell counting and MTT results should not be compared directly since they do not assess the same exact variables [124]. MTT is reported to assess critical biochemical cell function [125] and it has been described as a quantifier of mitochondrial activity. Cell counting assesses the number of cells, which depends on cell division, since the results show the relative percentage of cells compared to control (control was considered to be cells incubated only with adequate cell culture media). The latter procedure has an associated error of approximately 25% due to miscounting, errors in chamber loading and statistical errors generated by a low cell number in counting chamber.

Adding trypan blue after incubation was chosen for the screening of dead cells. It is described as a compound that takes advantage of affinity for some cell nuclear component and enters the cell due to the breakdown of the diffusion barriers in the membranes, possibly associated with a molecular rearrangement of the chromatin. A membrane from a healthy cell should not be permeable to trypan blue [126]. The number of dead cells was negligible for all cell lines and drug concentration, besides for 500μM of 5-FU in T-47D.

Cell counting results show a tendency similar to MTT: very strong inhibition of cells due to 5-FU; relatively weaker inhibition with FUAc, weak inhibition of MDA-MB-231 and MCF-7 due to FUAc-HSA (there was a high inhibition of T-47D) and no apparent effect on cells linked to HSA, except T-47D. Although, cell counting results show a stronger cell inhibition relative to T-47D and MCF-7 than MTT results, by direct comparison of substance and concentration effect. However, the difference is not so wide that the differences between MTT and cell counting could not be based on the different processes to which the assays assess. There are evidences that an increased tumor cell metabolism, namely the production of reactive oxygen species (ROS), is not necessarily associated with increased cellular proliferation and is dependent on several cell characteristics [127][128].

Conversion of MTT to formazan occurs in the presence of NADH, NADPH, mitochondrial dehydrogenases and free thiol group of cysteine [79][129]. Funk et al described an over-estimation of cell activity in MTT results when albumin was added to cell media [129], what can be considered by comparing our results from cell counting and MTT.

The most accentuated differences between MTT and cell counting results were registered for T-47D cell line incubated with 500μM HSA and all the three concentrations of FUAc-HSA and FUAc. Based on the cellular reduction chain of MTT to formazan, we considered the hypothesis that acetate present in FUAc and FUAc-HSA is cleaved and left free inside the cells, being posteriorly activated by acetyl-coA synthetase and thus creating acetyl-coenzyme A (Acetyl-coA) [130]. Acetyl-coA enters the citric-acid cycle, which produces NADH (a MTT reductor) so an acceleration of citric cycle can occur due to extra availability of acetyl-coA, as previously observed for prostate cancer cells [11][131]. The previously referred process can lead to over-availability of NADH, and consequently an over-reduction of MTT not merely connected to the cancer cell normal metabolism.

Another reason for this difference can be the different ways in which the tested drugs lead cells to stop or slow its proliferation. Mooney *et al* [132] reported different apoptic mechanisms between MCF-7 and T-47D cell lines, both in timing and in involved cellular entities. As so, can be considered that not all cell lines have the same mechanisms leading to its apoptosis.

Cell counting experiments were not performed with all the concentrations chosen for MTT since it is a time consuming procedure and we could not guarantee cell integrity by keeping them out of the $CO_2$ during such a long period. This change of incubator had to be carried out due to facility constraints. The reduction of the number of concentrations to test from six to three was tough seen as the more adequate option. Since MTT assay was performed before cell counting, its results were analyzed and the three highest concentrations were chosen for cell counting due to the apparent absence of cell metabolism inhibition associated with the lowest concentrations. The choice for the 72 hours time point was based on the previous experiments with FUAc-BSA, where cell counting was also performed at the same time point, and based on MTT results since cell inhibition was already evident. In the ANNEX II the standard deviation between MTT and cell counting results can be consulted.

### 4.2.3 Confocal scanning laser microscopy images

To support MTT and cell counting results, confocal laser scanning microscopy images were obtained to assess cell metabolism and cell anatomy. The obtained images can be seen from Figure 51 to Figure 53. Results from CLSM can be related with MTT results since it is clear, when comparing images relative to T-47D and MCF-7, a reduced fluorescence inside the cells incubated with FUAc-HSA if compared to control cells. Cell shape is also different from control cells and more similar to shapes exhibited by cells incubated with 5-FU. Images relative to MDA-MB-231 cell line do not exhibit such a difference in fluorescence between cells incubated with FUAc-HSA and control however there is a notorious lower cell confluence and modifications in shape. Since the referred microscopy images were intended to provide a qualitative idea of cell metabolism and anatomy, a further analysis do not seem pertinent.

## 4.3 Critical review

The most debatable procedures in this work are MTT and cell counting. Both the referred methods have a relatively high associated error. Referring to cell counting, associated error is between 20 and 30%, mainly due to pipetting, counting and statistical errors [133]. MTT in turn have biased results due to modifications in cell metabolism, interaction with compounds in culture media (like HSA, for instance) and even due to unequal evaporation associated with 96 wells cell culture plates [134][135].

As aforementioned, MTT results for 24 hours have a large standard deviation. Data relative to 48 hours tended to exhibit lower standard deviation, what led us to consider the data

relative to 72 and 96 hours more reliable to infer the drug influence on cell culture. One reason for such wide spread results mainly at 24 and 48 hours concerning MTT can be the influence on cell cycle exerted by trypsin, used for cell passaging [136]. A study performed with MCF-7 cell line to assess trypsin-induced proteome alteration found that several proteins known to regulate cell metabolism, cell growth, mitochondrial electron transportation and cell adhesion were down-regulated after trypsinization and proteins that regulate cell apoptosis were up-regulated [136]. It was previously reported that mitogen-stimulated mouse spleen cells are more active in MTT to formazan reduction than resting cells [79]. Therefore, the decreasing tendency of standard deviation along the time, which was observed in MTT results, can be associated with above-mentioned information. We hypothesized as well that with prolonged incubation period cells had time to recover their normal metabolic activity and the influence of trypsin was overtaken since it was removed from culture media when the drugs under research were added.

Concerning to cell counting, it proved to be a very useful technique for cell inhibition, although very time consuming. In order to have an adequate number of cells to count we had to seed them in a twenty-four well plate hence creating different conditions for the cells to grow, namely growth and gas-exchange area. The number of cells to seed for each cell line had also to be adjusted since they have different growth curves. Even trying our best to create conditions as similar as possible as the ones of MTT assay, they were inevitably different. Interestingly, previous publication focused on drug resistance related to cell confluence in colorectal and it was suggested that the more confluent the cells were, the more they were resistant to the drug [137]. This could be a hypothesis for explanation of discrepancies between MTT and cell counting results as well since cells were usual less confluent in 24 well plates than in the 96 well plates. The 24 well plates were used for cell incubation in cell counting procedure and 96 well plates for MTT assay.

IC50 values were calculated according to cell inhibition for each of the six concentrations of each substance used in the MTT assay and for the three concentrations of each drug substance in the cell counting experiments. This value was meant to provide a clear way to evaluate how strong the cells were inhibitied by a drug. We considered that it fulfilled its purpose, however it could be more significant by adding more drug concentrations, what would be interesting for future experiments. The discrepancy registered between IC50 values calculated from MTT and cell-counting data can be due to the differences already referred between the two assays, to the error associated with both of them or even with the differences between the cell lines and how fast they divide react to 5-FU. It should be considered that IC50 values were calculated using a fitting equation, so the less data points, the less accurate it can be. This difference can also be noticed by looking to the confidence intervals associated with

IC50 from MTT and cell counting: the ones relative to cell counting are much wider. Referring to results for T-47D cell line, the IC50 values obtained for inhibition due to 5-FU vary approximate and for FUAc the difference is not very wide (592 μM with MTT data and 413 μM with cell counting).

Finally, as mostly performed *in vitro* tests, the ones performed by us were intended to simulate real tumor environment, which were obviously impossible to achieve. Since there was a lack of media circulation, it is difficult to predict how different could the results be if taking body clearance of the drugs into account. Considering the inherent physiologic theory, it is possible to hypothesize an increasing gap between 5-FU/FUAc and FUAc-HSA cell inhibition since the latter would be cleared from circulating blood much latter than the first referred substances.

Incubation of the three cell lines with fluorescence stained HSA was attempted, although not successful due to technical issues in the stained protein synthesis. This experiment should however take place in the future in order to prove HSA uptake of cultured cells, what could give an overview about the hypothesis that HSA uptake by cell is directly connected to the presence of mABP and SPARC proteins in each cell line.

## 4.4 General considerations and major issues

Motivation for this work came mainly from the previous successful tests described by Koziol *et al* [11], in which bovine serum albumin was used instead of the human homonym protein. Based on the previously shown cytotoxic effect with FUAc-BSA, which was chosen due to its much lower price compared to HSA, the project was continued by substituting BSA with HSA.

Bovine and human albumins are very similar, sharing approximately 76% of their amino-acid sequence, similar secondary structure and net charge, being its main difference the fact that BSA contains one tryptophan residue while HSA contains two [138]. A recent study [139] supports however that the assumption of similar behavior between HSA and BSA should not be made due to different molecular characteristics. Considering the hypothesis of future human tests with this particle, BSA should not be used due to documented occurrence of allergic reactions [140][141].

Previous work on the FUAc-HSA particle lacked adequate particle characterization (HSA loading ratio) and a synthesis protocol description [10]. However they tested the particle in vivo and reported the detection of 5-FU in the rabbit's blood even thirty-six hours after injection and 5-FU was detected in the brain by intravenous administration of 5-Fluorouracil

acetic acid HSA conjugates. 5-FU could not be detected in the brain by administration of pure 5-FU and 5-FU acetic acid (FUAc). Therefore, we considered the hypothesis of a similar behavior from our FUAc-HSA conjugates, however in a careful way and requiring further confirmation.

In the previous work with FUAc-BSA conjugate, only three drug concentrations were chosen for *in vitro* tests: 100, 300 and 500 μM. As referred in the methods section, the FUAc-HSA concentration of 500 μM is equivalent to 500 μM of 5-FU. When designing the experiments for this project, there was a decision to change the tested concentrations taking into consideration works of Takimoto *et al.* and Furuya *et al.* [142][143]. They reported 5-FU serum concentrations of a maximum of approximately 12 and 10,5μM in humans treated with 5-FU infusions administered intravenously. Therefore we considered testing lower concentrations comparing to the ones previously chosen. Regarding the results, no significative cell inhibition was achieved with concentration under 100μM for FUAc-HSA, however 5-FU can be associated with strong cell inhibition even in the concentration of 1μM at 96 hours time point. These results suggest either that not all 5-FU was released from FUAc-HSA so the incubation time should be prolonged or that the drug released is not pure 5-FU so it has not the same cytotoxic power as 5-FU. Therefore, in future experiments, could be interesting to add at least one more time point (120 hours) in order to have a better overview of FUAc-HSA cytotoxicity and how dependent it is on the time of incubation.

HSA high loading ratio was associated to conformation changes and higher accumulation in liver (or other organs with mononuclear phagocytosis system) by Stehle *et al* [18]. When Stehle *et al* administrated HSA with less MTX bound particles to rats (1:1 ratio), they detected more accumulation in tumor (about 14% of total compound administered), as so we hypothesized that FUAc-HSA could have a similar pharmacokinetic profile. This could lead to differential HSA loading ratios to target either kidney or liver tumors or tumors located in another body structures, like breast for instance. A lower molecular weight of FUAc when compared to MTX should however be highlighted (188,1 to 454,56 Da [144]) what suggests that could be possible to load HSA with more FUAc than MTX molecules and maintain HSA native conformation.

Major issues faced when working in this project were to overtake uneven cell growth in cultures at 96 well plates for more than 48 hours and to optimize DNA extraction protocol. For approximately one month we had to dispose MTT assays since control cells were not reducing MTT after incubation for 48 hours. Plates and media were screened and finally we found that the problem seemed to be the way of placing the plates in the incubator. As for each run of MTT assay eight 96 well plates were needed, we used to place four of them in a pile, being the one corresponding to 24 hours assay on top and the one for 96 hours on the bottom of the pile.

After starting to place every plate directly on the incubator shelf the problem was solved. Our hypothesis was that placing the plates in such a way blocked airflow for plates on the bottom and cells started to die.

Regarding DNA extraction, the first extraction kit that we tried was apparently not effective and the respective protocol was also not very clear, so we decided to try it several times by adjusting the number of cultivated cells but this was not successful. This process took approximately one month and the first time a new extraction kit was tried (the kit referred in material section (2.1), we could obtain DNA from cells incubated with FUAc and 5-FU nonetheless was not possible to obtain further results on that experiment before the submission of this work.

## 4.5 Conclusion and suggestions for future work

As a conclusion, it seems reasonable to state that FUAc-HSA effect looks promising, however its relation with SPARC expression in cells was not very clear by considering the results of this work. Further tests on this conjugate, namely 5-FU release and half-life in blood-circulation would be of great interest if we take into account results obtained by other groups handling particles with similar characteristics to FUAc-HSA. Our results suggest that mABP plays a role in FUAc-HSA effect on the cells, perhaps more central than SPARC since the difference between results regarding to MDA-MB-231 and T-47D are wider than between T-47D and MCF-7. The role of SPARC and mABP proteins in cell endocytic uptake appear as an interesting subject to be focused on future investigation since it can reveal unknown pathways of albumin-bound drugs uptake.

Incubating the particles in a physiological solution and performing a HPLC analysis could assess 5-FU release from particles. In vivo tests would be of great help in order to improve the knowledge about the body clearance and stability of FUAc-HSA.

There could be interesting to find out if our reaction for FUAc-HSA synthesis could be adapted in a way that make possible the control of HSA loading ratio.

Based on the literature research done for this work, we found a lack of papers comparing non-tumorigenic cells to tumor cells. It could lift the veil on how selective the particles can be to test them with MCF10 cell line, for instance.

Different cytotoxicity tests might be important before moving to animal tests in order to validate the results already obtained. Tests based on substances like calcein and ethidium homodimer-1 assess at the same time membrane integrity and esterase activity and quantification is made by flow cytometry without the need of washing steps.

Considering the current world economy and therefore the unavoidable cost control in healthcare, this approach fit in cost reduction at long term. For FUAc-HSA synthesis, the most expensive material is HSA, being however not prohibitive. Besides that, all the other substances are fairly cheap and the synthesis reaction can be easily reproduced. If FUAc-HSA works as the theory predicts and previous preliminary tests suggest, treatment with this particle instead of pure 5-FU would prevent oncologic patients from further health issues due to 5-FU systemic toxicity. A higher dose of 5-FU could be reached in the vicinity of a tumor, keeping its systemic concentration lower. However this represents a mere hypothesis and several years of research on this compound will be needed in order to overtake human tests.

# 5 References


[1] American Cancer Society, “Global Cancer: Facts and Figures, 2nd Edition”, 2008.

[2] H. Maeda, J. Wu, T. Sawa, Y. Matsumura, and K. Hori, “Tumor vascular permeability and the EPR effect in macromolecular therapeutics : a review,” *J. Control. Release*, vol. 65, pp. 271–284, 2000.

[3] T. K. Pathway, C. Tiruppathi, W. Song, P. Sass, A. B. Malik, and M. Bergenfeldt, “Gp60 Activation Mediates Albumin Transcytosis in Endothelial Cells by Gp60 Activation Mediates Albumin Transcytosis in Endothelial Cells by Tyrosine Kinase-dependent Pathway *,” *J. Biol. Chem.*, vol. 272, no. 41, pp. 25968–25975, 1997.

[4] J. Ghuman, P. A. Zunszain, I. Petitpas, A. A. Bhattacharya, M. Otagiri, and S. Curry, “Structural Basis of the Drug-binding Specificity of Human Serum Albumin,” *J. Mol. Biol.*, vol. 353, pp. 38–52, 2005.

[5] C. Bertucci, G. Ascoli, G. Uccello-barretta, L. Di Bari, and P. Salvadori, “The binding of 5-fluorouracil to native and modified human serum albumin : UV , CD , and 1H and 19F NMR investigation,” *J. Pharm. Biomed. Anal.*, vol. 13, pp. 1087–1093, 1995.

[6] M. W. Saif, A. Choma, S. J. Salamone, and E. Chu, “Pharmacokinetically Guided Dose Adjustment of 5-Fluorouracil : A Rational Approach to Improving Therapeutic Outcomes,” *J. Nat. Cancer Inst.*, vol. 101, pp. 1543–1552, 2009.

[7] D. Farrell, K. Ptak, N. J. Panaro, and P. Grodzinski, “Nanotechnology-Based Cancer Therapeutics — Promise and Challenge — Lessons Learned Through the NCI Alliance for Nanotechnology in Cancer,” *Pharm. Res.*, vol. 28, pp. 273–278, 2011.

[8] M. Tada, “Antineoplastic agents. The preparation of 5-fluorouracil-1-acetic acid derivatives,” *Bull. Chem. Soc. Jpn.*, vol. 48, pp. 3427–3428, 1975.

[9] C.-K. Kim, M. Gull Lee, M. Ki Park, H. Lee, and H. Jin Kang, “In vitro Drug release characteristics of methotrexate-human serum albumin and 5-fluorouracil-acetic acid-human serum albumin conjugates,” *Arch. Pharm. Res.*, vol. 12, no. 3, pp. 186–190, Sep. 1989.

[10] S. M. Chung, “Pharmacokinetics of 5-fluorouracil after intravenous infusion of 5-fluorouracil-acetic acid-human serum albumin conjugates to rabbits,” *Int. J. Pharm.*, vol. 68, pp. 61–68, 1991.

[11] M. J. Koziol, T. K. Sievers, K. Smuda, Y. Xiong, F. Wojcik, A. Steffen, M. Dathe, M. Angelika, R. Georgieva, and B. Hans, “Kinetics and Efficiency of a Methyl-Carboxylated 5-Fluorouracil-Bovine Serum Albumin Adduct for Targeted Delivery,” *Macromol. Biosci.*, vol. 14, no. 3, pp. 428–439, 2014.

[12] N. Service and M. G. Hospital, “Zero-Length Crosslinking Procedure with the Use of Active Esters ’,” *Anal. Biochem.*, vol. 185, pp. 131–135, 1990.

[13] N. P. Desai, V. Trieu, L. Yuan, R. Wu, P. Soon-shiong, and W. J. Gradishar, “Improved effectiveness of nanoparticle albumin-bound ( nab ) paclitaxel versus polysorbate-based

docetaxel in multiple xenografts as a function of HER2 and SPARC status," *Anticancer. Drugs*, vol. 19, pp. 899–909, 2008.

[14] "The History of Cancer by The American Cancer Society." [Online]. Available: http://www.cancer.org/acs/groups/cid/documents/webcontent/002048-pdf.pdf. [Accessed: 10-Oct-2014].

[15] A. Y. Chow, "Nature Scitable: Cell Cycle Control by Oncogenes and Tumor Suppressors: Driving the Transformation of Normal Cells into Cancerous Cells," 2010. [Online]. Available: http://www.nature.com/scitable/topicpage/cell-cycle-control-by-oncogenes-and-tumor-14191459#.

[16] D. Hanahan and R. Weinberg, "The Hallmarks of cancer," *Cell*, vol. 100, pp. 57–70, 2000.

[17] A. C. S. OMS, "Global cancer, facts and figures," 2011. [Online]. Available: http://www.cancer.org/acs/groups/content/@epidemiologysurveilance/documents/document/acspc-027766.pdf.

[18] G. Stehle, H. Sinn, A. Wunder, H. Hermann, J. C. M. Stewart, G. Hartung, W. Maier-borst, and D. Ludwig, "Plasma protein ( albumin ) catabolism by the tumor itself-implications for tumor metabolism and the genesis of cachexia," *Crit. Rev. Oncol.*, vol. 26, no. 97, pp. 77–100, 1997.

[19] F. Kratz and B. Elsadek, "Clinical impact of serum proteins on drug delivery," *J. Control. Release*, vol. 161, no. 2, pp. 429–445, 2012.

[20] E. Frei, "Albumin binding ligands and albumin conjugate uptake by cancer cells.," *Diabetol. Metab. Syndr.*, vol. 3, no. 1, p. 11, Jan. 2011.

[21] H. Maeda, G. Y. Bharate, and J. Daruwalla, "Polymeric drugs for efficient tumor-targeted drug delivery based on EPR-effect.," *Eur. J. Pharm. Biopharm.*, vol. 71, no. 3, pp. 409–19, Mar. 2009.

[22] H. Maeda, "Tumor-Selective Delivery of Macromolecular Drugs via the EPR Effect : NATURE OF THE EPR EFFECT AND FACTORS," *Bioconjug. Chem.*, vol. 21, pp. 797–802, 2010.

[23] T. Lammers, F. Kiessling, W. E. Hennink, and G. Storm, "Drug targeting to tumors : Principles , pitfalls and ( pre- ) clinical progress," *J. Control. Release*, vol. 161, no. 2, pp. 175–187, 2012.

[24] M. R. Dreher, W. Liu, C. R. Michelich, M. W. Dewhirst, F. Yuan, and A. Chilkoti, "Tumor vascular permeability, accumulation, and penetration of macromolecular drug carriers.," *J. Natl. Cancer Inst.*, vol. 98, no. 5, pp. 335–44, Mar. 2006.

[25] A. Urruticoechea, R. Alemany, J. Balart, A. Villanueva, F. Viñals, and G. Capellá, "Recent Advances in Cancer Therapy : An Overview," *Curr. Pharm. Des.*, vol. 16, pp. 3–10, 2010.

[26] "Chemotherapy article wikipedia." [Online]. Available: http://en.wikipedia.org/wiki/Chemotherapy. [Accessed: 20-Oct-2014].

[27] H. Durivage, *Lippincott´s Cancer Chemotherapy Handbook*, Second. Lippincott Publishers, Williams & Wilkins, 2001.

[28] E. Chu and V. DeVita, *Physicians Cancer chemotherapy Drug Manual 2008*. Jones and Bartlett, 2008.

[29] D. B. Longley, D. P. Harkin, and P. G. Johnston, "5-FLUOROURACIL : MECHANISMS OF ACTION AND CLINICAL STRATEGIES," *Nat. Rev. Cancer*, vol. 3, no. May, pp. 330–338, 2003.

[30] J. B. Parker and J. T. Stivers, "Dynamics of Uracil and 5-Fluorouracil in DNA," *Biochemistry*, vol. 50, pp. 612–617, 2011.

[31] U. Amstutz and T. K. Froehlich, "Dihydropyrimidine dehydrogenase gene as a major predictor of severe 5-fluorouracil toxicity R eview," *Pharmacogenomics*, vol. 12, pp. 1321–1336, 2011.

[32] K. Cho, X. Wang, S. Nie, Z. G. Chen, and D. M. Shin, "Therapeutic nanoparticles for drug delivery in cancer.," *Clin. Cancer Res.*, vol. 14, no. 5, pp. 1310–6, Mar. 2008.

[33] Y. H. Bae and K. Park, "Targeted drug delivery to tumors: Myths, reality and possibility You," *J. Control. Release*, vol. 153, no. 3, pp. 198–205, 2012.

[34] I. K. Kwon, S. C. Lee, B. Han, and K. Park, "Analysis on the current status of targeted drug delivery to tumors.," *J. Control. Release*, vol. 164, no. 2, pp. 108–14, Dec. 2012.

[35] F. Kratz, "Albumin as a drug carrier: design of prodrugs, drug conjugates and nanoparticles.," *J. Control. Release*, vol. 132, no. 3, pp. 171–83, Dec. 2008.

[36] G. Fanali, V. Trezza, M. Marino, M. Fasano, and P. Ascenzi, "Molecular Aspects of Medicine Human serum albumin : From bench to bedside," *Mol. Aspects Med.*, vol. 33, no. 3, pp. 209–290, 2012.

[37] M. J. Hawkins, P. Soon-shiong, and N. Desai, "Protein nanoparticles as drug carriers in clinical medicine," *Adv. Drug Deliv. Rev.*, vol. 60, pp. 876–885, 2008.

[38] E. Miele, G. P. Spinelli, E. Miele, F. Tomao, and S. Tomao, "Albumin-bound formulation of paclitaxel ( Abraxane ® ABI-007 ) in the treatment of breast cancer," *Int. J. Nanomedicine*, vol. 4, pp. 99–106, 2009.

[39] B. Elsadek and F. Kratz, "Impact of albumin on drug delivery — New applications on the horizon," *J. Control. Release*, vol. 157, no. 1, pp. 4–28, 2012.

[40] C. E. Powell, A. M. Soto, C. L. Michaelson, F. Diba, F. Mounier, P. J. Verroust, and C. Sonnenschein, "Characterization of a plasma membrane-resident albumin-binding protein associated with the proliferation of estrogen-target , serum-sensitive cells," *Steroids*, vol. 68, pp. 487–496, 2003.

[41] A. Temple, T.-Y. Yen, and S. Gronert, "Identification of specific protein carbonylation sites in model oxidations of human serum albumin.," *J. Am. Soc. Mass Spectrom.*, vol. 17, no. 8, pp. 1172–80, Aug. 2006.

[42] P. Rondeau and E. Bourdon, “The glycation of albumin: structural and functional impacts.,” *Biochimie*, vol. 93, no. 4, pp. 645–58, May 2011.

[43] S. Sugio, A. Kashima, S. Mochizuki, and M. Noda, “Crystal structure of human serum albumin at 2 . 5 Å resolution,” *Protein Eng.*, vol. 12, no. 6, pp. 439–446, 1999.

[44] E. Neumann, E. Frei, D. Funk, M. D. Becker, C. Fiehn, H. Schrenk, and U. Mu, “Native albumin for targeted drug delivery,” *Expert Opin. Drug Deliv*, vol. 7, no. 8, pp. 915–925, 2010.

[45] “Abraxane webpage, Celgene Corporation,” *www.abraxane.com*. .

[46] F. Petrelli, K. Borgonovo, and S. Barni, “Targeted delivery for breast cancer therapy : the history of paclitaxel,” *Expert Opin. Pharmacother*, vol. 11, no. 8, pp. 1413–1432, 2010.

[47] J. Cortes, C. Saura, and C. El, “Nanoparticle albumin-bound ( nab ™ ) -paclitaxel : improving efficacy and tolerability by targeted drug delivery in metastatic breast cancer,” *Eur. J. Cancer Suppl.*, vol. 8, no. 1, pp. 1–10, 2010.

[48] A. Taheri, F. Atyabi, F. Salman Nouri, F. Ahadi, M. A. Derakhshan, M. Amini, M. H. Ghahremani, S. N. Ostad, P. Mansoori, and R. Dinarvand, “Nanoparticles of Conjugated Methotrexate-Human Serum Albumin: Preparation and Cytotoxicity Evaluations,” *J. Nanomater.*, vol. 2011, pp. 1–7, 2011.

[49] K. Wosikowski, E. Biedermann, B. Rattel, N. Breiter, and P. Jank, “In Vitro and in Vivo Antitumor Activity of Methotrexate Conjugated to Human Serum Albumin in Human Cancer Cells,” *Clin Cancer Res*, vol. 9, pp. 1917–1926, 2003.

[50] G. Hartung, G. Stehle, H. Sinn, A. Wunder, H. H. Schrenk, S. Heeger, M. Kra, L. Edler, E. Frei, H. H. Fiebig, D. L. Heene, and W. Maier-borst, “Phase I Trial of Methotrexate-Albumin in a Weekly Intravenous Bolus Regimen in Cancer Patients,” *Clin Cancer Res*, vol. 5, pp. 753–759, 1999.

[51] “FDA website,” *www.patientnetwork.fda.gov/learn-how-drugs-devices-get-approved/drug-development-process/step-1-discovery-and-development*. .

[52] A. von Heideman, “Exploring cancer drugs in vivo and in vitro,” University of Uppsala, 2011.

[53] D. D. Allen, R. Caviedes, A. M. Cárdenas, T. Shimahara, J. Segura-Aguilar, and P. A. Caviedes, “Cell Lines as In Vitro Models for Drug Screening and Toxicity Studies,” *Drug Dev. Ind. Pharm.*, vol. 31, no. 8, pp. 757–768, 2005.

[54] R. H. Shoemaker, “The NCI60 human tumour cell line anticancer drug screen,” *Nat. Rev. Cancer*, vol. 6, no. October, pp. 813–823, 2006.

[55] “Triple-Negative Breast Cancer.” [Online]. Available: http://www.breastcancer.org/symptoms/diagnosis/trip_neg. [Accessed: 10-Oct-2014].

[56] “Estrogen and Progesterone Receptor Testing for Breast Cancer - American society of clinical oncology.” [Online]. Available: http://www.cancer.net/research-and-

advocacy/asco-care-and-treatment-recommendations-patients/estrogen-and-progesterone-receptor-testing-breast-cancer. [Accessed: 15-Oct-2014].

[57] X. Wang, M. Nakamura, I. Mori, K. Takeda, Y. Nakamura, H. Utsunomiya, G. Yoshimura, T. Sakurai, and K. Kakudo, "Calcitonin receptor gene and breast cancer: Quantitative analysis with laser capture microdissection," *Breast Cancer Res. Treat.*, vol. 83, pp. 109–117, 2004.

[58] Q. Qu, Y. Mao, X. Fei, and K. Shen, "The impact of androgen receptor expression on breast cancer survival: a retrospective study and meta-analysis.," *PLoS One*, vol. 8, p. e82650, 2013.

[59] S. Karmakar, Y. Jin, and A. K. Nagaich, "Interaction of glucocorticoid receptor (GR) with estrogen receptor (ER) α and activator protein 1 (AP1) in dexamethasone-mediated interference of ERα activity," *J. Biol. Chem.*, vol. 288, pp. 24020–24034, 2013.

[60] C. V Clevenger, W. Chang, W. Ngo, T. L. M. Pasha, K. T. Montone, and J. E. Tomaszewski, "Expression of Prolactin and Prolactin Receptor in Human Breast Carcinoma Evidence for an Autocrine / Paracrine Loop," *Am. J. Pathol.*, vol. 146, no. 3, pp. 695–705, 1995.

[61] F. Brugnoli, S. Grassilli, M. Piazzi, M. Palomba, E. Nika, A. Bevelloni, S. Capitani, and V. Bertagnolo, "In triple negative breast tumor cells, PLC-β2 promotes the conversion of CD133high to CD133low phenotype and reduces the CD133-related invasiveness," *Mol. Cancer*, vol. 12, no. 165, 2013.

[62] "ATCC company website," *www.lgcstandards-atcc.org*. .

[63] C. E. Powell, A. M. Soto, and C. Sonnenschein, "Identification and characterization of membrane estrogen receptor from MCF7 estrogen-target cells," *J. Steroid Biochem. Mol. Biol.*, vol. 77, pp. 97–108, 2001.

[64] T. J. Liu, B. C. Sun, X. L. Zhao, X. M. Zhao, T. Sun, Q. Gu, Z. Yao, X. Y. Dong, N. Zhao, and N. Liu, "CD133+ cells with cancer stem cell characteristics associates with vasculogenic mimicry in triple-negative breast cancer.," *Oncogene*, vol. 32, no. 5, pp. 544–53, Jan. 2013.

[65] K. Subik, J.-F. Lee, L. Baxter, and T. Strzepek, "The Expression Patterns of ER, PR, HER2, CK5/6, EGFR, Ki-67 and AR by Immunohistochemical Analysis in Breast Cancer Cell Lines," *Breast cancer basic Clin. Res.*, vol. 4, 2010.

[66] G. J. Quinlan, G. S. Martin, and T. W. Evans, "Albumin: biochemical properties and therapeutic potential.," *Hepatology*, vol. 41, no. 6, pp. 1211–9, Jun. 2005.

[67] I. Chary, K.V.R. (Tata Institute of Fundamental Research, Mumbai and I. Govil, Girjesh ( Tata Institute of Fundamental Research, Mumbai, *NMR in Biological Systems: From Molecules to Humans*. Springer, 2008.

[68] K. V. R. Chary and G. Govil, "NMR in Biological Systems: From molecules to humans," Springer.

[69] "NMR spectroscopy J-coupling." [Online]. Available: http://en.wikipedia.org/wiki/J-coupling. [Accessed: 11-Oct-2014].

[70] "nuclear magnetic resonance decoupling." [Online]. Available: http://en.wikipedia.org/wiki/Nuclear_magnetic_resonance_decoupling. [Accessed: 10-Oct-2014].

[71] "Thermo Scientific webpage: NHS and Sulfo-NHS." [Online]. Available: http://www.piercenet.com/product/nhs-sulfo-nhs. [Accessed: 05-Aug-2014].

[72] N. Cooke, "DDW - Drug Discovery World website." [Online]. Available: www.ddw-online.com/enabling-technologies/p148395-recent-advances-in-mass-spectrometry-for-drug-discovery-and-development-fall-03.html. [Accessed: 10-Aug-2014].

[73] "Wikipedia page about MALDI-TOF." [Online]. Available: http://en.wikipedia.org/wiki/Time-of-flight_mass_spectrometry#equation_9. [Accessed: 15-Oct-2014].

[74] C. Bertucci, M. Pistolozzi, and A. De Simone, "Circular dichroism in drug discovery and development : an abridged review," *Anal Bioanal Chem*, vol. 398, pp. 155–166, 2010.

[75] "Photophysics Company webpage," *http://www.photophysics.com/tutorials/circular-dichroism-cd-spectroscopy/3-chirality-and-biology*. .

[76] D. H. A. Corrêa and C. H. I. Ramos, "The use of circular dichroism spectroscopy to study protein folding , form and function," *African J. Biochem. Res.*, vol. 3, no. 5, pp. 164–173, 2009.

[77] O. Bastidas, "Cell counting with Neubauer Chamber. Basic Hematocytometer Usage."

[78] N. S. Foundation, "Counting Cells with a Hemocytometer - protocol," 2006.

[79] T. Mosmann, "Rapid Colorimetric Assay for Cellular Growth and Survival : Application to Proliferation and Cytotoxicity Assays," *J. oflmmunologicalMethods*, vol. 65, pp. 55–63, 1983.

[80] M. V Berridge, P. M. Herst, and A. S. Tan, "Tetrazolium dyes as tools in cell biology : New insights into their cellular reduction," *Biotechnol. Annu. Rev.*, vol. 11, no. 05, pp. 127–152, 2005.

[81] T. L. Riss, A. L. Niles, and L. Minor, "Cell Viability Assays Assay Guidance Manual," *Cell Viability Assays, Promega Corp.*

[82] J. A. Plumb, "Cell Sensitivity Assays: The MTT assay," *Cancer Cell Culture, Methods in Molecular Medicine*, pp. 165–169, 2004.

[83] J. Carmichael, W. G. Degraff, A. F. Gazdar, J. D. Minna, and J. B. Mitchell, "Evaluation of a Tetrazolium-based Semiautomated Colorimetric Assay : Assessment of Chemosensitivity Testing Evaluation of a Tetrazolium-based Semiautomated Colorimetrie Assay : Assessment," *Cancer Res.*, vol. 47, pp. 936–942, 1987.

[84] W. Strober, “Trypan Blue Exclusion Test of Cell Viability,” *Curr. Protoc. Immunol.*, 2001.

[85] Operating Manual, “LSM 510 Laser Scanning Microscope.”

[86] “Confocal laser scanning microscope - tutorial, Confocal and Advanced Light Microscopy Facility of The University of Edinburgh.” [Online]. Available: http://www.calm.ed.ac.uk/CALM UoE-CLSM tutorial 01.html. [Accessed: 03-Aug-2014].

[87] H. Sauer, M. Wartenberg, and J. Hescheler, “Reactive Oxygen Species as Intracellular Messengers During Cell Growth and Differentiation,” *Cell. Physiol. Biochem.*, vol. 11, no. 4, pp. 173–186, 2001.

[88] L. M. Henderson and J. B. Chappell, “Dihydrorhodamine 123: a fluorescent probe for superoxide generation?,” *Eur. J. Biochem.*, vol. 217, no. 3, pp. 973–80, Nov. 1993.

[89] J. P. Crow, “Dichlorodihydrofluorescein and dihydrorhodamine 123 are sensitive indicators of peroxynitrite in vitro: implications for intracellular measurement of reactive nitrogen and oxygen species.,” *Nitric Oxide*, vol. 1, no. 2, pp. 145–57, Apr. 1997.

[90] QIAGEN, “QIAamp DNA Mini and Blood Mini Handbook,” 2012.

[91] “Life Technologies website - DNase I Demystified.” [Online]. Available: http://www.lifetechnologies.com/pt/en/home/references/ambion-tech-support/nuclease-enzymes/general-articles/dnase-i-demystified.html. [Accessed: 04-Aug-2014].

[92] P. Noordhuis, U. Holwerda, C. L. Van Der Wilt, C. J. Van Groeningen, K. Smid, S. Meijer, H. M. Pinedo, and G. J. Peters, “5-Fluorouracil incorporation into RNA and DNA in relation to thymidylate synthase inhibition of human colorectal cancers,” *Ann. Oncol.*, vol. 15, pp. 1025–1032, 2004.

[93] R. D. M. Stepenes, “Tests for Normal Distribution,” in *Goodness-Of-Fit Techniques*, Macel Decker, 1986.

[94] “Graphpad prism statistics guide.” [Online]. Available: http://www.graphpad.com/guides/prism/6/statistics/index.htm?stat_qa_normality_tests.htm. [Accessed: 25-Sep-2014].

[95] “Ilustrated Glossary of Organic Chemistry.” [Online]. Available: http://www.chem.ucla.edu/harding/IGOC/N/n+1_rule.html. [Accessed: 16-Sep-2014].

[96] “UCLA NMR solvent chemical shifts guide.” [Online]. Available: http://www.chem.ucla.edu/~webspectra/NotesOnSolvents.html. [Accessed: 17-Sep-2014].

[97] “Sigma Aldrich HSA.” [Online]. Available: http://www.sigmaaldrich.com/catalog/product/sigma/a9511?lang=de&region=DE. [Accessed: 10-Jul-2014].

[98] B. A. Chabner and T. G. R. Jr, “Chemotherapy and the war on cancer,” *Nat. Rev. Cancer*, vol. 5, no. January, pp. 65–72, 2005.

[99] G. D. Heggie, D. S. Cross, W. J. Huster, and R. B. Diasio, "Clinical Pharmacokinetics Urine , and Bile1 of 5-Fluorouracil and Its Metabolites in Plasma ," *Cancer Res.*, vol. 47, pp. 2203–2206, 1987.

[100] K. S. Kim, D. S. Lim, and S. H. Cho, "Synthesis of Polymeric Drugs Containing D-Glucosamine as a Spacer," *Korea Polym. J.*, vol. 4, no. 1, pp. 16–22, 1995.

[101] S. S. Wong and L. C. Wongt, "Chemical crosslinking and the stabilization of proteins and enzymes," *Enzym. Microbiol. Techonology*, vol. 14, no. June, pp. 866–874, 1992.

[102] "Carbodiimide Crosslinker Chemistry - Thermo Scientific." [Online]. Available: http://www.piercenet.com/method/carbodiimide-crosslinker-chemistry. [Accessed: 20-Oct-2014].

[103] "NHS and Sulfo-NHS - Thermos Scientific." [Online]. Available: http://www.piercenet.com/product/nhs-sulfo-nhs. [Accessed: 20-Oct-2014].

[104] C. Pan, S. Xu, H. Zhou, Y. Fu, M. Ye, and H. Zou, "Recent developments in methods and technology for analysis of biological samples by MALDI-TOF-MS," *Anal. Bioanal. Chem.*, vol. 387, pp. 193–204, 2007.

[105] Y.-T. Cho, C.-W. Chen, M.-P. Chen, J.-L. Hu, H. Su, J. Shiea, W.-J. Wu, and D.-C. Wu, "Diagnosis of albuminuria by tryptic digestion and matrix-assisted laser desorption ionization/time-of-flight mass spectrometry.," *Clin. Chim. Acta.*, vol. 420, pp. 76–81, May 2013.

[106] "Application note for MALDI-TOF technique - Bruker GmbH." [Online]. Available: http://www.bruker.com/fileadmin/user_upload/8-PDF-Docs/Separations_MassSpectrometry/Literature/literature/ApplicationNotes/MT-112_Intact_Protein_2012_6-seitig_eBook.pdf. [Accessed: 04-Oct-2014].

[107] M. Guilhaus, "Principles and Instrumentation in Time-of-flight Mass Spectrometry Physical and Instrumental Concepts," *J. Mass Spectrosc.*, vol. 30, no. September, pp. 1519–1532, 1995.

[108] F. Dosio, P. Brusa, P. Crosasso, S. Arpicco, and L. Cattel, "Preparation, characterization and properties in vitro and in vivo of a paclitaxel–albumin conjugate," *J. Control. Release*, vol. 47, no. 3, pp. 293–304, Sep. 1997.

[109] G. Stehle, A. Wunder, H. Sinn, H. H. Schrenk, S. Schütt, E. Frei, G. Hartung, W. Maier-Borst, and D. L. Heene, "Pharmacokinetics of methotrexate-albumin conjugates in tumor-bearing rats.," *Anticancer. Drugs*, vol. 8, pp. 835–844, 1997.

[110] M. Rezaei-tavirani, S. H. Moghaddamnia, B. Ranjbar, M. Amani, and S. Marashi, "Conformational Study of Human Serum Albumin in Pre-denaturation Temperatures by Differential Scanning Calorimetry , Circular Dichroism and UV Spectroscopy Native →," vol. 39, no. 5, pp. 530–536, 2006.

[111] A. Varlan and M. Hillebrand, "Bovine and Human Serum Albumin Interactions with 3-Carboxyphenoxathiin Studied by Fluorescence and Circular Dichroism Spectroscopy," *Molecules*, vol. 15, pp. 3905–3919, 2010.

[112] F. Zsila, Z. Bikádi, and M. Simonyi, “Probing the binding of the flavonoid, quercetin to human serum albumin by circular dichroism, electronic absorption spectroscopy and molecular modelling methods,” *Biochem. Pharmacol.*, vol. 65, pp. 447–456, 2003.

[113] C. Louis-Jeune, M. a Andrade-Navarro, and C. Perez-Iratxeta, “Prediction of protein secondary structure from circular dichroism using theoretically derived spectra.,” *Proteins*, no. September, pp. 374–381, Sep. 2011.

[114] P. M. Calabro-jones, J. E. Byfield, J. F. Ward, and T. R. Sharp, “Time-Dose Relationships for 5-Fluorouracil Cytotoxicity against Human Epithelial Cancer Cells in Vitro,” *Cancer Res.*, vol. 42, pp. 4413–4420, 1982.

[115] J. Wesierska-Gadek, T. Schreiner, M. Maurer, A. Waringer, and C. Ranftler, “Phenol red in the culture medium strongly affects the susceptibility of human MCF-7 cells to roscovitine.,” *Cell. Mol. Biol. Lett.*, vol. 12, no. 2, pp. 280–93, Jan. 2007.

[116] E. Leung, J. E. Kim, M. Askarian-Amiri, G. J. Finlay, and B. C. Baguley, “Evidence for the existence of triple-negative variants in the MCF-7 breast cancer cell population.,” *Biomed Res. Int.*, vol. 2014, p. 836769, Jan. 2014.

[117] X. Guo, E. Goessl, G. Jin, E. S. R. Collie-duguid, J. Cassidy, W. Wang, and V. O. Brien, “Cell Cycle Perturbation and Acquired 5-Fluorouracil Chemoresistance,” *Anticancer Res.*, vol. 14, pp. 9–14, 2008.

[118] Q. Luo, P. Wang, Y. Miao, H. He, and X. Tang, “A novel 5-fluorouracil prodrug using hydroxyethyl starch as a macromolecular carrier for sustained release,” *Carbohydr. Polym.*, vol. 87, no. 4, pp. 2642–2647, 2012.

[119] “organic chemistry wikibooks.” [Online]. Available: http://en.wikibooks.org/wiki/Organic_Chemistry. [Accessed: 05-Oct-2014].

[120] R. M. Wohlhueter, R. S. McIvor, and P. G. Plagemann, “Facilitated transport of uracil and 5-fluorouracil, and permeation of orotic acid into cultured mammalian cells.,” *J. Cell. Physiol.*, vol. 104, pp. 309–319, 1980.

[121] B. Chan, N. Dodsworth, J. Woodrow, A. Tucker, and R. Harris, “Site-specific N-terminal auto-degradation of human serum albumin,” *Eur. J. Biochem*, vol. 528, pp. 524–528, 1995.

[122] A. Sułkowska, “Interaction of drugs with bovine and human serum albumin,” *J. Mol. Struct.*, vol. 614, pp. 227–232, 2002.

[123] N. Dhanesuan, J. a. Sharp, T. Blick, J. T. Price, and E. W. Thompson, “Doxycycline-Inducible Expression of SPARC/ Osteonectin/ BM40 in MDA-MB-231 Human Breast Cancer Cells Results in Growth Inhibition,” *Breast Cancer Res. Treat.*, vol. 75, no. 1, pp. 73–85, Sep. 2002.

[124] L. Galluzzi, S. a Aaronson, J. Abrams, E. S. Alnemri, D. W. Andrews, E. H. Baehrecke, N. G. Bazan, M. V Blagosklonny, K. Blomgren, C. Borner, D. E. Bredesen, C. Brenner, M. Castedo, J. a Cidlowski, a Ciechanover, G. M. Cohen, V. De Laurenzi, R. De Maria, M. Deshmukh, B. D. Dynlacht, W. S. El-Deiry, R. a Flavell, S. Fulda, C. Garrido, P. Golstein, M.-L. Gougeon, D. R. Green, H. Gronemeyer, G. Hajnóczky, J. M. Hardwick, M. O. Hengartner, H. Ichijo, M. Jäättelä, O. Kepp, a Kimchi, D. J. Klionsky, R. a

Knight, S. Kornbluth, S. Kumar, B. Levine, S. a Lipton, E. Lugli, F. Madeo, W. Malomi, J.-C. W. Marine, S. J. Martin, J. P. Medema, P. Mehlen, G. Melino, U. M. Moll, E. Morselli, S. Nagata, D. W. Nicholson, P. Nicotera, G. Nuñez, M. Oren, J. Penninger, S. Pervaiz, M. E. Peter, M. Piacentini, J. H. M. Prehn, H. Puthalakath, G. a Rabinovich, R. Rizzuto, C. M. P. Rodrigues, D. C. Rubinsztein, T. Rudel, L. Scorrano, H.-U. Simon, H. Steller, J. Tschopp, Y. Tsujimoto, P. Vandenabeele, I. Vitale, K. H. Vousden, R. J. Youle, J. Yuan, B. Zhivotovsky, and G. Kroemer, "Guidelines for the use and interpretation of assays for monitoring cell death in higher eukaryotes.," *Cell Death Differ.*, vol. 16, no. 8, pp. 1093–107, Aug. 2009.

[125] D. Lobner, "Comparison of the LDH and MTT assays for quantifying cell death: validity for neuronal apoptosis?," *J. Neurosci. Methods*, vol. 96, no. 2, pp. 147–152, Mar. 2000.

[126] K. Grankvist and I. Taljedal, "Alloxan Cytotoxicity in vitro," *Biochemistry*, vol. 162, pp. 19–24, 1977.

[127] J. E. Klaunig and L. M. Kamendulis, "The role of oxidative stress in carcinogenesis.," *Annu. Rev. Pharmacol. Toxicol.*, vol. 44, pp. 239–67, Jan. 2004.

[128] N. S. Brown and R. Bicknell, "Hypoxia and oxidative stress in breast cancer Oxidative stress : its effects on the growth , metastatic potential and response to therapy of breast cancer," 2001.

[129] D. Funk, H. Schrenk, and E. Frei, "Serum albumin leads to false-positive results in the XTT and the MTT assay," *Biotechniques*, vol. 43, no. 2, pp. 2–4, 2007.

[130] M. Karaayvaz, H. Zhai, and J. Ju, "miR-129 promotes apoptosis and enhances chemosensitivity to 5-fluorouracil in colorectal cancer.," *Cell Death Dis.*, vol. 4, p. e659, Jan. 2013.

[131] Y. Liu, "Fatty acid oxidation is a dominant bioenergetic pathway in prostate cancer.," *Prostate Cancer Prostatic Dis.*, vol. 9, no. 3, pp. 230–4, Jan. 2006.

[132] L. M. Mooney, K. a Al-Sakkaf, B. L. Brown, and P. R. M. Dobson, "Apoptotic mechanisms in T47D and MCF-7 human breast cancer cells.," *Br. J. Cancer*, vol. 87, no. 8, pp. 909–17, Oct. 2002.

[133] "Error in cell counting." [Online]. Available: http://www.celeromics.com/en/resources/docs/Articles/Counting-Chamber-Error.pdf. [Accessed: 25-Sep-2014].

[134] D. A. Scudiero, R. H. Shoemaker, K. D. Paull, D. A. Scudiere, K. D. Paul, A. Monks, S. Tierney, T. H. Nofziger, M. J. Currens, D. Seniff, and M. R. Boyd, "Evaluation of a Soluble Tetrazolium / Formazan Assay for Cell Growth and Drug Sensitivity in Culture Using Human and Other Tumor Cell Lines," *Cancer Res.*, vol. 48, pp. 4827–4833, 1988.

[135] M. I. Patel, R. Tuckerman, and Q. Dong, "A Pitfall of the 3-(4,5-dimethylthiazol-2-yl)-5(3-carboxymethonyphenol)-2-(4-sulfophenyl)-2H-tetrazolium (MTS) assay due to evaporation in wells on the edge of a 96 well plate.," *Biotechnol. Lett.*, vol. 27, no. 11, pp. 805–8, Jun. 2005.

[136] H.-L. Huang, H.-W. Hsing, T.-C. Lai, Y.-W. Chen, T.-R. Lee, H.-T. Chan, P.-C. Lyu, C.-L. Wu, Y.-C. Lu, S.-T. Lin, C.-W. Lin, C.-H. Lai, H.-T. Chang, H.-C. Chou, and H.-L. Chan, "Trypsin-induced proteome alteration during cell subculture in mammalian cells.," *J. Biomed. Sci.*, vol. 17, p. 36, Jan. 2010.

[137] C. Garrido, P. Ottavi, A. Fromentin, A. Drugs, A. Hammann, and B. Chauffert, "HSP27 as a Mediator of Confluence-dependent Resistance to Cell Death Induced by Anticancer Drugs," *Cancer Res.*, vol. 57, pp. 2661–2667, 1997.

[138] U. Anand and S. Mukherjee, "Binding, unfolding and refolding dynamics of serum albumins.," *Biochim. Biophys. Acta*, vol. 1830, no. 12, pp. 5394–404, Dec. 2013.

[139] M. Poór, Y. Li, G. Matisz, L. Kiss, S. Kunsági-Máté, and T. Kőszegi, "Quantitation of species differences in albumin–ligand interactions for bovine, human and rat serum albumins using fluorescence spectroscopy: A test case with some Sudlow's site I ligands," *J. Lumin.*, vol. 145, pp. 767–773, Jan. 2014.

[140] S. Tanabe, Y. Kobayashi, Y. Takahata, F. Morimatsu, R. Shibata, and T. Nishimura, "Some human B and T cell epitopes of bovine serum albumin, the major beef allergen.," *Biochem. Biophys. Res. Commun.*, vol. 293, no. 5, pp. 1348–53, May 2002.

[141] P. Restani, C. Ballabio, A. Cattaneo, P. Isoardi, L. Terracciano, and A. Fiocchi, "Characterization of bovine serum albumin epitopes and their role in allergic reactions," *Allergy*, vol. 59, pp. 21–24, 2004.

[142] C. H. Takimoto, L. K. Yee, D. J. Venzon, B. Schuler, F. Grollman, C. Chabuk, J. M. Hamilton, A. P. Chen, C. J. Allegra, and J. L. Grem, "High Inter- and Intrapatient Variation in 5-Fluorouracil Plasma Concentrations during a Prolonged Drug Infusion High Inter- and Intrapatient Variation in 5-Fluorouracil Plasma Concentrations during a Prolonged Drug Infusion," *Clin Cancer Res*, vol. 5, pp. 1347–1352, 1999.

[143] Y. Furuya, K. Yamamoto, N. Kohno, M. Yamamoto, and Y. Saitoh, "Serum concentrations of 5-fluorouracil achieved with nocturnal constant-rate infusion in patients with disseminated cancer.," *Cancer Lett.*, vol. 94, no. 2, pp. 207–11, Aug. 1995.

[144] M. J. Alvarez-Figueroa and J. Blanco-Méndez, "Transdermal delivery of methotrexate: iontophoretic delivery from hydrogels and passive delivery from microemulsions," *Int. J. Pharm.*, vol. 215, no. 1–2, pp. 57–65, Mar. 2001.

[145] S. Kaneda, J. Nalbantoglu, K. Takeishi, O. Gotoh, T. Seno, D. Ayusawa, and I. Nalbantoglu, "Structural and functional analysis of the Structural Synthase and Functional Gene * Analysis of the Human Thymidylate," *J. Biol. Chem.*, vol. 265, pp. 20277–20284, 1990.

[146] C. D. Blanke, M. Teng, and H. Choy, "The role of UFT in combined-modality therapy.," *Oncology (Williston Park).*, vol. 13, pp. 47–54, 1999.

[147] A. J. Hao, Y. J. Deng, S. City, L. Province, Y. H. Cao, T. Chinese, M. Hospital, and H. Province, "Synthesis and characteristics of the fluorouracil-dextran conjugates", *Pharmazie*, vol. 61, pp. 489–490, 2006.

[148] “Sigma Aldrich Webpage.” [Online]. Available: http://www.sigmaaldrich.com/life-science/custom-ol. [Accessed: 20-Jun-2014].

[149] “Principles of PRotein Structure Assignment 1996.” [Online]. Available: http://www.cryst.bbk.ac.uk/PPS2/assignments/A1/CD_info.html. [Accessed: 07-Aug-2014].

[150] “Celeromics web page.” [Online]. Available: http://www.celeromics.com/en/resources/Technical Notes/cells-chamber-concentration.php. [Accessed: 20-Aug-2014].

[151] “Microbehunter microbiology magazine.” [Online]. Available: http://www.microbehunter.com/the-hemocytometer-counting-chamber/. [Accessed: 20-Oct-2014].

[152] M. H. Aghdaie, B. Geramizadeh, N. Azarpira, E. Esfandiari, M. Darai, M. Rahsaz, S. Nikeghbalian, and S. A. Malekhosseini, “Hepatocyte Isolation From Unused / Rejected Livers for Transplantation : Ini- tial Step Toward Hepatocyte Transplantation , the First Experience From Iran,” *Hepat. Mon.*, vol. 13, no. 8, 2013.

[153] “Graphpad curve fitting Guide.” [Online]. Available: http://www.graphpad.com/guides/prism/6/curve-fitting/. [Accessed: 25-Sep-2014].

# ANNEX I

## Mann-Whitney test results (p-value) – MTT

### 24 hours

| T-47D | CTL vs HSA | CTL vs FUAc-HSA | CTL vs FUAc | CTL vs 5-FU |
|---|---|---|---|---|
| 1µM | 0,0006 | 0,1147 | 0,7591 | 0,0652 |
| 5µM | 0,0015 | 0,7591 | 0,1611 | 0,0005 |
| 10µM | 0,0063 | 0,1289 | 0,6738 | < 0.0001 |
| 50µM | 0,0462 | 0,7810 | 0,1793 | < 0.0001 |
| 100µM | 0,0297 | 0,1989 | 0,0084 | < 0.0001 |
| 500µM | 0,0015 | < 0.0001 | 0,0131 | < 0.0001 |

Table 1: p-values for Mann-Whitney test of T-47D cell line MTT data at 24 hours

| MDA-MB-231 | CTL vs HSA | CTL vs FUAc-HSA | CTL vs FUAc | CTL vs 5-FU |
|---|---|---|---|---|
| 1µM | 0,6739 | 0,3637 | 0,9716 | 0,5452 |
| 5µM | 0,6326 | 0,9149 | 0,3714 | 0,1813 |
| 10µM | 0,9149 | 0,2795 | 0,3870 | 0,0609 |
| 50µM | 0,6739 | 0,0570 | 0,4276 | 0,0035 |
| 100µM | 0,9148 | 0,0652 | 0,8698 | 0,0759 |
| 500µM | 0,0013 | 0,1443 | 0,0063 | < 0.0001 |

Table 2: p-values for Mann-Whitney test of MDA-MB-231 cell line MTT data at 24 hours

| MCF-7 | CTL vs HSA | CTL vs FUAc-HSA | CTL vs FUAc | CTL vs 5-FU |
|---|---|---|---|---|
| 1µM | 0,0008 | < 0.0001 | 0,4800 | 0,0606 |
| 5µM | < 0.0001 | 0,0018 | 0,8655 | 0,1439 |
| 10µM | < 0.0001 | 0,0159 | 0,1063 | 0,3424 |
| 50µM | < 0.0001 | 0,2399 | 0,2257 | 0,7346 |
| 100µM | < 0.0001 | 0,8655 | > 0.9999 | 0,1422 |
| 500µM | < 0.0001 | 0,2548 | 0,3564 | 0,1061 |

Table 3: p-values for Mann-Whitney test of MCF-7 cell line MTT data at 24 hours

## 48 hours

| T-47D | CTL vs HSA | CTL vs FUAc-HSA | CTL vs FUAc | CTL vs 5-FU |
|---|---|---|---|---|
| 1µM | 0,0697 | 0,8810 | 0,1081 | < 0.0001 |
| 5µM | 0,0610 | 0,5346 | 0,8474 | < 0.0001 |
| 10µM | 0,0156 | 0,4318 | 0,8473 | < 0.0001 |
| 50µM | 0,0479 | 0,9602 | 0,0017 | < 0.0001 |
| 100µM | 0,0792 | 0,5730 | < 0.0001 | < 0.0001 |
| 500µM | 0,3870 | < 0.0001 | < 0.0001 | < 0.0001 |

Table 4: p-values for Mann-Whitney test of T-47D cell line MTT data at 48 hours

| MDA-MB-231 | CTL vs HSA | CTL vs FUAc-HSA | CTL vs FUAc | CTL vs 5-FU |
|---|---|---|---|---|
| 1µM | 0,1217 | 0,9829 | < 0.0001 | 0,6327 |
| 5µM | 0,1216 | 0,0652 | 0,0003 | < 0.0001 |
| 10µM | 0,1148 | 0,0065 | 0,0172 | < 0.0001 |
| 50µM | 0,0860 | 0,0286 | 0,0846 | < 0.0001 |
| 100µM | 0,3060 | 0,0845 | < 0.0001 | < 0.0001 |
| 500µM | 0,2546 | 0,0532 | < 0.0001 | < 0.0001 |

Table 5: p-values for Mann-Whitney test of MDA-MB-231 cell line MTT data at 48 hours

| MCF-7 | CTL vs HSA | CTL vs FUAc-HSA | CTL vs FUAc | CTL vs 5-FU |
|---|---|---|---|---|
| 1µM | 0,0001 | 0,0044 | 0,9502 | < 0.0001 |
| 5µM | 0,9219 | 0,6750 | 0,0103 | 0,3029 |
| 10µM | 0,3758 | 0,5737 | < 0.0001 | < 0.0001 |
| 50µM | 0,6235 | 0,0717 | 0,0034 | < 0.0001 |
| 100µM | 0,0607 | 0,0323 | 0,0658 | < 0.0001 |
| 500µM | 0,0115 | 0,0020 | 0,0007 | < 0.0001 |

Table 6: p-values for Mann-Whitney test of MCF-7 cell line MTT data at 48 hours

## 72 hours

| T-47D | CTL vs HSA | CTL vs FUAc-HSA | CTL vs FUAc | CTL vs 5-FU |
|---|---|---|---|---|
| 1µM | 0,1747 | 0,0092 | 0,0121 | 0,0052 |
| 5µM | 0,0276 | 0,0019 | 0,9149 | < 0.0001 |
| 10µM | 0,0043 | 0,0084 | 0,6739 | < 0.0001 |
| 50µM | 0,2607 | 0,7375 | < 0.0001 | < 0.0001 |
| 100µM | 0,9376 | 0,0120 | < 0.0001 | < 0.0001 |
| 500µM | 0,6533 | < 0.0001 | < 0.0001 | < 0.0001 |

Table 7: p-values for Mann-Whitney test of T-47D cell line MTT data at 72 hours

| MDA-MB-231 | CTL vs HSA | CTL vs FUAc-HSA | CTL vs FUAc | CTL vs 5-FU |
|---|---|---|---|---|
| 1µM | 0,0114 | 0,1499 | 0,9579 | < 0.0001 |
| 5µM | 0,0017 | 0,2335 | 0,0285 | < 0.0001 |
| 10µM | 0,0009 | 0,3606 | 0,0017 | < 0.0001 |
| 50µM | 0,7212 | 0,0850 | < 0.0001 | < 0.0001 |
| 100µM | 0,5277 | 0,0850 | < 0.0001 | < 0.0001 |
| 500µM | 0,1884 | < 0.0001 | < 0.0001 | < 0.0001 |

Table 8: p-values for Mann-Whitney test of MDA-MB-231 cell line MTT data at 72 hours

| MCF-7 | CTL vs HSA | CTL vs FUAc-HSA | CTL vs FUAc | CTL vs 5-FU |
|---|---|---|---|---|
| 1µM | 0,1061 | 0,8094 | 0,9219 | < 0.0001 |
| 5µM | 0,3378 | 0,7546 | 0,3953 | < 0.0001 |
| 10µM | 0,0013 | > 0.9999 | 0,0776 | < 0.0001 |
| 50µM | 0,4150 | < 0.0001 | 0,0023 | < 0.0001 |
| 100µM | 0,8097 | < 0.0001 | < 0.0001 | < 0.0001 |
| 500µM | 0,7549 | < 0.0001 | < 0.0001 | < 0.0001 |

Table 9: p-values for Mann-Whitney test of MCF-7 cell line MTT data at 72 hours

## 96 hours

| T-47D | CTL vs HSA | CTL vs FUAc-HSA | CTL vs FUAc | CTL vs 5-FU |
|---|---|---|---|---|
| 1µM | 0,3773 | 0,3973 | 0,0237 | < 0.0001 |
| 5µM | 0,6738 | 0,8641 | 0,0003 | < 0.0001 |
| 10µM | 0,6491 | 0,6905 | 0,5695 | < 0.0001 |
| 50µM | 0,3950 | 0,6696 | < 0.0001 | < 0.0001 |
| 100µM | 0,3546 | 0,5314 | < 0.0001 | < 0.0001 |
| 500µM | 0,8489 | < 0.0001 | < 0.0001 | < 0.0001 |

Table 10: p-values for Mann-Whitney test of T-47D cell line MTT data at 96 hours

| MDA-MB-231 | CTL vs HSA | CTL vs FUAc-HSA | CTL vs FUAc | CTL vs 5-FU |
|---|---|---|---|---|
| 1µM | 0,0062 | 0,3447 | 0,0381 | < 0.0001 |
| 5µM | 0,0485 | 0,5156 | 0,0009 | < 0.0001 |
| 10µM | 0,2613 | 0,2884 | < 0.0001 | < 0.0001 |
| 50µM | 0,5230 | 0,5230 | < 0.0001 | < 0.0001 |
| 100µM | 0,0794 | 0,1412 | < 0.0001 | < 0.0001 |
| 500µM | 0,0231 | < 0.0001 | < 0.0001 | < 0.0001 |

Table 11: p-values for Mann-Whitney test of MDA-MB-231 cell line MTT data at 96 hours

| MCF-7 | CTL vs HSA | CTL vs FUAc-HSA | CTL vs FUAc | CTL vs 5-FU |
|---|---|---|---|---|
| 1µM | 0,6490 | 0,9501 | 0,8653 | < 0.0001 |
| 5µM | 0,3202 | 0,0044 | 0,9785 | < 0.0001 |
| 10µM | 0,0390 | 0,0177 | 0,1232 | < 0.0001 |
| 50µM | 0,1422 | < 0.0001 | < 0.0001 | < 0.0001 |
| 100µM | 0,7013 | < 0.0001 | < 0.0001 | < 0.0001 |
| 500µM | 0,1989 | < 0.0001 | < 0.0001 | < 0.0001 |

Table 12: p-values for Mann-Whitney test of MCF-7 cell line MTT data at 96 hours

# ANNEX II

Standard deviation of MTT and cell counting values for the three cell lines at 72 hours time point

| T-47D | HSA | FUAc-HSA | FUAc | 5-FU |
|---|---|---|---|---|
| 50µM | 12,73 | 19,80 | 17,68 | 2,121 |
| 100µM | 14,14 | 29,70 | 19,09 | 11,31 |
| 500µM | 23,33 | 28,99 | 12,73 | 0,0 |

Table 1: Standard deviation between MTT and cell counting percentage values relative to T-47D cell line at the 72 hours time point

| MDA-MB-231 | HSA | FUAc-HSA | FUAc | 5-FU |
|---|---|---|---|---|
| 50µM | 11,31 | 10,61 | 13,44 | 0,7071 |
| 100µM | 4,950 | 7,778 | 16,97 | 4,243 |
| 500µM | 7,778 | 3,536 | 21,92 | 2,121 |

Table 2: Standard deviation between MTT and cell counting percentage values relative to MDA-MB-231 cell line at the 72 hours time point

| MCF-7 | HSA | FUAc-HSA | FUAc | 5-FU |
|---|---|---|---|---|
| 50µM | 9,899 | 5,657 | 1,414 | 1,414 |
| 100µM | 1,414 | 0,7071 | 9,899 | 12,02 |
| 500µM | 6,364 | 7,071 | 3,536 | 12,02 |

Table 3: Standard deviation between MTT and cell counting percentage values relative to MCF-7cell line at the 72 hours time point

# ANNEX III

Subtraction of HSA from FUAc-HSA CD-spectroscopy spectra.

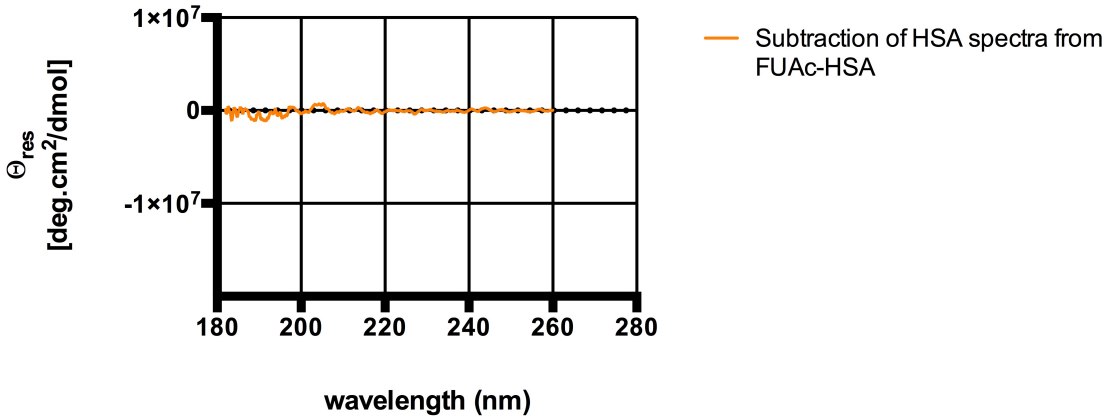


Figure 1 : Subtraction of HSA from FUAc-HSA CD-spectroscopy spectra